The
ENGINEERS' DIGEST

REVIEW OF WORLD ENGINEERING PROGRESS

VOL. X. No. 7 JULY, 1949

ENGINEERING LIBRARY

AUG 9 1949

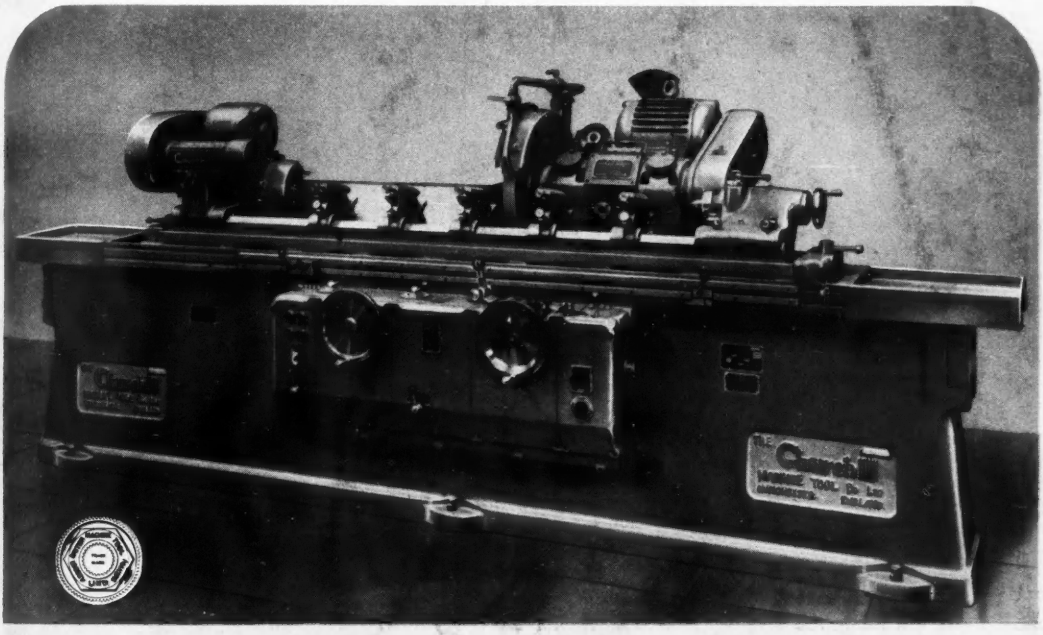

The Churchill Model 'BW'

10" X 60" PLAIN GRINDING MACHINE

Standardisation at its best is in the interest of the user but often helps only the manufacturer. The new Churchill Standard Control Apron for Precision Grinding Machines helps the operator by convenience and sensitivity of control—maintenance by get-at-ability—the makers by line assembly and service without headaches—and, most important of all, the customer—with a still better machine.

THE CHURCHILL MACHINE TOOL Co LTD
BROADHEATH MANCHESTER

Home Selling Agents: Charles Churchill and Co., Ltd., Birmingham and Branches
Export Sales Organisation: Associated British Machine Tool Makers Ltd., London Branches and Agents

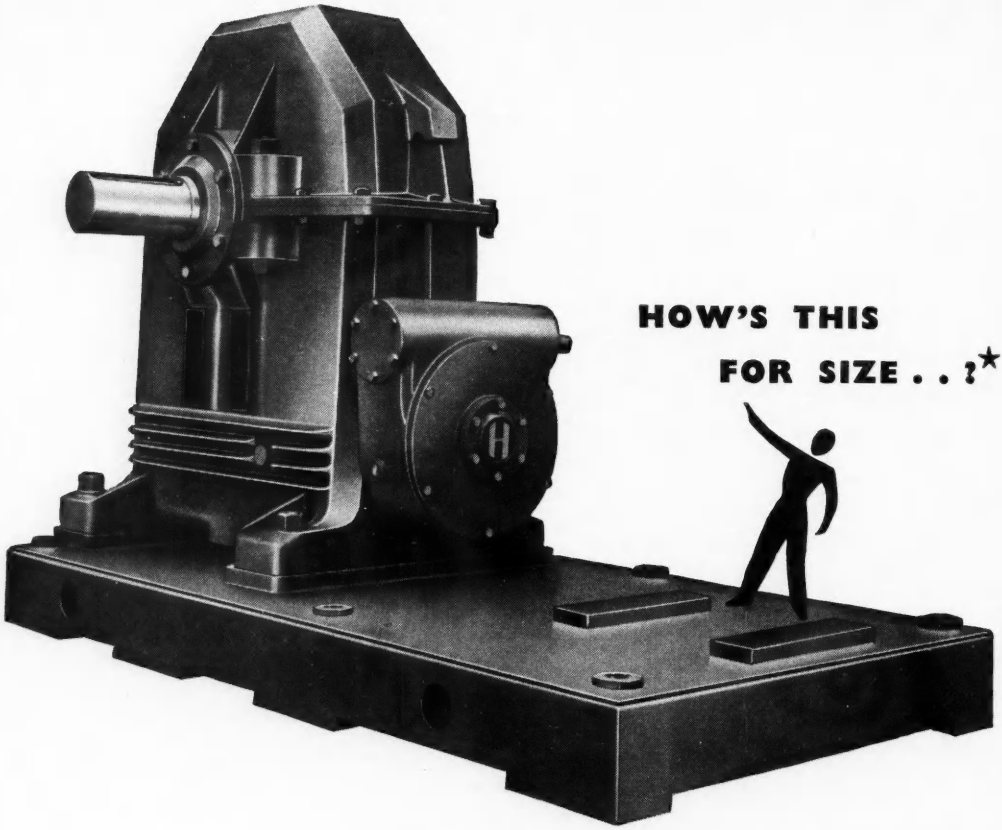

★ **Yes, yes! We have exaggerated a bit in the picture. But if you're a fisherman you'll sympathise — we hope.**

It is reported that our advertising is giving the wrong impression. Avid readers now think that we produce *only* miniature worm reduction units. The very idea! Why here is a Holroyd Giant — the father and mother of our standard units. It has an overall ratio of 120/1, is used for a barring gear drive and will transmit nearly half a million lb. ins. on the forged steel output shaft. The two Holfos Phosphor Bronze wheels are 18 ins. and 44 ins. diameter. There are ball and roller bearings fitted throughout and the worms are case hardened and ground from nickel steel. In fact this model, the 10/24H, is very big and very tough. Is that clear? **Very big and very tough.**

Holroyd

WORM GEAR UNITS UP TO 24" CENTRES

JOHN HOLROYD & COMPANY LIMITED · MILNROW · LANCASHIRE

CRC 134

THE ENGINEERS' DIGEST

REVIEW OF WORLD ENGINEERING PROGRESS

VOL. X. No. 7 JULY, 1949

IN THIS ISSUE

WITH modern machines running at the limit of endurance of their materials, an accurate determination of the geometrical pattern of stresses occurring in machine parts becomes increasingly important. At the same time, the complexity of stress analysis grows, the less permissible it becomes to make idealised assumptions which would simplify calculation and experiment. Various, often expensive, methods of experimental stress analysis have been evolved on the basis of model tests or measurements " on the job." The theoretical determination of stresses from the laws of elasticity, though it appears to be the most direct primary approach, involves, in nearly all practical cases, mathematical difficulties and arithmetical complications constituting a source of embarrassment whenever the time factor is an essential consideration. Even Prof. Southwell's relaxation methods which avoid the worst mathematical difficulties, leave a residue of semi-skilled computational work beyond the scope of most research departments, even when equipped with the necessary calculating machines.

In the search for mechanical methods of solving the arithmetical difficulties involved in theoretical stress determination, the Metrology Department of Liège University has developed the apparatus described on page 233. Taking the mathematical background of photo-elastic experimental stress analysis as the point of departure, the author develops the theory and demonstrates the manipulation of this new instrument, which has been designed to cope quickly and easily with complicated two-dimensional stress problems, e.g., stresses in flat plates. Examples are given, and it is shown that in certain special cases three-dimensional problems can be dealt with. Moreover, since the instrument is not dependent on experimental conditions, but merely offers a mechanical method of solving the complicated mathematical problems of theoretical stress analysis, it can also be used for the solution of all those problems in physics and engineering which lead to the same fundamental mathematical equations, such as, e.g., the transverse bending of plates, two-dimensional electric fields, steady fluid flow, and torsion of beams.

The author invites those concerned with investigations on similar lines, and using this instrument, or instruments of a similar character, to communicate with him regarding their experience and any difficulties they may happen to have encountered.

* * *

During the war considerable research was carried out in Germany on the reduction of noise in electric motors. The interest in this ostensibly peace-time problem was primarily due to the desire to eliminate the noise of submarines as far as possible, so as to make their detection more difficult. The field of investigation was extended to cover all types of electric motors, and the article " Approximate Calculation of the Noise produced by Squirrel-Cage Motors " is typical of the theoretical approach of the A.E.G. research engineers to the advance calculation of the noise of squirrel-cage motors. Not only do the resulting formulae give an objective measure for comparison of the anticipated noise of various designs of squirrel-cage motors under various load conditions, but, in addition, the calculations lead to the establishment of various rules for the design of low-noise motors.

* * *

A brief but interesting note on page 241 in this issue refers to new types of ultrasonic generators which have been successfully developed in the United States for the removal of dust and polluting substances from the atmosphere. The equipment is already being used in industrial plants, and powerful ultrasonic generators of considerable capacity are now a practical possibility.

* * *

In the second part of the article " Fundamentals of Automatic Control," presented in this issue, Dr. Oppelt deals first with the calculation of the loci of series and parallel connected systems, branched systems, and feedback networks. Mention is made of a cylindrical slide rule for the multiplication of complex numbers, and of an apparatus with a transparent rotatable disc, which enables complex multiplication to be carried out directly on the locus plane, without additional calculations. The article continues with the determination of open-and-closed-loop systems, control elements for variation of the reference datum, and the effect of load disturbances. The conclusion of this article, dealing with stability criteria, will be published in our September issue.

Approximate Calculation of the Noise produced by Squirrel-Cage Motors

By Dr. JORDAN. (From *A.E.G. Technical Report*, No. U. 38242, by courtesy of the Board of Trade, German Division.)

ACCORDING to current ideas, the noise produced by squirrel-cage motors is due to radial oscillations of the laminations.

The intensity of sound at the surface of the packet of laminations, i.e., the sound energy emitted per cm² of the surface, is a physical (objective) measure of the noise.

It is customary not to express this intensity $\mathcal{J}$ in Watt/cm², but to indicate it in the form of a ratio to the energy corresponding to the intensity of the audio threshold $\mathcal{J}_s$, and thus to express the sound energy as a dimensionless factor. As the magnitude of the sound energy to be specified covers the range from the audio threshold to the threshold of feeling (pain level), which corresponds to a range of 1 to 10^{12}, it was found convenient to express the ratio $\mathcal{J}/\mathcal{J}_s$ in a logarithmic form, thus:—

$$B = k \log_{10} \frac{\mathcal{J}}{\mathcal{J}_s} \text{ [Bel].} \quad .. \quad (1)$$

According to Weber's law, the value of B is then, incidentally, also an approximate measure of the subjective sensation, or the loudness, of sound.

As the human ear can already detect an energy increase of 25 per cent, i.e.,

$$\mathcal{J}_1/\mathcal{J}_2 = 1{\cdot}25,$$

the factor k in eq. (1) is chosen so that

$$1 = k \log_{10} 1{\cdot}25 \quad .. \quad .. \quad (2)$$

which means $k = 10$; the ratio of the sound energies

$$D = 10 \log_{10} \frac{\mathcal{J}}{\mathcal{J}_s} \text{ [db]} \quad .. \quad .. \quad (3)$$

is called the "decibel scale."

At a frequency of 1000 cps the decibel scale is, by definition, identical with the phon scale of the loudness of sound L:

$$L = 10 \log_{10} \frac{\mathcal{J}}{\mathcal{J}_s}, \text{ or } \Delta L = 10 \log_{10} \frac{\mathcal{J}_1}{\mathcal{J}_2} \text{ [phons],}$$
$$\text{for } f = 1000 \text{ cps} \quad .. \quad .. \quad (4)$$

It can be seen that the loudness L depends not only on the intensity $\mathcal{J}$ of the sound, but also on the threshold value $\mathcal{J}_s$. According to the Fletcher-Munson curves shown in Fig. 1, the audio threshold for a frequency of 1000 cps equals 10^{-16} W/cm², corresponding to a sound pressure of 2×10^{-4} dyne/cm² [μ bar]. Furthermore, these curves show that the phon and decibel scales still approximately coincide at frequencies as low as 500 cps and as high as 2000 cps.

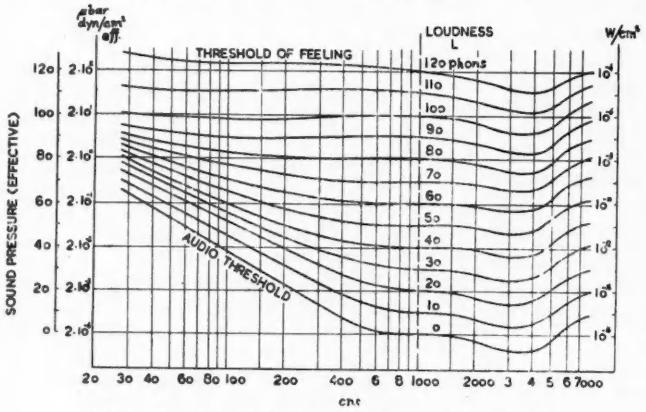

Fig. 1. **Curves of equal loudness (after Fletcher-Munson).**

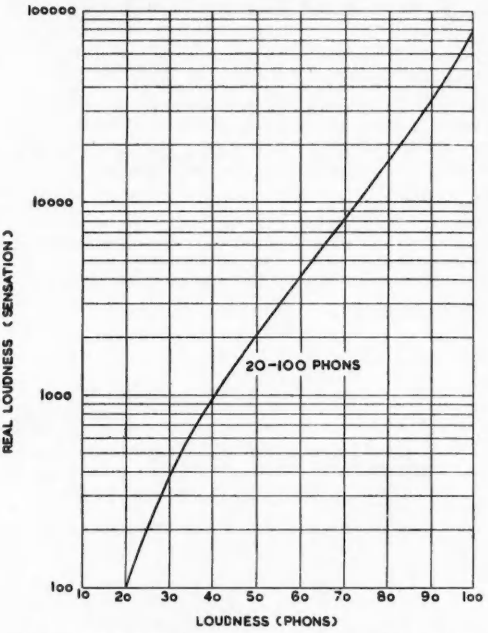

Fig. 2. **Real loudness (sensation) as a function of the loudness.**

At the same time, Weber's law, which states that the sensation increases as the logarithm of the stimulus, is also approximately valid only within a frequency range in the neighbourhood of 1000 cps and for a medium loudness of somewhere between 40 and 90 phons. Fig. 2 shows the relation, according to Fletcher-Munson, between the real subjective sensation of loudness and the loudness L as physically defined (phons). It can be seen that in the medium range, the real loudness is doubled for an increase of the physical loudness from 8 to 10 phons. In the loudness range below 40 phons, the doubling of the real loudness is already achieved by a smaller change in loudness.

To determine the loudness L (phons) at the surface of a motor or generator, it is necessary to know the specific emitted energy, i.e., the sound energy $\mathcal{J}$ emitted from 1 cm² of the surface of the machine (W/cm²). This can be calculated as the mean value over a period of time of the product of sound pressure p [dyne/cm²] and speed of the sound impulse [cm/sec] at the (effective) emitting surface.

In the case of an infinite plane oscillating at a speed of $v = 2\pi f X$ [cm sec⁻¹], where f is the frequency in cps,

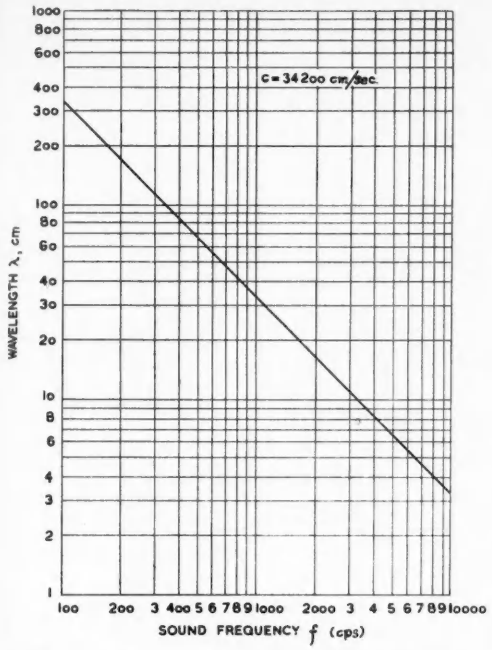

Fig. 3. **Wavelength of sound as a function of the frequency** f. Air temperature 18° C

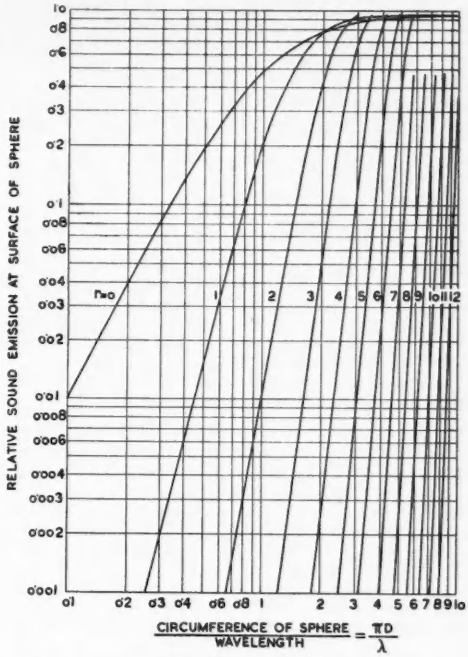

Fig. 4. **Relative sound emission of spherical emitters.** $r = 0$ to 12

and X the amplitude in cm, sound pressure p and sound speed v are in phase and proportional, the proportionality factor $\rho_c = 41{\cdot}5$ [g cm^{-2} sec] being independent of frequency and called the " sound wave resistance of air."

$$\mathcal{J}_{\text{plane}} = \int_0^T pv\,dt = \frac{1}{2}(\rho_c)\,v^2\,10^{-7} = 83\,\pi^2\,10^{-7} f^2 X^2 \quad [\text{Watt cm}^{-2}] \quad (5)$$

Calculation of the sound intensity based on eq. (5) is also permissible when the dimensions of the sound emitter are large when compared with the emitted wave length λ (cm).

This assumption will not generally be applicable to motors or generators, as the sound frequencies of 500 to 4000 cps, as produced, for instance, by the conventional asynchronous motors, correspond to wavelengths of 69 to 8·5 cm, which is of the same order as the diameters of medium-size motors.

To enable an approximate determination to be made of the loudness at the surface of the machine also for the above-mentioned general case, the oscillating packet of laminations can be assumed to form a section of a spherical emitter, the order of which is determined by the pulsating radial forces, and the diameter of which D approximately equals the outer diameter of the stator laminations.

For instance, if the whole inner circumference of the stator laminations is subject to a uniformly distributed alternating force ($r = 0$) which causes the pocket to be deformed in a manner similar to that of a tube subjected to an alternating internal pressure, the sound emitter is called a " zero emitter " (respirating sphere).

If there is a shaking force ($r = 1$) such as, for instance, an unbalanced rotor, the oscillating rotor behaves as an emitter of the order one (pulsating sphere).

If the radial forces cause an elliptic deformation of the stator laminations the motor acts as an emitter o the order two.

Similarly, for higher orders, as in the case of a plane emitter, sound pressure and sound speed are proportional also in the case of an oscillating sphere; but they are generally out of phase and the proportionality factor is frequency-dependent. It depends—as can easily be deduced for the zero emitter—on the ratio between the circumference πD of the sphere and

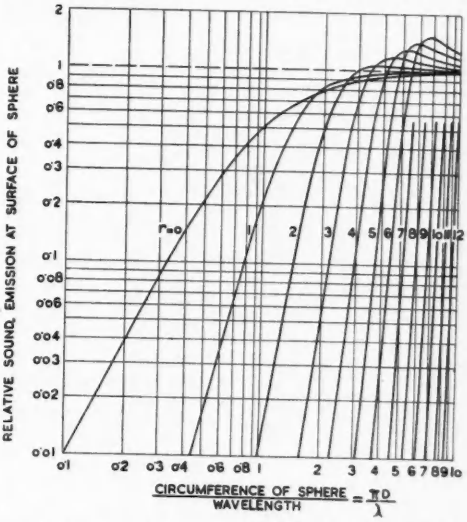

Fig. 5. **Relative sound emission of spherical emitters.** $r = 0$ to 12

the wavelength. The ratio of the specific sound intensity of an emitter of the order r to the specific sound intensity of an infinite plane emitter oscillating with the same speed is called the "relative sound intensity," $N_{\text{rel } r}$.

It is represented by the real component of the above-mentioned complex proportionality factor of sound pressure and sound speed, and it is shown in Figs. 4 and 5 for the orders $r = 0$ to $r = 12$ as a function of the ratios of the circumference of the sphere and the wavelength λ. For small values of $\pi D/\lambda$, $N_{\text{rel } r}$ increases with the $(2r + 2)$th power, and for

$$\pi D/\lambda \gg 1$$

approaches a limit of 1 independently of the order r. It is worth noting that for certain frequency ranges the specific sound intensity of a spherical emitter of an order higher than $r = 2$ can assume higher values than that of an oscillating plane. This fact is due to interference phenomena.

The sound intensity at the surface of an electric motor is, therefore, approximately:

$$\mathfrak{J}_r = \mathfrak{J}_{\text{plane}} N_{\text{rel } r} = 83\,\pi^2\,10^{-7}\,N_{\text{rel } r}\,f_r^2\,X_r^2 \text{ [Watt cm}^{-2}\text{]} \quad (6)$$

where X_r [cm] is the peak value of the amplitude of the rth deformation wave at the surface of the stator packet and f_r [cps] is the corresponding sound frequency.

To evaluate the sound intensity $\mathfrak{J}_r$ at the surface of the motor it is necessary to know the relative sound intensity $N_{\text{rel } r}$ (from Figs. 4 and 5), the sound frequency f_r and the amplitude X_r of the oscillation.

The sound frequencies corresponding to the various deformation (or force) waves resulting from the winding harmonics can be calculated from the following formula:

$$f_r = f_N \left[g'' \frac{Z''}{p} (+ s) \right] + (0 \text{ or } 2 f_N) \quad \text{[cps]} \quad (7)$$

where Z'' is the number of rotor slots, $2p$ the number of poles, f_N the supply frequency, s the slip and g'' any positive or negative integer. In the case of deformation waves due to saturation, these frequencies are increased by twice the supply frequency f_N.

All factors in eq. (6) are now determined, except for the peak amplitude X_r of the radial oscillations. This equals

$$X_r = X_{r\,\text{stat}} \cdot \xi_r \quad \text{[cm]}, \quad \ldots \quad \ldots \quad (8)$$

where $X_{r\,\text{stat}}$ is the "static" deformation amplitude and ξ_r a factor taking into account the influence of resonance. This resonance factor depends on the ratio f_r/F_r (F_r = natural frequency of the packets of laminations for the rth wave), and on the attenuation. The latter is not easily determined theoretically in advance. This fact, however, is of no importance as endeavours will, of course, always be made to avoid operating within the resonance range.

This means that the following frequencies will have to be avoided, as has been deduced elsewhere:—

$$\left.\begin{aligned} \text{for } r = 0\text{:}\quad & F_0 = \frac{526000}{2\pi R_m}\,\varphi_z \text{ [cps]} \\ \text{for } r \geq 2\text{:}\quad & F_r = \frac{1}{2\sqrt{3}} \cdot \frac{r\,(r^2-1)}{\sqrt{r^2+1}} \cdot \frac{h}{R_m} F_0 \text{ [cps]} \end{aligned}\right\} \quad (9)$$

where R_m = mean radius of the laminations (cm),
h = the height of the laminations (cm), and

$$\varphi_z = \sqrt{\frac{\text{weight of the yoke}}{\text{weight of the yoke} + \text{weight of the teeth}}}$$

For $r = 1$ only a deflection of the shaft and not a deformation of the pockets of laminations takes place, and it will always be endeavoured to avoid this case by choosing the number of slots Z'' of the rotor as an even number:—

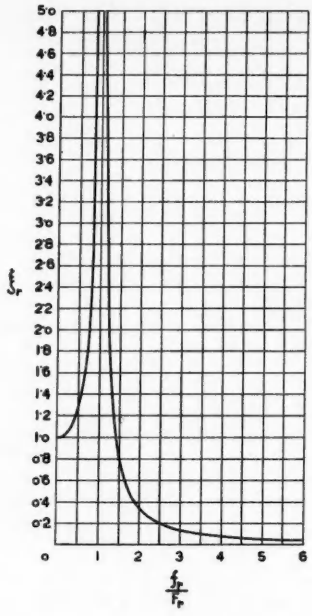

Fig. 6.
Resonance factor.

$$\xi_r = \frac{1}{\left(1 - \frac{f_r}{F_r}\right)^2}$$

If these frequencies are avoided the resonance factor can be approximated

$$\xi_r = \frac{1}{\left(1 - \frac{f_r}{F_r}\right)^2} \quad \text{(see Fig. 6)} \quad \ldots \quad (10)$$

The static deformation amplitude $X_{r\,\text{stat}}$ has been deduced elsewhere as:—

$$\left.\begin{aligned} \text{for } r = 0\text{:}\quad & X_{0\,\text{stat}} = K_0 \frac{R_m}{2{\cdot}2 \times 10^6} \left(\frac{R_m}{h}\right), \text{[cm]} \\ \text{for } r \geq 2\text{:}\quad & X_{r\,\text{stat}} = K_r \frac{R_m}{2{\cdot}2 \times 10^6} \left(\frac{R_m}{h}\right)^3 \frac{12}{(r^2-1)^2}, \text{[cm]} \end{aligned}\right\} \quad (11)$$

where K_0 and K_r are the amplitudes of the radial deformation (force) waves [kg/cm²].

It is also important to bear in mind that in the case of slow-running rotors, the zero oscillation is by far the most predominant. In such machines the number of rotor slots is always chosen as a multiple of the number of poles, and it is for this reason that radial force waves occur only as multiples of the number of poles $2p$, i.e., $r = 0, 2p, 4p, \ldots$ However, for a 12-pole machine with $h/R_m = 0{\cdot}1$, the ratio X_{12}/X_0 is already smaller than 1/10.

Of main interest is the ratio, for equal force wave amplitude, of the deformation amplitudes given by eq. (11).

$$\frac{X_{r\,\text{stat}}}{X_{0\,\text{stat}}} = \frac{12}{(r^2-1)^2} \cdot \frac{1}{(h/R_m)^2} \ldots \quad \ldots \quad (12)$$

This ratio, as a function of h/R_m and with r as the parameter, is shown in Fig. 7. It will be seen that the relative static deformation amplitudes of the lower

orders are—at least in the range of h/R_m as used in induction motors—much more dangerous than the uniform deformation $r = 0$. On the other hand, the higher orders $r \geq 6$ show—in the range of

$$0{\cdot}1 \leq \frac{h}{R_m} \leq 0{\cdot}25$$

used, as a rule, in fast-running machines—smaller deformations than those for $r = 0$.

The following example illustrates the relative magnitudes of the deformation amplitudes:—In the case of a motor with a mean stator yoke radius of $R_m = 20$ cm, a height of the yoke of $h = 0{\cdot}2\ R_m = 4$ cm, a deformation or force wave of order 2 ($r = 2$) and a corresponding force wave amplitude of

$$R_2 = 0{\cdot}05\ \text{kg/cm}^2,$$

the actual static deformation is $0{\cdot}76 \times 10^{-4}$ cm; the deformations are thus extremely small.

From the foregoing, all the factors required for the calculation of the loudness L at the machine surface, caused by any force wave K_r, are now known.

The radial force waves are caused by the combined actions of fields in the air gap. Of all the possibilities of field combination, only one case need be taken into account as a first approximation. This is the interference of a basic field harmonic of the order $\nu = p\,(6g' + 1)$ with one of the fields of the basic rotor current of the order of $\lambda = g''\ Z'' + p$. This produces radial force waves of the orders

$$r = g''\ Z'' + p \pm \nu \quad .. \quad .. \quad (13)$$

and of frequencies (according to eq. 7) of

$$K_r = \frac{1}{1 + \sigma_{dp}''} \frac{1}{\sqrt{1 + \left(\frac{\sigma s_k}{s}\right)}} \left(\frac{\mathfrak{J}'}{\mathfrak{J}_{m\nu}'}\right)^2 \left(\frac{\mathbf{B}_{dp}}{5000}\right)^2 \times \left| \frac{p}{\nu} \frac{\xi_\nu'}{\xi_p'} f_{sp} \right| \times \left| \frac{\xi_p''^2}{1 + g'' \dfrac{Z''}{p}} \right| \text{[kg/cm}^2\text{]} \quad (14)$$

where σ_{dp}'' = geometrical rotor stray factor for the basic harmonic.

σ = total stray factor for the basic harmonic.

s_k = breakdown slip.

s = slip.

$\mathfrak{J}'$ = stator current [amp.]

$\mathfrak{J}_{m\nu}'$ = magnetisation current.

$\mathbf{B}_{dp}$ = induction amplitude of the basic wave $\nu = p$ (gauss).

$\xi\nu'$ = stator winding factor for the νth field.

From this the loudness L_0 at the surface of the machine for a zero oscillation is derived as

$$L_0 = 20 \log_{10} \left[2250 \sqrt{N_{\text{rel}\,0}} \times \xi_0 \left(\frac{2\pi R_m}{\lambda}\right) \left(\frac{R_m}{h}\right) K_0 \right], \text{[phons]} \quad (15)$$

Taking into account that:—

$$N_{\text{rel}\,0} = \frac{\left(\frac{2\pi R}{\lambda}\right)^2}{1 + \left(\frac{2\pi R}{\lambda}\right)^2}$$

where R = outer radius of the stator packet [cm], it

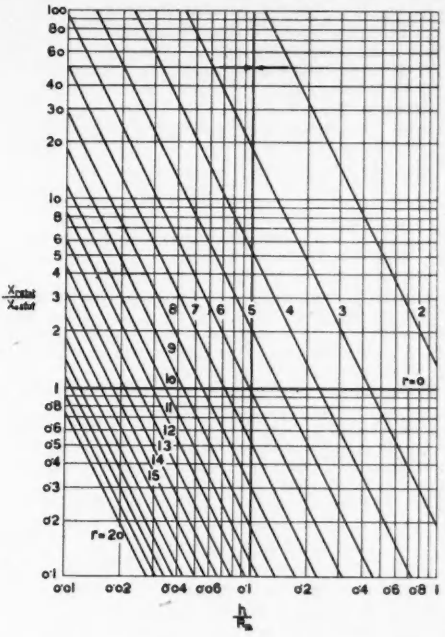

Fig. 7. **Relative static deformation amplitudes.**

follows that:—

$$L_0 = 20 \log_{10} \left[2250 \frac{\left(\frac{2\pi R}{\lambda}\right)^2}{\sqrt{1 + \left(\frac{2\pi R}{\lambda}\right)^2}} \xi_0 \left(\frac{R_m}{h}\right) K_0 \right] \text{[phons]} \quad (17)$$

In the case of large motors which oscillate as zero oscillators, it is normally

$$\frac{2\pi R}{\lambda} \gg 1.$$

Therefore $N_{\text{rel}\,0} = 1$ and eq. (17) is simplified to:

$$L_0 = 20 \log_{10} \left[2250 \left(\frac{2\pi R}{\lambda}\right) \left(\frac{R_m}{h}\right) \xi_0 K_0 \right] \text{[phons]} \quad (18)$$

This equation is valid, in particular, for large machines with a large number of poles where, in addition to the force waves $r = 0$, only force waves of a high order (multiples of $2p$) occur.

On the other hand, for emitters of the order r (including $r = 2$) the following general equation is valid:—

$$L_r = 20 \log_{10} \left[27000 \sqrt{N_{\text{rel}\,r}}\ \xi_r \left(\frac{2\pi R_m}{\lambda}\right) \times \left(\frac{R_m}{h}\right)^3 \frac{1}{(r^2 - 1)^2} K_r \right] \text{[phons]} \quad (19)$$

The following example illustrates the order of magnitude of the loudness at the machine surface. It is a continuation of the earlier example where a static deformation amplitude of $0{\cdot}76 \times 10^{-4}$ was obtained. If the frequency is $f_2 = 1000$ cps, the corresponding sound wavelength according to Fig. 3 is $\lambda = 34$ cm and the relative power of emission accord-

ing to Fig. 5 for $2R_m + h = 44$ cm is $N_{rel\ 2} = 1{\cdot}075$

The natural frequency for oscillations of the order 2 is in accordance with eq. (9) and for $\varphi_z = 0{\cdot}85$, $F_2 = 550$ cps, which means that the resonance factor is $\xi_2 = 0{\cdot}435$ (Fig. 6). The loudness according to eq. (19), is, therefore: $L = 90$ phons. If the rotor produces a force wave of the order 4 of the same amplitude and frequency, then $N_{rel\ 4} = 0{\cdot}8$, $F_4 = 3000$ cps $\xi_4 = 1{\cdot}12$ and $L = 68$ phons.

For larger slow-running machines, $N_{rel\ r}$ is again equal to 1, and this also applies in the case of $r = 2$. The factor $N_{rel\ r}$ is the main reason why it is relatively simple to build small motors with low noise level. Small motors also have, in general, a small number of rotor slots per pair of poles and, therefore, produce relatively low sound frequencies and sound waves of longer wavelengths, which in themselves are large as compared with the dimensions of the motor. In addition, the amplitudes of the oscillations decrease proportionately with the mean radius R_m.

With eqs. (15) and (19) as a basis for comparison, individual machines can now be compared.

Geometrically similar machines with identical number-of-slot ratios and identical magnetic saturation, differ from each other by the relative radiation power $N_{rel\ r}$, the resonance factor ξ_r and the mean yoke radius. The difference in loudness of two geometrically similar machines is, therefore,:

$$\Delta L_{12} = 20 \log_{10} \left[\sqrt{\frac{N_{rel\ r1}}{N_{rel\ r2}}} \; \frac{\xi_{r1}}{\xi_{r2}} \; \frac{R_{m1}}{R_{m2}} \right] \text{[phons]} \quad (20)$$

If the dimensions of a machine are increased threefold, all other conditions remaining unchanged, the loudness at the surface of the machine increases by about 10 phons, which corresponds to a doubling of the real loudness.

A doubling of the height h of the yoke results in a decrease of the loudness at the surface of the machine by 18 phons if $r = 2$; if, however, the sound is due to a zero oscillation, the loudness, in this case, is reduced by only about 6 phons.

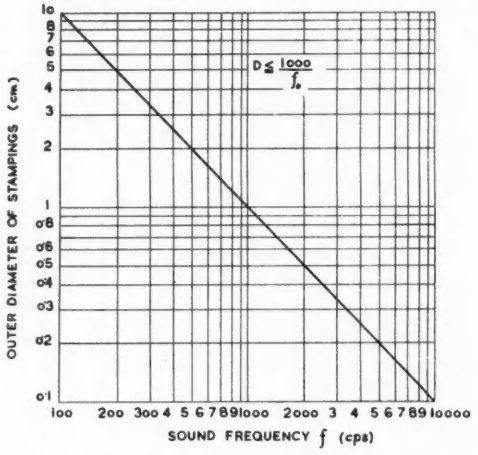

Fig. 8. **Critical diameter for zero-oscillations** ($r = 0$).

An increase of the magnetic induction by 20 per cent increases the forces, according to eq. (14), by a factor 1·44, which corresponds to an increase in loudness by about 3 phons. By changing connections from star to delta, the forces increase threefold, which corresponds to an increase in loudness of 10 phons.

If the motor load is doubled, the forces due to the basic rotor current increase four times. This means an increase in loudness by 12 phons, which again corresponds to a doubling or the real loudness, as compared with conditions under the original load. From this, it is obvious that the magnetically produced sounds increase considerably with the load. The whining of motors on no-load, especially those with straight slots, is dealt with elsewhere.

It is also of importance to compare emitters of different orders, but with the same force and frequency, within one machine, as is the case when one machine is tested with various rotors. Assuming $N_{rel\ r} = 1$ and $\xi_r = 1$, the difference in loudness in comparison with the zero oscillation is

$$\Delta L_{ro} = 40 \log_{10} \left[\frac{2\sqrt{3}}{r^2 - 1} \left(\frac{R_m}{h} \right) \right] \text{[phons]} \quad .. \quad (21)$$

This shows that for the usual values of h/R_m which, for fast-running motors, are between 0·1 and 0·3, emitters of the order 2 are especially unfavourable. For $h/R_m = 0{\cdot}2$ and $r = 2$, for instance, $\Delta L_{20} = 40 \log_{10} 0{\cdot}76 = 31$ phons. However, the emitter of the order 4 is only louder by $\Delta L\ 40 = 40 \log_{10} 1{\cdot}16 = 2$ to 3 phons than a zero emitter.

Also of some importance is the critical diameter below which a substantial emission of certain wavelengths may no longer be expected. These data are shown in Figs. 8 and 9. A plane oscillating at the same frequencies has been taken as the basis for comparison.

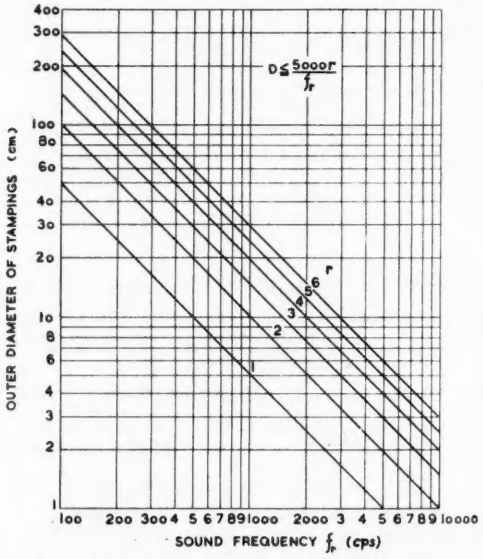

Fig. 9. **Critical diameter for oscillations of the order** r.

Finally, the loudness which a motor produces in a closed room also depends on the absolute sound output, which can be obtained by multiplying the relative sound output with the emitter surface $4\pi R^2$ and with the factor $\frac{1}{2r+1}$, which takes account of the distribution of the sound amplitude over the whole surface. It is for this reason, too, that smaller motors produce less noise.

Based on the above deliberations, the choice of the number of slots will be discussed in another paper.*

*We have not been able to find out whether this paper has ever been published.—EDITOR, E.D.

Nomogram for the Calculation of Condenser Bushings

By F. ČEŘOVSKÝ. (From *Elektrotechnický Obzor*, Vol. 36, No. 16, August, 1947, pp. 298-304, 6 illustrations.)

(*Continued from June issue*)

Maximum Stress in Radial Direction

According to eq. (3) the radial stress

$$\rho = \frac{\text{const.}}{r\,l} = \frac{\text{const.}}{y},$$

The radial stress values at the inside (terminal) and outside radii of the bushing are (Fig. 3):

$$\rho_i = \frac{E}{2}\,\frac{l_0 + l_n}{\log_e r_n/r_0}\,\frac{1}{l_0\,r_0}, \quad .. \quad (12)$$

and

$$\rho_e = \frac{E}{2}\,\frac{l_0 + l_n}{\log_e r_n/r_0}\,\frac{1}{l_n\,r_n}, \quad .. \quad (13)$$

If ρ_d is the maximum permissible radial stress of the material, and $\rho_i \leq \rho_e = \rho_d$, we obtain from eq. (13)

$$\frac{E}{2}\,\frac{l_0 + l_n}{\log_e r_n/r_0}\,\frac{1}{r_n\,l_n} = \rho_d$$

from which r_n can be calculated if the other values are known. We thus obtain:

$$\frac{E}{\rho_d}\,\frac{l_0 + l_n}{2\,l_n} = r_n \log_e \frac{r_n}{r_0}, \quad .. \quad (13a)$$

Similarly for $\rho_e \leq \rho_i = \rho_d$,

$$\frac{E}{2}\,\frac{l_0 + l_n}{\log_e r_n/r_0}\,\frac{1}{l_0\,r_0} = \rho_d,$$

and

$$\frac{E}{\rho_d}\,\frac{l_0 + l_n}{2\,l_0} = r_0 \log_e \frac{r_n}{r_0} \quad .. \quad (12a)$$

To obtain simpler equations (12a) and (13a) are divided by r_0 and the following new symbols are introduced:

$$\alpha = \frac{l_0}{l_n} > 1, \quad .. \quad .. \quad (14)$$

$$\beta = \frac{r_n}{r_0} = \frac{d_n}{d_0} > 1, \quad .. \quad (15)$$

and

$$\kappa = \frac{E}{\rho_d\,d_0}, \quad .. \quad .. \quad (16)$$

and diameters are used instead of radii, e.g.

$$d_0 = 2\,r_0, \quad d_n = 2\,r_n, \quad \text{etc.},$$

and we obtain from eq. (13a):

$$\kappa(1 + \alpha) = \beta \log_e \beta \quad .. \quad .. \quad (17)$$

valid for $\rho_i \leq \rho_e$ (max. radial stress near the outside cylinder, i.e. if

$$\frac{1}{r_0\,l_0} \leq \frac{1}{r_n\,l_n}, \quad \text{or re-written} \quad \frac{r_n}{r_0} \leq \frac{l_0}{l_n}, \quad \text{and } \beta \leq \alpha$$

Inserting eqs. (14), (15), and (16) into eq. (12a), we obtain:

$$\kappa(1 + \alpha) = \alpha \log_e \beta \quad .. \quad .. \quad (18)$$

which is valid for $\rho_e \leq \rho_i$ (max. radial stress on the terminal side), i.e. for $\alpha \leq \beta$.

Basic Principle of the Condenser Bushing

Without metal foil inserts the bushing is a simple cylindrical condenser and the terminal and the outer cylinder are its electrodes. The radial stress at any radius represented by

$$\rho_v = \frac{E}{r \log_e r_n/r_0}$$

The same result is obtained by using eq. (3) for l = const. The maximum radial stress is at the minimum radius, r_0, i.e., at the terminal.

$$\rho_{v0} = \frac{E}{r_0 \log_e r_n/r_0} \quad .. \quad .. \quad (19)$$

If intermediate metal layers are to be of any value the maximum radial stress has to be reduced to a value smaller than the one obtained by eq. (19), or

$$\rho/\rho_{v0} < 1,$$

and introducing the values from eq. (11) and (19) we obtain

$$\frac{\rho}{\rho_{v0}} = \frac{l_0 + l_n}{2\,l}\,\frac{r_0}{r} < 1, \quad .. \quad (20)$$

If the radial stress has its maximum at the terminal, l and r in eq. (20) should be replaced by the values l_0 and r_0, and we obtain

$$\frac{l_0 + l_n}{2\,l_0} < 1.$$

This condition is always fulfilled, because $l_n < l_0$. It is, therefore, obvious that the radial stress at the terminal is always smaller in the case of a condenser bushing than in the case of a bushing without metal inserts. If the inequality (20) has also to be fulfilled for the stress at the (outside) sleeve, the following relation applies:

$$\frac{l_0 + l_n}{2\,l_n}\,\frac{r_0}{r_n} < 1,$$

and using eqs. (14) and (15), this can be re-written:

$$\frac{1 + \alpha}{2} < \beta \quad .. \quad .. \quad (21)$$

As

$$\alpha > 1, \quad \frac{1 + \alpha}{2} > 1,$$

and

$$\log_e \frac{1 + \alpha}{2} > 0.$$

It is also true that

$$\log_e \beta > \log_e \frac{1 + \alpha}{2},$$

and

$$\beta \log_e \beta > \frac{1 + \alpha}{2} \log_e \frac{1 + \alpha}{2} \quad .. \quad (22)$$

For maximum radial stress at the sleeve eq. (17) is applicable:

$$\beta \log_e \beta = \kappa(1 + \alpha), \quad .. \quad .. \quad (17)$$

We, therefore, obtain

$$\kappa > \frac{1}{2} \log_e \frac{1+\alpha}{2}, \quad .. \quad .. \quad (23)$$

or

$$\alpha < 2\, e^{2\kappa} - 1$$

It is obvious from the latter inequality that α, the ratio between the total length of the bushing and the length of the earthed sleeve, has an upper limit, which is given by the inequality (23) and is also plotted in the nomogram of the solution of eqs. (17) and (18) representing the limiting curve of the family of curves, thus eliminating incorrect solutions.

Nomogram of the Equations (17) *and* (18)

The equations (17) and (18) required for calculation of β can easily be represented by straight-line nomograms, but such representation would be impractical, because the validity of one of the equations would have to be assumed at the beginning of the calculation, and if this assumption were to be proved wrong it would be necessary to recommence the calculation, using the other equation. This disadvantage can be eliminated by using a nomogram, which enables simultaneous representation of both equations (17) and (18) by plotting two families of curves β in a κ and α-field respectively. Eq. (17) can also be written:

$$\log_{10} \kappa + \log_{10} (1+\alpha) = \log_{10} (\beta \log_e \beta) \quad .. \quad (17a)$$

$$\left.\begin{aligned} \text{In co-ordinates: } y &= \eta \log_{10} (1+\alpha) \\ x &= \xi \log_{10} \kappa \end{aligned}\right\} \quad .. \quad (24)$$

This represents eq. (17a), and is a straight line for β = const., the equation of which is:

$$y = -\frac{\eta}{\xi} x + \eta \log_{10} (\beta \log_e \beta), \quad .. \quad (17b)$$

This straight line is only valid where $\alpha \geq \beta$, and $\alpha = \beta$ is the last point still valid. The geometrical locus of all points $\alpha = \beta$ is a curve, and its equation is obtained by inserting $\alpha = \beta$ in either eq. (17), or (18), e.g., $\kappa (1+\alpha) = \alpha \log_e \alpha$

or

$$\kappa = \frac{\alpha \log_e \alpha}{1+\alpha}, \quad .. \quad .. \quad (25)$$

The values κ for various $\alpha = \beta$ are given in Table 1, and the $\alpha = \beta$ curve is plotted in Figs. 4 and 5 and the nomogram, Fig. 6, as the limiting curve of the family

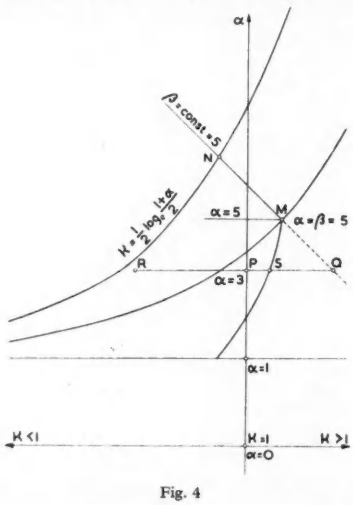

Fig. 4

TABLES I AND II. CONDENSER BUSHING CALCULATIONS.

TABLE I.

$\alpha = \beta$	$\kappa = \frac{\alpha \log_e \alpha}{1+\alpha}$
1·0	0·000
1·1	0·050
1·2	0·100
1·3	0·149
1·4	0·196
1·5	0·244
2·0	0·462
2·5	0·655
3·0	0·824
3·5	0·974
4·0	1·111
4·5	1·23
5·0	1·34
6·0	1·54
7·0	1·70
8·0	1·85
9·0	1·98
10	2·09
15	2·54
20	2·86
30	3·29
40	3·60
50	3·84
60	4·03
70	4·18
80	4·33

TABLE II.

α	$\kappa = \frac{1}{2} \log_e \frac{1+\alpha}{2}$
1·0	0·000
1·5	0·112
2·0	0·203
2·5	0·280
3·0	0·347
3·5	0·406
4·0	0·459
4·5	0·506
5·0	0·550
6·0	0·626
7·0	0·693
8·0	0·752
9·0	0·804
10	0·852
15	1·040
20	1·175
30	1·37
40	1·51
50	1·62
60	1·71
70	1·79
80	1·85
90	1·91
100	2·01

of curves β. The straight lines eq. (17b) are, therefore, only valid to the left of this curve, which represents the region where $\alpha \geq \beta$. It is advantageous to use a logarithmic scale for both co-ordinate axes of the nomogram, and if the two modules ξ, η are equal, eq. (17b) can be written:

$$y = -x + \eta \log_{10} (\beta \log_e \beta) \quad .. \quad (17c)$$

The equation represents a family of straight lines for various constant values of β, and these lines enclose an angle of 135° with the direction of the positive x-axis. Attention has to be paid to correct marking of the nomogram scales (Fig. 4). The κ scale is plotted on the x-axis, and for $x = 0$ ($x = \xi \log_{10} \kappa = 0$, and as $\xi \neq 0$, it follows that for $x = 0$, $\log_{10} \kappa = 0$), or $\kappa = 1$. The further marking of the κ-scale does not present difficulties. The α-scale is on the y-axis, and for $y = 0$ ($y = \eta \log_{10} (1+\alpha) = 0$, as $\eta \neq 0$, it follows that $\log_{10} (1+\alpha) = 0$), $\alpha = 0$. For $1+\alpha = 2$, $\alpha = 1$, etc. After marking the α and κ-scales and plotting the curve $\alpha = \beta$, the family of parallel (17c) straight lines can easily be entered in the diagram. The plotting of one curve for $\beta = 5$ is indicated in Fig. 4. the line is drawn under an angle of 135° from the point M of the $\alpha = \beta$ curve, for which $\alpha = \beta = 5$. Only the part of the line to the left of $\alpha = \beta$, i.e., point M is valid.

It was shown earlier that there is an upper limit for α, i.e., a lower limit for κ, if the condenser bushing is to reduce the stress, and the basic requirement is:

$$\kappa > \tfrac{1}{2} \log_e \frac{1+\alpha}{2} \quad .. \quad .. \quad .. \quad (23)$$

This means that the characteristic point of the bushing, given by the co-ordinates κ, α, must be situated to the right of the curve

$$\kappa = \tfrac{1}{2} \log_e \frac{1+\alpha}{2}, \quad .. \quad .. \quad .. \quad (26)$$

and all points to the left of this curve do not represent conditions of favourable condenser bushings; these lines should, therefore, not be drawn.

$$\kappa = \tfrac{1}{2} \log_e \frac{1+\alpha}{2},$$

and the above mentioned curve, therefore, ends in point N. The points of this limiting curve have to be calculated and also entered in the diagram.

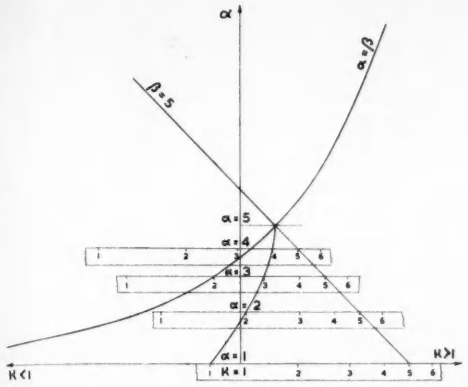

Fig. 5

Plotting of the family of curves for $\beta > \alpha$: If eq. (17a) were applicable it could also be written in the form

$$\log_{10} \kappa_\alpha = \log_{10} (\beta \log_e \beta) - \log_{10} (1 + \alpha), \qquad (27)$$

The symbol κ_α is only used temporarily, to discriminate it from κ_β of the eq. (18) solely valid in this zone. Eq. (18) could also be written in the following form:

$$\kappa_\beta (1 + \alpha) = \frac{\alpha}{\beta} . \beta \log_e \beta,$$

which can also be rewritten:

$$\log_{10} \kappa_\beta = \log_{10} (\beta \log_e \beta) - \log_{10} (1 + \alpha) + \log_{10} \alpha - \log_{10} \beta \qquad (28)$$

or $$\log_{10} \kappa_\beta = \log_{10} \kappa_\alpha + \log_{10} \alpha - \log_{10} \beta, \quad .. \quad (28a)$$

This equation enables easy construction of $\log_{10} \kappa_\beta$ by using $\log_{10} \kappa_\alpha$ (Fig. 4). For a given α characterized by point P, $\log_{10} \kappa_\alpha$ is given by the distance $\overline{PQ}$. The required distance $\overline{PS}$ is obtained by plotting $\log_{10} \beta = \overline{QR}$ to the left and $\log_{10} \alpha = \overline{RS}$ to the right again, using modulus ξ for both values:

$$\overline{PS} = \overline{PQ} - \overline{QR} + \overline{RS} =$$

$$= \log_{10} \kappa_\alpha - \log_{10} \beta + \log_{10} \alpha = \log_{10} \kappa_\beta \qquad (29)$$

It is advantageous to use a logarithmic scale of the modulus ξ drawn on a strip of paper for plotting the curves, and the points are entered one by one along the β = const. curve, starting, for example, from point $\alpha = 1$ and progressing to the point $\alpha = \beta$. The plotting can be carried out quickly, and is demonstrated for $\beta = 5$ in Fig. 5. The auxiliary scale is shown as applied to $\alpha = 1, 2, 3$ and 4. Fig. 6 represents the finished nomogram.

Calculation of the Principal Dimensions (Practical Example).

The results obtained can be utilized for calculating the principal dimensions of the condenser bushing, and this is demonstrated by a practical example. A paper-insulated non-symmetrical condenser bushing is to be designed; one end of the bushing is in oil, the other in air, the test voltage $E = 100$ kV, the inside dia. $d_0 = 50$ mm, the length of the outside cylinder, $l_n = 200$ mm. The permissible maximum stresses are $\rho_d = 7{\cdot}5$ kV per mm in the radial direction, and $\lambda_{ed} = 0{\cdot}31$ kV per mm in the axial direction in air, and $\lambda_{id} = 0{\cdot}62$ kV per mm in oil.

We obtain, according to eq. (5):

$$\lambda_d = \frac{\lambda_{ed} \lambda_{id}}{\lambda_{ed} + \lambda_{id}} = \frac{0{\cdot}31 \times 0{\cdot}62}{0{\cdot}31 + 0{\cdot}62} = 0{\cdot}206 \text{ kV/mm}$$

and using eq. (10):

$$l_0 - l_n = \frac{E}{\lambda_d} = \frac{100}{0{\cdot}206} = 486 \text{ mm},$$

$$l_0 = l_n + 486 = 686 \text{ mm}$$

and according to eq. (14):

$$\alpha = \frac{l_0}{l_n} = \frac{686}{200} = 3{\cdot}43$$

According to eq. (16):

$$\kappa = \frac{E}{\rho_d d_0} = \frac{100}{7{\cdot}5 \times 50} = 0{\cdot}267$$

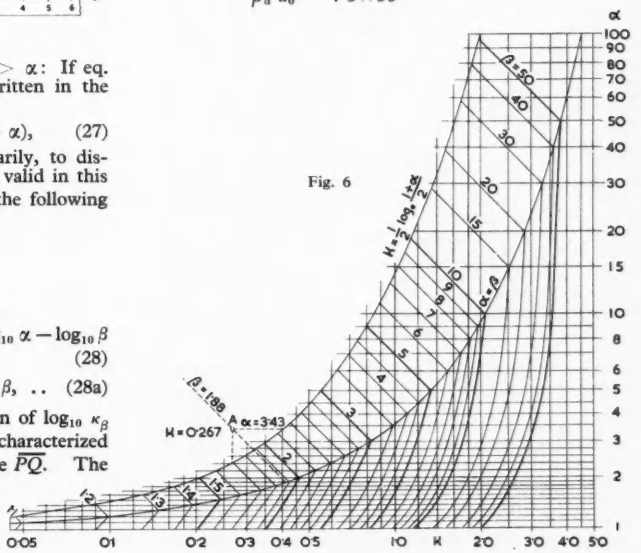

Fig. 6

For these values of α and κ we obtain point A in the nomogram, Fig. 6, and it is obvious that this point represents an incorrectly designed condenser bushing. It is already known from previous chapters that the maximum stress of this bushing will be at the sleeve (because $\alpha > \beta$), and that the stress will be higher than if there were no metal inserts at all. This theoretical result is somewhat outweighed by the fact that the metal foils subdivide the insulator into thinner layers which withstand a relatively higher stress than does a single insulator of equal thickness without subdivisions.

For the mentioned values of κ and α we obtain by interpolation (drawing a line parallel to the β = const. curves to the curve $\alpha = \beta$), $\beta = 1{\cdot}88$.

The external diameter (sleeve dia.):

$$d_n = \beta d_0 = 1{\cdot}88 \times 50 = 94 \text{ mm}$$

The radial stress at the sleeve for an infinite number of foil inserts according to eq. (13):

$$\rho_e = \frac{E}{2} \frac{l_0 + l_n}{\log_e r_n/r_0} \frac{1}{l_n r_n}$$

$$= \frac{100}{2} \times \frac{686 + 200}{\log_e 1{\cdot}88} \times \frac{1}{200 \times 47} = 7{\cdot}46 \text{ kV/mm}$$

Without foil inserts (ordinary bushing), the maximum radial stress at the terminal (inside dia.) would be, according to eq. (19):

$$\rho_{r0} = \frac{E}{r_0 \log_e r_n/r_0} = \frac{100}{25 \log_e 1{\cdot}88} = 6{\cdot}34\,\text{kV/mm}$$

It is obvious that the insertion of metal foils is disadvantageous for this bushing, and to obtain an improvement it would be necessary either to decrease α or to increase κ. Increase of κ would necessitate a smaller diameter d_o, as the other values determining κ are constant (eq. 16), and this is not possible because of the current which has to flow through the terminal. The easiest way out is to decrease α by increasing l_n and keeping $l_0 - l_n$ constant, but not by making l_0 smaller.

U.S.A.

High Speed Trains—A Field for Gas Turbines

By W. A. GIGER, Consulting Engineer, Allis-Chalmers Manufacturing Company, Milwaukee, Wisconsin.

BEFORE the beginning of this century, that is, long before the aeroplane or the automobile offered serious competition to the railways, investigations were conducted into the possibility of adopting high speeds to trains. As far back as 1902, an experimental electric rail car was operated at 126 mph. While this speed may have since been exceeded during special runs, the fact still remains that the maximum station-to-station speed of modern streamlined trains amounts to about 70 to 75 mph.

Since the advent of the automobile and the tremendous expansion of commercial aviation after the second world war, these means of transport have become a real competitive consideration, mainly for passenger transport and, lately, also for light freight transport by the railways all over the world. The speeds and sizes of aircraft are continuously and rapidly increasing, as compared with the rather conservative attempts to boost speeds in railway passenger transport.

The railways, particularly on long-distance runs, are improving the service rendered to the travelling public, by providing faster and smoother transport, and more comfortable and more aesthetically equipped cars.

In order to regain a large part of the passenger business, train speeds should, however, be increased very materially, even over those now adopted by express trains. By the use of present-day propelling machinery and materials now available, which, in conjunction with aerodynamic shapes established theoretically and in wind tunnels, are transformed into new forms of locomotives and cars, it is, in the writer's opinion, possible to increase speeds substantially for trains operating over existing tracks still in good condition.

Various solutions for high-speed train operations have been proposed in years past, and new proposals are still being made from time to time. Without becoming too involved in details of these systems, a few of them are mentioned here.

A. MONORAIL TRAINS, STABILIZED BY GYROSCOPES.

For these trains it was claimed that the right-of-way and track construction would be cheap because only one rail is needed. Relatively sharp curves could be safely negotiated because the gyroscope would always give the vehicle the necessary natural banking and stabilizing force to keep it from jumping the track. One disadvantage of this system is that the vehicles must be held with special mechanisms to keep them from falling to the side if the gyros stop. Entirely new track systems would have to be built, which, considering the fact that standard two-rail tracks are now available, would be an immense handicap when trying to finance such a system and prove it to be economically satisfactory. An exchange of vehicles of standard track with the new system would be impossible.

A question of great importance would also be that concerning the kind of propelling system which should be used. Driving through the carrying wheels or by means of propellers, with an electric transmission system or by means of diesel engines or other prime movers, such as gas turbine mechanical or jet propulsion units, would have to be considered. The results of full-scale experiments which have been carried out with monorail gyro vehicles would not justify recommending the adoption of this system for large-scale high-speed train operation.

B. OVERHEAD MONORAIL RAILWAY SYSTEM.

Overhead monorail systems have been built and are in use for slow-speed operation with electric drive arrangements. Some promoters claim this to be one of the solutions for city transport and high-speed railway systems. Entirely new overhead rail systems would be necessary. The drive system would be approximately as under Section A, but also in this case costly development work would have to be undertaken before a satisfactory and economical high-speed system could be built.

C. TWO-RAIL SYSTEM WITH SPECIAL TRACK.

One such system, having two rails inclined at an angle of 30 degrees towards the centreline of the track, was developed some time ago, but not carried through to full-scale experiments. The wheels are tilted at the same angle and have quite high flanges reaching under the heads of the rails. The vehicle is thus claimed to be well protected against derailment. This railway system, which has been built and tested in models only, is claimed to be suitable for speeds of up to about 300 mph. Cars would be extremely light (aircraft construction) and would be operated preferably as single units at small time intervals. The driving system could be as mentioned in Sections A and B. Stresses in the track would be low on account of the light weight of the vehicles. This system, so far as the special track system is concerned, probably represents the nearest approach to the standard track system now used on railway main lines. Existing tracks could be changed over quickly and without unreasonable expense, but, again, vehicles of one system could not be used on the other tracks. Also, in this case, much development work would have to be undertaken to create satisfactory full-scale operating units.

D. DEVELOPMENT OF HIGH-SPEED VEHICLES FOR IMPROVED EXISTING TRACKS.

The system, which necessitates a minimum of experimental work and expenditure but which permits the least speed increase over existing speeds, is to use

existing tracks, improve them where necessary, and develop vehicles which can operate at higher sustained speeds than are now generally used.

The power necessary to move a railway vehicle (or a whole train) is dependent on the total train resistance and the speed at which it travels. The power requirement determines the space which has to be utilized for the propulsion machinery as well as its cost. This space cost and its operating expense compared with the useful space available for the transportation of passengers, and the revenue gained therefrom, largely determines the economy of the arrangement.

It is, therefore, very important that for very high speed vehicles the power required should be a minimum. Since the speed of a train and the gradients of the line are in most cases given by the time-table and the profile, the remaining elements, determining this required power equipment space, are the tractive resistance and the weight. To obtain minimum horsepower for a certain run, this tractive resistance and the weight should preferably be a minimum.

Because at high speed the air resistance becomes the major portion of the total train resistance, highly streamlined light-weight vehicles are needed.

A " passenger " vehicle has primarily to support the weight of the passengers and to provide shelter for them during operation. A certain amount of luggage weight and the equipment to provide heat, light and air conditioning must be included in the total weight, and if operated in a train, considerable traction and shock forces must be dealt with. At this point, attention should be directed to the method of designing new passenger vehicles which do not operate in compositions of existing cars. It may be advantageous to produce all auxiliary power required per car within the car structure itself, or it may be simpler, cheaper and more reliable to obtain this power from the locomotive or a special auxiliary power car.

Since passenger cars are sometimes involved in collisions, the Government requires that certain safety measures be provided to protect the passengers. These safety measures are such that the car must withstand a certain impact force without damage. The impact energy varies in direct proportion with the masses of the colliding bodies and with the square values of their speeds. Car bodies and car ends are, therefore, designed to be telescope-proof to withstand such forces. Low-weight cars must also be designed to give about the same safety factor and the impact forces used in the calculations must be determined as established by their weight and speed conditions.

Ultra-light passenger cars should not be operated in so-called standard car combinations; because of the great difference in their weight, they are at a decided disadvantage in the event of a collision.

One very effective means of increasing schedule speeds is to lower the centres of gravity of the locomotive and cars. This permits higher speeds around curves. Such an attempt, when combined with the lowering of the floor and roof lines, also reduces the cross-section of the vehicle. The reduced cross-sectional area again results in a lower air resistance of the vehicle. Reducing the cross-section of the passenger compartments also results in a lighter and cheaper car. All equipment suspended on the car underframe must be closed in carefully to present as smooth a surface as possible, and the front and tail ends of the train must be streamlined to reduce frontal air resistance and drag.

Skin friction is reduced by providing a smooth outside surface and by closing the openings between the cars. Because of the lower weight of cars and motive power units of such special design, the wear on the track and, above all, the stresses and misalignment created due to the passage of trains over the track will be greatly reduced. Needless to say, such lighter cars, having less deteriorating effect on existing tracks, result in lower maintenance costs.

In recent years, a new prime mover applicable to railways has been created, namely, the gas turbine. This machine is excellently suited for railway motive power. It contains no reciprocating parts and, therefore, operates very smoothly. In its simplest form, no water is needed, which is highly appreciated during summer and winter operation, and it consists of few types of parts as compared with other propulsion machinery now used.

Because the air resistance of a vehicle increases very rapidly when speeds of 70 to 80 mph and higher are contemplated, it is essential that for such high-speed trains, the total train resistance should be carefully studied.

The train resistance of a railway vehicle consists of many factors, i.e. :—

(1) those which are constant in relation to the speed.
(2) those which are a function of the first power of the speed.
(3) those which are a function of the second power of the speed.

Assuming the case of a vehicle operating on straight tangent track, its total resistance consists of the following components :—

(a) track and journal resistance.
(b) flange resistance.
(c) air resistance.

The resistance component which varies most is the air resistance. Since railway vehicles, locomotives, and cars in general are of very different designs, depending to a large extent on the time they were built and on the purpose for which they were to be used, we find many older vehicles designed with very little attempt to reduce air resistance. In most of these cases, no thought was given to the air resistance at all, and other supposedly more important considerations determined the design.

So-called efficient streamlining of a fast moving body is only possible if the smooth-flowing medium surrounding this body (air, water or gas) is not disturbed by other objects. This is the reason why the specific resistance of a body moving through air at some distance above the earth is lower than will ever be reached by a vehicle moving on rails. No matter how carefully all parts of high-speed railway vehicles are closed in, particularly those located under its body, such as bogies, air-brake equipment and air-conditioning and heating equipment, the presence of the bogies themselves, as the carrying medium of the vehicle, and the close proximity of the track, greatly disturbs the smooth flow of the air on that side of the vehicle and increases the total air resistance. Therefore, the air resistance of railway locomotives and cars varies greatly, depending on their general design and on the extent of streamlining.

For instance, a steam locomotive of current design, with all axles arranged comparatively close together, shows a different air resistance from an electric or diesel locomotive running on two widely spaced bogies, with the underframe between the bogies carefully closed in, representing a smooth surface to the air rushing along it. With the speeds of fast trains as they are to-day, streamlining has been carried out to various degrees. While it is true that streamlining of cars and locomotives can be carried very far in the interests of reducing air resistance, it is also true that the more streamlined a vehicle, the more difficult it will be properly to maintain it. For this reason, many locomotives, even for fairly fast schedules and with so-called streamlining of their boiler front, or body sections, are left entirely open on the sides of the driving wheels and other vital

parts, in order to make them readily accessible for inspection and maintenance (lubrication, adjustments, etc.). It is now quite clear that the higher the operating speed of a vehicle, or an entire train, the more valuable becomes the closing-in of all protruding parts or empty spaces between coupled vehicles, in order to avoid air disturbances.

Due to the various degrees of streamlining possible, the only way to determine the practical design limits as accurately as possible is to make air resistance tests in a wind tunnel with scale models of the real vehicle or train and the track.

While it is not within the scope of this article to enumerate the actual values of the components of train resistances of various kinds of railway vehicles and their combinations, in relation to the speed at which they travel, it may be mentioned that exhaustive tests and verifications of such tests, in actual service, have been carried out by numerous organizations and scientists.

AUSTRIA

Research into Boundary Lubrication

By I. MORGHEN. (From *Maschinenbau und Wärmewirtschaft*, Vol. 3, Nos. 4 and 5, April and May, 1948, pp. 57-61, and 75-78 respectively, 2 illustrations.)

ACCORDING to Newton's equation, friction in hydrodynamic lubrication depends only on the viscosity of the lubricant. If, however, oil film thickness is too small to establish hydrodynamic conditions, the importance of the viscosity recedes with respect to other " boundary" influences, determined mainly by the tear strength of the lubricant and bearing metal (force required to tear molecules out of the surface layers), by the viscosity, which, for very thin films, varies from point to point, and by the atmospheric pressure. The chemical affinity of lubricant and metal influences the tear strength; amorphous, highly viscous " corrosion " products may be formed, which favour lubrication. Friction heat may re-transform the amorphous Beilby layer of polished surfaces into the metallic state. Previous testing apparatus has not been sensitive enough to differentiate reliably between friction qualities of different lubricants. The author has designed a special instrument of great sensitivity for the normal friction range ($\mu = 0{\cdot}06$ to $0{\cdot}12$), giving reproducable results with an accuracy of $\pm\ 0{\cdot}001$ for the friction co-efficient. The instrument is based on the four-ball testing principle, with three steel balls constituting the bearing proper, whilst a fourth ball, loosely guided in a counter-bearing, is free to rotate and carries a small symmetrically constructed fan wheel. An air stream guided through two nozzles on to the fan wheel keeps the ball in slow constant rotation. The amount of air passing through the nozzles per minute is a measure of the force required to keep the ball just revolving against friction. Small disks placed on top of the fan wheel serve to vary the bearing pressure. The friction qualities of different lubricants under specified conditions and the influence of different friction factors can be measured very accurately with this instrument. These factors are:

Dry Friction. In spite of thorough cleaning, the balls do not show dry-friction values until after several revolutions. The friction value starts with $\mu = 0{\cdot}3$ to $0{\cdot}4$, increases to $0{\cdot}7$ after about 3 revolutions, then quickly approaches dry-friction values.

Ball Uniformity. Ten different ball pairings showed friction results straying by $0{\cdot}005$ (accuracy $\pm\ 0{\cdot}001$). New balls, therefore had to be calibrated with a neutral hydrocarbon oil. Measured friction values, referred to calibration values, could then be used to compare the frictions of different lubricants.

Change of Geometrical Shape. According to Hertz's equation, the spherical balls flatten out at the contact point, and wear further increases the diameter of the contact circle. The mean sliding velocity of normal balls was $^{3}/_{16}$ ips. Up to 600 revolutions, i.e., 30 minutes running time, friction does not change appreciably with dimensional changes due to wear. Friction with machine oil lubricant only increased from $\mu = 0{\cdot}101$ to $0{\cdot}106$.

Film Thickness. Friction can be measured during running in an oil bath or with well wetted balls (μ in the latter case increased by $0{\cdot}005$). Results with wetted balls were shown to be the most practicable; they also exclude viscosity influences. Very thin films, with oil centrifuged off, show different friction behaviour according to the lubricant used. Hydrocarbon oils show normal friction values up to 15 revolutions; μ then rises quickly. With fatty oils, μ already increases after 2/3 of a revolution and rises to dry-friction values. Fatty oils show a smaller starting-friction value than mineral oils, and also smaller friction values with thin films than with thicker films, i.e., friction at rest decreases with decreasing film thickness. Thin films are quickly destroyed, the more so with fatty oils than with mineral oils.

Gas Atmosphere. If films are very thin and temperatures high, the atmosphere may become important. Oxygen accelerates destruction of the film.

Change in Bearing Surface. Fatty oils tend to form deep grooves under conditions of wear; hydrocarbon oils, although showing a greater μ, lead to uniform smooth wear. μ also varies according to surface smoothness. Changes ranging up to $0{\cdot}01$ were noted when one oil was replaced by another after running-in.

Surface Roughness. Sand-blasted or etched balls show a friction increase by about $0{\cdot}035$. Results begin to stray to a greater extent.

Lubricant. Tests were conducted under 250 gram loads, at 20° C and at atmospheric pressure. Viscosity has no influence within certain limits. Outside these limits, μ increases and, for low-molecular lubricants, approaches dry friction. Contrary to conventional belief, " active " oils show no difference in friction qualities. Results were corroborated by tests on oils of very widely varying viscosity.

Load. μ is independent of the load within the limits of 50 to 1000 grams.

Temperature. Temperature influences are too small to be measured within the limits of 20 to 200° C.

Bearing Metals. Variations of μ for different bearing metals are of the same order of magnitude as those for different lubricants.

Stick-slip Motion. When running fast, especially with thin oils, the rotor assumes a peculiar " stick-slip " motion[2] attended with a singing noise and with lowered friction values. Since this is not a sliding motion proper, it should be avoided during normal running tests.

BIBLIOGRAPHY

(1) G. D. BOERLAGE, Four-ball testing, *Engineering* 136, 46 (1933) and 144, 1 (1937).

(2) MORGAN, MUSKAT, REED: Studies in Lubrication X, *J. appld. Physics* 12, 743 (1941).

A New Instrument for the Theoretical Determination of Stress Distributions in Flat Plates of Irregular Shape

By CH. MASSONNET. (From *Revue Universelle des Mines*, 9th Series, Vol. 5, No. 2, February, 1949, pp. 41-51, 22 illustrations.)

EXCEPT where the very simplest problems are concerned mathematical methods of stress analysis entail highly complicated arithmetical calculations and often insurmountable practical difficulties. A graphical and, if possible, mechanical method of determining stresses in flat plates of irregular shape under any loading would, therefore, be of great importance. The author has developed an instrument for such purposes.

I. *Theory.*

The principle of superposition of the effects of applied forces derives immediately from Hooke's Law. Any complex state of stress can, therefore, be regarded as being built up by the superposition of certain simple and known component states of stress. The fundamental component stress distribution may be, for example, the simple radial stress distribution in a flat disc (Fig. 1). Let b = unity be the thickness of the disc and let a force P [pounds per unit thickness] act

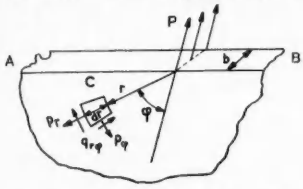

Fig. 1

on the horizontal straight face $A - B$ of the disc, which extends to infinity below that face. Let the force P be uniformly distributed over the thickness of the disc. The element C in the disc, at a distance r from the point of application of force P, then carries a direct radial stress

$$p_r = -\frac{2P}{\pi r}\cos\varphi,$$

where the angle φ is measured clockwise from the positive direction of force P. The direct circumferential stress p_φ and the shear stress q on the radial and circumferential faces of the element are zero. Hence p_r is a principal stress and the sum of the principal stresses at point C is

$$S = -\frac{2P}{\pi r}\cos\varphi$$

Let us now consider an element of unit thickness and of very small breadth dl stressed in simple tension by a force $p_r\,dl$ acting in direction 1_r (Fig. 2). A face,

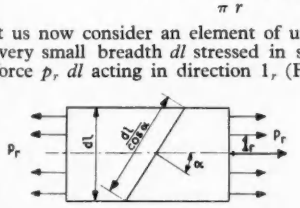

Fig. 2

the normal of which forms the angle α with the direction of applied tension, has a length $dl/\cos\alpha$ and the resultant stress on this face can be written in vector form:

$$\mathbf{F}_\alpha = p_r\cos\alpha = -\frac{2P}{\pi r}\cos\varphi\cos\alpha\times\mathbf{1}_r$$

where $\mathbf{1}_r$ is the unit stress vector in direction 1_r. This simple state of radial stress just described corresponds to the well known " isotropic region " of photo-elasticity, and can thus be shown to be a physical reality in flat discs. A superposition of several such simple states of stress will, therefore, also correspond to a physical reality in flat discs of any shape.

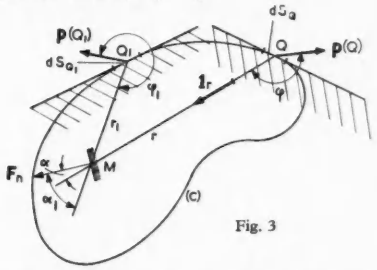

Fig. 3

Let us consider, further, a disc C of unit thickness subjected to external forces uniformly distributed along parts of the circumference (Fig. 3). A tangent to the circumference is drawn at point Q and the disc considered to extend indefinitely below this tangent. The elemental length ds_Q at point Q then forms part of both the disc circumference and the tangent, and carries the " fictitious " elementary loading $p(Q)\,ds_Q$. At every point of the disc (regarded as extending indefinitely below the tangent) a simple radial stress distribution will then exist, but the intensity of the stress will be infinitely small. Thus, at a point M of the disc, a face, the normal of which has the direction $\mathbf{F}_n$, will carry an infinitely small resultant stress which can be written in vector form:

$$d\mathbf{F}_n(p) = -\frac{2p}{\pi r}\cos\varphi\cos\alpha\times\mathbf{1}_r\,ds_Q$$

The sum of the principal stresses at point M will then be:

$$dS = -\frac{2p}{\pi r}\cos\varphi\,ds_Q.$$

At the point Q of the circumference, however, there will be a finite stress of direction and intensity $\mathbf{p}(Q)$. By similar reasoning, a fictitious loading $p_1(Q_1)\times ds_{Q_1}$ at point Q_1 will produce at point M (in a disc extending indefinitely below the tangent at Q_1) an infinitely small resultant stress on a face normal to the direction of $\mathbf{F}_n$:

$$d\mathbf{F}_n(p_1) = -\frac{2p_1}{\pi r_1}\cos\varphi_1\cos\alpha_1\,\mathbf{1}_{r1}\,ds_{Q1}.$$

If all the infinitely small stresses due to the loading along the whole of the circumference are superimposed, the resulting state of stress at point M can be expressed in vector form:

$$\mathbf{F}_n(p) = -\frac{2}{\pi}\int p(Q)\,\frac{\cos\varphi\cos\alpha}{r}\,\mathbf{1}_r\,ds_Q,$$

the integral extending over the whole length of the circumference. The sum of the principal stresses at M is then:

$$S(p) = -\frac{2}{\pi}\int p(Q)\,\frac{\cos\varphi}{r}\,ds_Q.$$

The problem may be simplified by dividing the disc circumference into segments of equal length Δs and by replacing the distributed loads by single loads con-

centrated at the centre of each segment. The integrals are thus transformed into ordinary sums and the stress produced on any small face inside the disc can be expressed as a vector:

$$\boldsymbol{B}(P) = \boldsymbol{F}_n \, \Delta s = -\frac{2\,\Delta s}{\pi} \sum_{\text{contour}} P \cos\varphi \, \frac{\cos\alpha}{r} \, \mathbf{1}_r \quad (1)$$

where the P values are the fictitious concentrated loads acting on the circumferential segments. The resulting error can be kept so small as to be negligible if the length of the segments is chosen correspondingly small. The sum of the principal stresses is then:

$$S(P) = -\frac{2\,\Delta s}{\pi} \sum_{\text{contour}} P \, \frac{\cos\varphi}{r} \quad .. \quad .. \quad (2)$$

The loads $p\,ds$ (or P) distributed over the circumference are each applied to a different semi-infinite disc limited only by the tangent at the corresponding point of the circumference. They have nothing in common with the actually applied, given, forces and have, therefore, been called "fictitious" loads. The state of stress inside the disc will thus correspond to a different external loading from that given. The problem remains of finding the particular distribution of fictitious loads which will result in internal forces (measured, e.g., in elements of material along the circumference of the given disc) which exactly balance the given external loads. Let us assume, e.g., a flat square plate subjected to simple tension (Fig. 4). Let the circumference be divided into 20 equal segments

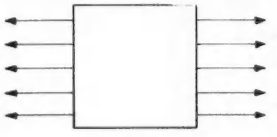

Fig. 4

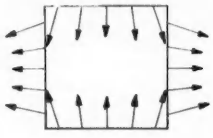

Fig. 5

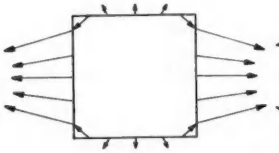

Fig. 6

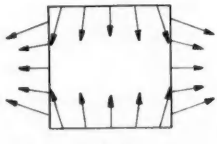

Fig. 7

and consider the *given* surface forces $\boldsymbol{T}$ as being fictitious concentrated loads $\boldsymbol{T}$, acting at various points R on segments of length Δs. These fictitious loads $\boldsymbol{T}$ produce internal forces $\boldsymbol{B}(T)$ on any element of material of the semi-infinite plate extending below the tangent to the circumference at R. An element Q situated at the circumference of the given disc will then be stressed (a) by a force $\boldsymbol{B}(T)$ due to the fictitious loads acting on all circumferential points other than Q and (b) by a force $\boldsymbol{T}$ due to the fictitious load externally applied at the surface segment Δs_Q. In general, the resultant internal force, $\boldsymbol{B}(T) + \boldsymbol{T}$, on the small boundary element at point Q will differ by an amount $\boldsymbol{B}(T) \neq 0$ from the *given* external force $\boldsymbol{T}$ at Q. If, therefore, a new and improved fictitious load distribution (Fig. 5) $\boldsymbol{P}_1 = \boldsymbol{T} - \boldsymbol{B}(T)$ is assumed, the resulting internal force on the element at Q will differ from the applied external force at Q by an amount $\boldsymbol{B}(P_1) < \boldsymbol{B}(T)$. A third approximation can then be made with a fictitious load distribution (Fig. 6) $\boldsymbol{P}_2 = \boldsymbol{P}_1 - [\boldsymbol{B}(P_1) + \boldsymbol{P}_1 - \boldsymbol{T}] = \boldsymbol{T} - \boldsymbol{B}(P_1)$. This procedure should be repeated until $\boldsymbol{P}_n$ does not differ any longer from $\boldsymbol{P}_{n-1}$, i.e., until $\boldsymbol{B}(P_{n-1}) = 0$. However, the result is not always determinate and consecutive approximations may, as shown in Figs. 4 to 7, fluctuate indefinitely about a mean

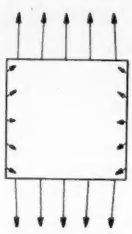

Fig. 8

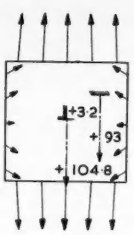

Fig. 9

Fig. 10

value. The corrections applied to successive approximations should, therefore, equal only half the errors $\boldsymbol{B}(T)$, $\boldsymbol{B}(P_1)$, etc. It can then be shown that the series converges mathematically for any given shape of the disc. Figs. 8 to 10 (replacing 5 to 7) illustrate this latter method and show that approximations converge rapidly. Two or three attempts give a satisfactory degree of accuracy. In Fig. 9 are indicated internal stresses at two points inside the disc, as calculated from the second approximation of the fictitious circumferential loading. Theoretically correct figures would be + 100 vertically, + 0 horizontally. The error is, therefore, small.

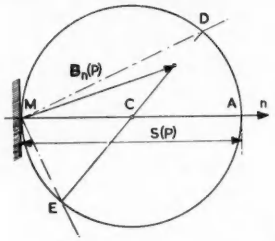

Fig. 11

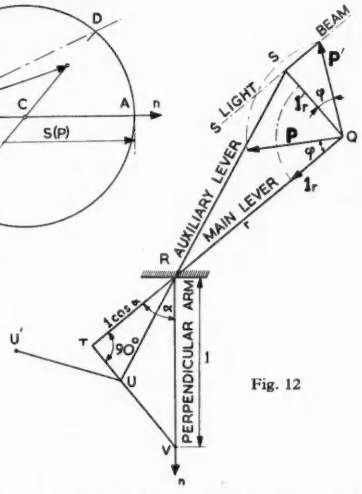

Fig. 12

Once the correct distribution of the fictitious loads has been obtained, the stresses at any point M inside the given disc are easily obtained. The vectorial sum $\boldsymbol{B}_n(P)$ of all the elementary induced stresses, eq. (1), represents the resultant stress on any given face of the element of material at point M, and the scalar sum $S(P)$, eq. (2), the sum of the principal stresses at that point. Mohr's stress circle can then be drawn as follows (Fig. 11): Let the face represented by hatched lines (point M) be the face to be considered, $MI = \boldsymbol{B}_n(P)$ the resultant stress vector from eq. (1), Mn the normal to the face. On Mn lay out the distance $MA = S(P)$ and draw a circle with MA as diameter and with C as centre. Draw line CI and project to intersections D and E with the circle. The circle is then Mohr's stress circle, MD and ME are the principal planes, and ID and IE are the values of the principal stresses. The state of stress is thus completely defined.

II. *Mechanical Conversion.*

Let $\boldsymbol{P}'$, $\mathbf{1}_r'$, $\boldsymbol{B}'$ represent the vectors $\boldsymbol{P}$, $\mathbf{1}_r$, $\boldsymbol{B}$ rotated clockwise through 90 degrees (Fig. 12). The device

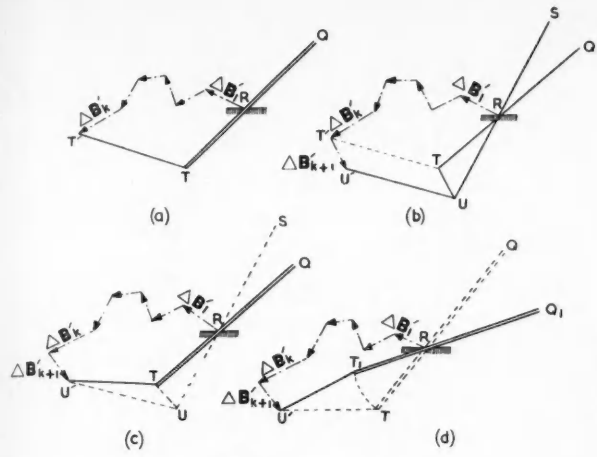

Fig. 13

to be described should then produce, firstly, the elementary vector at a point R :

$$\Delta B' = -\frac{2}{\pi} \Delta S \times P'(Q) \cos \varphi \frac{\cos \alpha}{r} \times \mathbf{1}_r',$$

secondly, the vectorial sum, and, thirdly, the scalar sum of the elementary vectors for all the fictitious loads along the circumference.

Let R be the point at which the state of stress is to be determined, and Q the point on the circumference of the given disc at which the elementary load $P(Q)$ is applied; then $QR = r$. The mechanism (see Fig. 12) consists of a main lever TRQ pivoting about point R, a slider Q carrying link SQ perpendicularly to RQ and sliding on RQ, a slider S sliding on SQ and carrying an electric bulb and special lens through which a narrow beam of light $S - S$ parallel to TRQ is projected onto a cardboard surface. If slider S is adjusted until the beam of light passes through the end point of vector P', then: $QS = P' \cos (\mathbf{P}', \mathbf{1}_r') = P \cos \varphi$. Link TV is fixed at T to a roller carrier travelling along TR and is constrained to slide through the fixed point V on Rn, i.e., the normal, at point R, to the face considered (hatched). Angle VTR always remains 90 degrees and if the fixed length VR is chosen equal to $2\,\Delta s_Q/\pi$, then:

$$RT = RV \cos \alpha = \frac{2\,\Delta s_Q}{\pi} \cos \alpha.$$

Finally, an auxiliary lever URS which also pivots about point R, is constrained to pass through point S, and carries at U a slider which may slide on TV as well as URS. Thus,

$$TU = \frac{QS \times RT}{QR}$$

and vector

$$\mathbf{TU} = -\frac{2\Delta s_Q}{\pi} \times P(Q) \cos\varphi \times \frac{\cos\alpha}{r} \times \mathbf{1}_r' = \Delta \mathbf{B}'$$

The actual apparatus has been designed for work on discs smaller than 320 mm (12·6 inches) across and with vectors $\mathbf{P}$ up to 100 mm (4 inches) length. Normal length of segment Δs has been assumed to be 60 mm ($2\frac{3}{8}$ in.); hence $RV = 120/\pi = 38{\cdot}197$ mm (about $1\frac{1}{2}$ in.). If another length Δs is chosen, the resultant vector $\Delta \mathbf{B}'$ varies proportionally if RV remains unchanged.

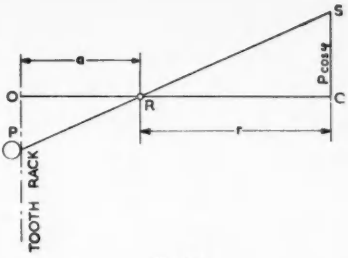

Fig. 14

For the summation of the various elementary vectors, eq. (1), a link UU' is pivoted at point U on the slider, but can be blocked in position by an electro-magnet at U so that angle TUU' remains constant. A roller carrier at U' may travel along UU' but can be blocked in position by a second electro-magnet at U'. It carries a needle at U' which is forced into the cardboard underneath the instrument by the action of a spring, but is drawn back when the magnet is energised. Suppose now the vectorial addition has been partially completed and the partial vector sum $\sum_1^k \Delta B'$ is represented by vector RT' (Fig. 13a). The following operations will then serve to add another elementary vector $\Delta \mathbf{B}'_{k+1}$ to the sum already completed:

(1) In the starting position, the levers QRT and SRU coincide and link UU' is in position TT' (Fig. 13a). A switch, arranged at point S of the device, is pressed and energises the two magnets. U' is thus blocked on link UU', the needle is withdrawn from the paper, and the link U' is blocked on slider U so that angle $U'UT$ remains constant.

(2) Lever URS is moved and adjusted so that the beam of light S–S passes through the end of vector P_{k+1}'. The link UU' then moves from position TT' to a new position UU' by simple translation and $T'U'$ is parallel and equal to TU (Fig. 13b), i.e., equal to $\Delta \mathbf{B}_{k+1}'$. RU' is then the new vectorial sum $\sum_1^{k+1} \Delta B'$. The addition has been made.

(3) Switch S is released, the magnets are de-energised, and the needle U' is pressed into the cardboard. Lever URS is then moved back to the position of lever QRT whilst point U' remains fixed on the cardboard and link UU' turns about point U (Fig. 13c).

(4) The levers QRT and URS are finally moved together to a new position Q_1RT_1 whilst U' still remains fixed. (Fig. 13d). The device is now ready for addition of the next elementary stress vector, due to the fictitious load at Q_1.

For the calculation of the scalar sum $S(P)$, according to eq. (2), the main lever QRT is extended to point O and the auxiliary lever SRU to P (Fig. 14). At O, a rack is fastened in a direction perpendicular to QRO, and at P, a pinion meshes with the rack and slides on lever SRP. The pinion carries a revolution counter which is coupled to the pinion when a third electro-magnet, arranged in series with the other two, is energised, i.e., during operations (1) and (2) described above. The connection is broken when switch S is released, i.e., during operations (3) and (4). The counter thus indicates a number of revolutions proportional to distance

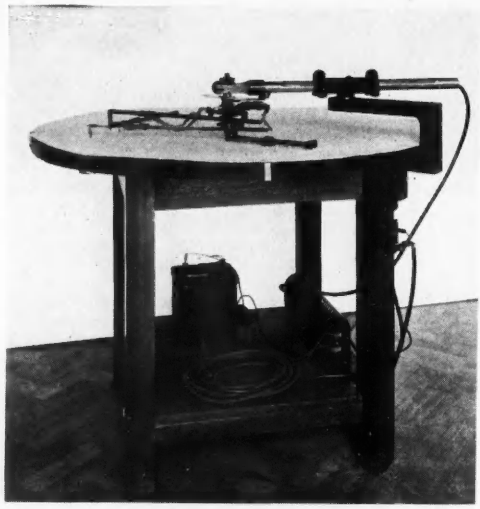

Fig. 15. **View of working table and suspension arrangement of instrument.**

$$OP = OR\frac{SQ}{RQ} = a\frac{P\cos\varphi}{r}$$

Length a and the diameter of the pinion are so chosen that the revolutions counted are proportional, on a scale of 5 units to 1 mm, to:

$$\Delta S\,(P) = \frac{2}{\pi}\,\Delta s \times \frac{P\cos\varphi}{r}.$$

During the operations mentioned, the scalar sum of the various $\Delta S(P)$ is thus formed automatically and can be read off the counter when summation over the whole circumference of the disc has been completed.

Although the operations described can be completed very easily and speedily, the design of the actual mechanism is rather complicated. It must be able to furnish the summation of the elementary stresses at any point inside the disc, i.e., the main lever must be able to rotate a full circle about its pivot. Any shape, convex or concave, of the circumference, any size and direction of the fictitious loads, any direction of the internal face to be considered, must be covered. However, the apparatus has been successfully built by the Metrology Department of Liège University and is shown in Figs. 15 to 17.

III. *Examples.*

Fig. 18 shows a three-branched hinge plate under the action of bending moments and certain forces, as well as the resulting fictitious loading. The resulting stresses in the interior of the plate, and at its circumference, are given in Fig. 19. Measurements on a model, with Huggenberger extensometers, agreed so well that it is not possible to say whether the small differences are due to errors in measurement or in mathematical approximation.

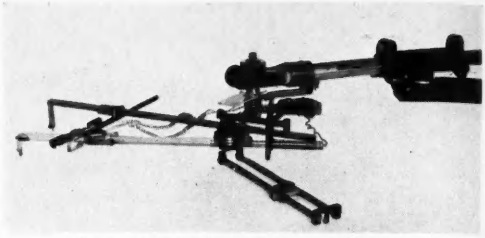

Fig. 16. **View of instrument assembled.**

Stresses in masonry dams can be calculated accurately by this method, even when taking into account the connection of the masonry with the underlying sub-soil.

The examples given so far are those of plain discs, without internal holes. If a plate contains internal holes, the stress distribution is no longer independent of the elastic constants of the material. The problems are then difficult to study by photo-elasticity, but can be solved by an extension of the mechanical methods indicated in this article. This method can equally well be applied when, instead of the circumferential

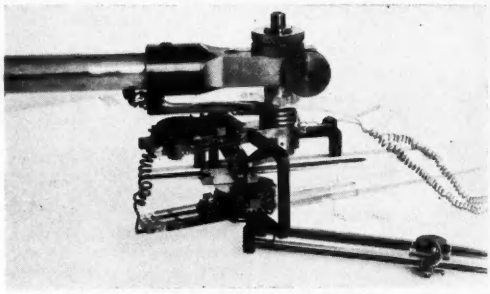

Fig. 17 **Detail of central mechanism.**

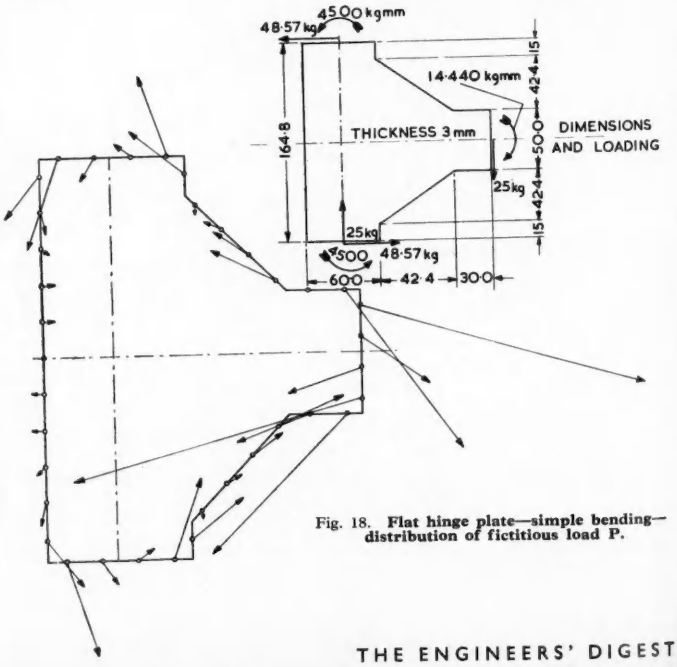

Fig. 18. **Flat hinge plate—simple bending—distribution of fictitious load P.**

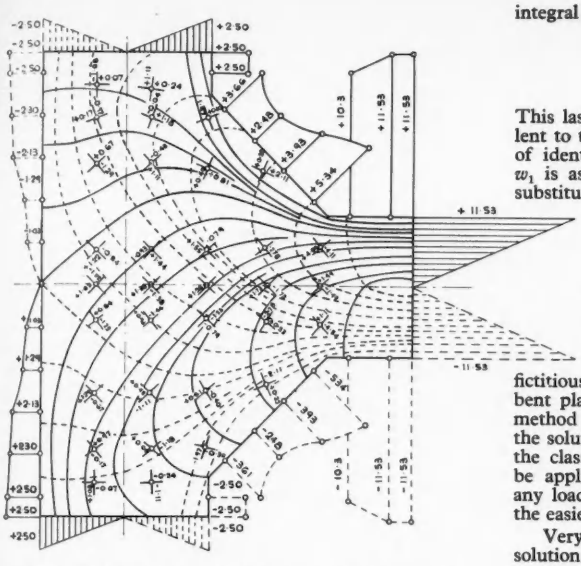

Fig. 19. **Simple bending—principal stresses and stresses at the circumference.**

loading, the circumferential displacements are given, or when partly displacements and partly loads are specified. In a prism compressed between plates without lubrication, the displacements are zero on the surfaces contacting the plates and the stresses are zero on the free surfaces.

The method also permits of studying stresses and deformations of flat plates bent by the action of transverse forces. The vertical displacement of any point of a horizontal plate under vertical transverse loading is given by

$$\Delta\Delta\, w = \frac{\partial^4 w}{\partial x^4} + 2\frac{\partial^4 w}{\partial x^2\, dy^2} + \frac{\partial^4 w}{\partial y^4} = \frac{p\,(x, y)}{D},$$

where $p\,(x, y)$ is the force per unit area exerted by the distributed loading and D the rigidity of the plate. The solution of this equation consists of a particular integral w_0 that can usually be found easily and a general integral w_1 satisfying the equation

$$\frac{\partial^4 w_1}{\partial x^4} + 2\frac{\partial^4 w_1}{\partial x^2\, \partial y^2} + \frac{\partial^4 w_1}{\partial y^4} = 0$$

This last equation, however, is mathematically equivalent to the one which would be obtained for a flat disc of identical shape under circumferential loading. If w_1 is assumed to be a certain stress function in this substituted problem, then the stresses at a point inside the fictitious flat disc would be

$$p_x = \frac{\partial^2 w_1}{\partial y^2}\ ;\ p_y = \frac{\partial^2 w_1}{\partial x^2};\ q_{xy} = -\frac{\partial^2 w_1}{\partial x\, dy}.$$

By determining these stresses, the stress function w_1 and, hence, the deflection of the bent plate can be found. The load to be applied at the circumference of the fictitious disc would depend on the way the actual bent plate is supported. The author has applied this method to a uniformly loaded built-in square plate and the solution found conforms closely to that obtained by the classical theory. The new method can, however, be applied equally well to discs of any shape under any loading, the problem of built-in plates being only the easiest for treatment by this method.

Very complex problems for which no method of solution has yet been found can be treated by the method described, such as stresses in discs of variable thickness, transverse bending of plates of variable thickness, and bending of discs under forces applied in the plane of the disc. Moreover, the scalar sum $S(P)$ giving the sum of the principal stresses at any point inside a flat disc satisfies the Laplace equation

$$\frac{\partial^2 S}{\partial x^2} + \frac{\partial^2 S}{\partial y^2} = 0.$$

Hence, the scalar summation alone will solve mechanically all those physical problems which lead to harmonic functions or, more generally, to functions of the form

$$\frac{\partial^2 f}{\partial x^2} + \frac{\partial^2 f}{\partial y^2} = g\,(x, y).$$

Some of these problems are: two-dimensional magnetic and electric fields; stable flow of fluids, heat, and electricity; filtration through permeable ground; torsion of beams and bending under shearing forces.

GERMANY

Fundamentals of Automatic Control

By W. OPPELT. (From "Fundamentals of automatic control," *Wolfenbütteler-Verlagsanstalt G.m.b.H.*, Hannover, 1947, 118 pp., 32 illustrations; "Graphical methods for complex multiplication," *A.E.Ü.*, Vol. 2, 1948, pp. 76-78, 4 illustrations; "New methods for assessing the stability of automatic control processes," *Die Technik*, Vol. 3, No. 7, July, 1948, pp. 312-314, 7 illustrations.)

(*Continued from June issue.*)

5. POSSIBILITIES OF CONNECTION OF CONTROLLER ELEMENTS

A considerable increase in the types of operations which can be performed is obtained by connecting various controller elements in series or in parallel. Parallel-connected elements can act in combination or in opposition. Furthermore, the polarity of the elements, i.e., their positive or negative swing, can be reversed without altering their orientation in the circuit. The frequency characteristics or transfer functions of the resultant controller blocks will now be determined.

Series or Cascade Connection: In series-connected elements, the input of the second element is the output of the first, so that

$$\varphi_{e2} = \varphi_{a1} \quad .. \quad .. \quad .. \quad (19)$$

and since $\varphi_{a1} = \varphi_{e1}\, \boldsymbol{F}_1\,(i\omega)$, and $\varphi_{a2} = \varphi_{e2}\, \boldsymbol{F}_2\,(i\omega)$, we have $\varphi_{a2}/\varphi_{e1} = \boldsymbol{F}_{1\times 2}\,(i\omega) = \boldsymbol{F}_1\,(i\omega)\, \boldsymbol{F}_2\,(i\omega)$ .. (19′) therefore, if

$$\varphi_{a2} = \varphi_{a2_0} e^{i a_2 t} \quad \text{and} \quad \varphi_{a1} = \varphi_{a2_0} e^{i a_1 t}$$

are the transient response functions corresponding to unit step disturbances φ_{e2} and φ_{e1}, the overall transfer function of the cascade connection will be

$$\begin{aligned} \boldsymbol{F}_{1\times 2}(i\omega) &= \varphi_{a1_0} e^{i a_1 t} \; \varphi_{a2_0} e^{i a_2 t} \\ &= \varphi_{a1_0} \varphi_{a2_0} e^{i(a_1+a_2)t} \qquad .. \quad (20) \end{aligned}$$

The locus of the overall transfer function can thus be obtained point by point, by adding the phase angles and multiplying the amplitudes of the two vectors φ_{a1} and φ_{a2} determined for the same frequency ω. The operation is simplified by taking the natural logarithms of φ_{a1} and φ_{a2}

$$w_{a1} = \log \varphi_{a1}, \quad w_{a2} = \log \varphi_{a2},$$

and plotting in the (u, iv) plane their phase angles α as ordinates v, against the logarithms of the amplitudes taken as abscissae, u, beginning with the value of w for which $(u, v) = (\log \varphi, \alpha) = 0$. The resultant locus of the overall transfer function is then obtained by drawing from the origin the vectors to points of the loci corresponding to the same value of ω, and determining the resultant vector by means of a " multiplication parallelogram." The curves can thus be added together to give the product curve (Fig. 16), and this method is particularly effective when the resultant locus for several identical series-connected elements is to be found, this being the logarithm of the n-th power of a complex function. The transfer function is finally obtained by plotting the function $\boldsymbol{F}_{1\times 2}(i\omega) = e^{w_{\text{res}}}$ A change in polarity of the cascade circuit is equivalent to changing the + or − sign of $\boldsymbol{F}_{1\times 2}(i\omega)$. The addition of a zero-order element $\boldsymbol{F}(i\omega) =$ const. causes a change in the scale (magnification) of the co-ordinate axes*.

The multiplication in the (u, v) plane is thus obtained by adding two corresponding vectors. The addition of $\boldsymbol{F}_1(i\omega)$, $\boldsymbol{F}_2(i\omega)$ can be achieved in two manners: (1) by conformal mapping of the (x, y) plane on the (u, v) plane, and addition of corresponding x and y values by themselves; (2) by mapping the (u, v) plane on the original (x, y) plane. In this second case, logarithmic spirals are obtained, since a straight line $u = c \times iv$ passing through the origin, will in the (x, y) plane, because $u = \log A$, be converted to the form $A = b^{icv} = b^{ica}$ which represents a logarithmic spiral passing through the point $(+1, 0)$. This leads, therefore, to the device with logarithmic spirals on a transparent rotatable disc, shown in Fig. 17, which enables the complex multiplication to be carried out directly on the (x, y) locus plane, without additional calculations.

Parallel Connections: In the case of parallel-connected elements, the input quantity is the same for all the elements, and the outputs are added together:

$$\varphi_{e1} = \varphi_{e2} = \varphi_e \qquad .. \qquad .. \quad (21)$$

$$\begin{aligned} \varphi_{a1} &= \boldsymbol{F}_1(i\omega)\, \varphi_{e1} = \boldsymbol{F}_1(i\omega)\, \varphi_e \\ \varphi_{a2} &= \boldsymbol{F}_2(i\omega)\, \varphi_{e2} = \boldsymbol{F}_2(i\omega)\, \varphi_e \quad .. \qquad .. \quad (21') \end{aligned}$$

so that

$$\begin{aligned} \boldsymbol{F}_{1\times 2}(i\omega) &= \varphi_a/\varphi_e = (\varphi_{1a} + \varphi_{2a})/\varphi_e \\ &= \boldsymbol{F}_1(i\omega) + \boldsymbol{F}_2(i\omega) \qquad .. \quad (22) \end{aligned}$$

The addition is obtained graphically by means of vector parallelograms for corresponding points (see Fig. 18). It will be noticed that phase-leads can occur even when only lag elements are used.

Branched Systems: When the input of an element is the sum of the outputs of two previous elements,

*Tables for complex multiplication have been developed by F. Reinhardt (" Tables for conversion from rectangular to polar co-ordinates," Siemens & Halske Report: Measuring devices for telecommunications engineering, Berlin, 1944). Reinhardt has also designed a cylindrical slide rule for complex multiplication (see " E.T.Z.", Vol. 69, No. 3, 1948).

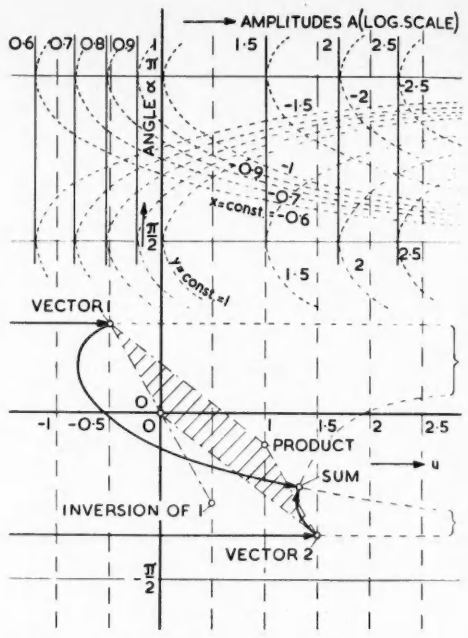

Fig. 16. **The $w = (u, iv)$ plane as a conformal representation of the $z = (x, iy)$ locus plane using the image function $w = \log z$.**

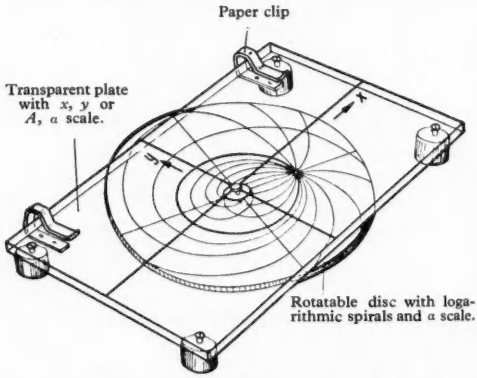

Fig. 17. **Apparatus for multiplication of complex numbers in the locus plane.**

then each of these inputs can be assumed to be going through the latter element independently, and the resultant output is then the sum of the individual outputs:—

$$\begin{aligned} \varphi_a &= \boldsymbol{F}(i\omega)(\varphi_{e1} + \varphi_{e2}) \\ &= \boldsymbol{F}(i\omega)\, \varphi_{e1} + \boldsymbol{F}(i\omega)\, \varphi_{e2} = \varphi_{a1} + \varphi_{a2} \quad .. \quad (23) \end{aligned}$$

Thus, for instance, in Fig. 1 the effect of the load disturbance σ on the controlled quantity φ is the same as that of an external force acting on the controlled unit, with an amplitude $\boldsymbol{F}_S(i\omega)\, \sigma$.

Opposite Connections: Oppositely-connected elements (with regenerative feedback) consist of parallel elements orientated in opposite directions. If the reversed or feed-back element is the second element, then the input of the first element will be the sum of

the network input and the output of the second element. Therefore the network output will be

$$\varphi_a = \mathbf{F}_1(i\omega)(\varphi_e + \varphi_{a2}) = \varphi_{a1} = \mathbf{F}_1(i\omega)\,\varphi_{e1} \quad .. \quad (24)$$

Furthermore, the output of the first element is both the input of the second and the network output; therefore

$$\mathbf{F}_2(i\omega)\,\varphi_{a1} = \mathbf{F}_2(i\omega)\,\varphi_a = \mathbf{F}_2(i\omega)\,\varphi_{e2} = \varphi_{a2} \quad .. \quad (25)$$

The transfer function of the parallel system with regenerative feedback is therefore

$$\mathbf{F}_{1-2}(i\omega) = \frac{1}{\dfrac{1}{\mathbf{F}_1(i\omega)} - \mathbf{F}_2(i\omega)} \quad .. \quad .. \quad (26)$$

It should be noted that this expression differs from that of a parallel network in which the polarity of one element has been changed; for instance, a change of polarity of the second element gives:—

$$\mathbf{F}_{1+2}(i\omega) = \mathbf{F}_1(i\omega) + (-\mathbf{F}_2(i\omega)) = \mathbf{F}_1(i\omega) - \mathbf{F}_2(i\omega).$$

The addition of rod or linkage displacements is achievable by means of differential levers, the addition of forces by allowing the forces to act at the same point. The addition of electric currents is generally obtained as an addition of ampere-turns in a transformer, relay or measuring instrument, or in a specially designed circuit.

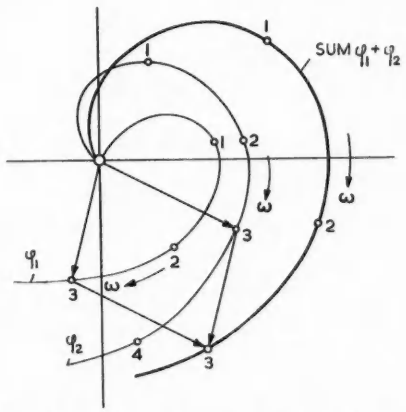

Fig. 18. **Addition of complex vectors for determination of locus of parallel elements.**

6. GRAPHICAL DETERMINATION OF CONTROLLER SYSTEM

Graphical methods for the solution of the differential equations of controller systems have been developed by O. Martin.* To determine a curve which is a function of time, the axis of the abscissae is subdivided into a number of time-intervals, which are taken as small as required for the accuracy of the representation. The curve is then constructed by referring to the initial conditions, and the plot of the output curve of the first network element is begun. The main point in the process is that each consecutive element is assumed to start moving by one time-interval later than the one preceding it in the circuit. Thus, the entire motion of each element can be determined step by step since the input quantity of each element is known, this being the output quantity of the preceding element for the previous time-interval.

*"Graphical controller dynamics," (Dissertation), Dresden, 1939, and Wiss. Ver. Siemens, Vol. 18, 1939, pp. 24-44.

7. SUBDIVISION INTO CONTROLLER AND CONTROLLED NETWORKS

The system can be subdivided into a controller and a controlled unit. The regulator elements r_n and the time-lag elements T_i of the controller are usually limited in number, and this also applies to the characteristic coefficients s_k of the controlled unit, so that most systems will still be covered if the restrictive assumptions are made:

$$T_i : i \leq 3;\ s_k : k \leq 2;\ r_n : -1 \geq n \geq +1 \quad .. \quad (27)$$

The controller network is then determined by its differential equation, transfer function, and transient function:

$$T_3\mu''' + T_2\mu'' + T_1\mu' + \mu = r_{-1}\int \varphi\,dt + r_0\,\varphi + r_1\,\varphi'$$

$$\mathbf{F}_R(i\omega) = \frac{r_{-1}(i\omega)^{-1} + r_o + r_1(i\omega)}{1 + T_1(i\omega) + T_2(i\omega)^2 + T_3(i\omega)^3} \quad (28)$$

$$\varphi_R(t) = \frac{1}{2\pi i}\int_{-\infty}^{+\infty} d\omega\,\frac{\mathbf{F}_R(i\omega)}{\omega}\,e^{i\omega t}$$

The corresponding equations for the controlled unit are

$$s\varphi'' + s_1\varphi' + s_0\varphi = -\mu$$

$$\mathbf{F}_S(i\omega) = \frac{-1}{s_0 + s_1(i\omega) + s_2(i\omega)^2} \quad .. \quad (29)$$

$$\varphi_S(t) = \frac{1}{2\pi i}\int_{-\infty}^{+\infty} d\omega\,\frac{\mathbf{F}_S(i\omega)}{\omega}\,e^{i\omega t}$$

8. OPEN-LOOP SYSTEMS

A control circuit can be cut open at any point, for instance between the controller and the controlled unit. The open system is easier to calculate, particularly with a sinusoidal excitation. The differential equation of the open-loop system is of the form

$$\Sigma\Sigma\, T_i s_k\, \varphi_a^{(i+k)} = -\Sigma\, r_n\, \varphi_e^{(n)} \quad .. \quad (30)$$

and with the restrictions defined by eq. (27) this gives

$$\left.\begin{aligned} &T_3 s_2\,\varphi_a^{(V)} + (T_3 s_1 + T_2 s_2)\,\varphi_a^{(IV)} \\ &\quad + (T_3 s_0 + T_2 s_1 + T_1 s_2)\,\varphi_a''' \\ &\quad + (T_2 s_0 + T_1 s_1 + s_2)\,\varphi_a'' \\ &\quad + (T_1 s_0 + s_1)\,\varphi_a' + s_0\,\varphi_a \\ &= -r_{-1}\int \varphi_e\,dt - r_0\,\varphi_e - r_1\,\varphi_e'. \end{aligned}\right\} \quad (31)$$

In the case of harmonic excitation, the various elements of the equations can be represented by vectors forming a vector polygon, in which the influence of each individual element can be assessed. The transfer function of the open-loop system is obtained with a series connection between the controller R and the controlled unit S by multiplying the corresponding transfer functions of these two networks:

$$\left.\begin{aligned} \varphi_a/\varphi_e = \mathbf{F}(i\omega) &= \mathbf{F}_R(i\omega)\,\mathbf{F}_S(i\omega) \\ &= -\Sigma r_n(i\omega)^n/[\Sigma T_i(i\omega)^i\ \Sigma s_k(i\omega)^k] \\ &= -\Sigma r_n(i\omega)^n/[\Sigma\Sigma T_i s_k(i\omega)^{(i+k)}] \end{aligned}\right\} \quad .. \quad (32)$$

and this is in fact equal to the ratio of the right-hand member to the left-hand member of eq. (31) after substituting $(i\omega)^m$ for d^m/dt^m and solving for φ_a/φ_e.

The system transient function $\varphi_{\ddot{u}}$ is obtained from eq. (32) as

$$\varphi_{\ddot{u}}(t) = \frac{1}{2\pi i}\int_{-\infty}^{+\infty} d\omega\,\frac{\mathbf{F}(i\omega)}{\omega}\,e^{i\omega t} \quad .. \quad (33)$$

If the input quantity is not a unit step function but any given function, then this latter function can be resolved into a number of step functions, each of which begins at an instant t_x and has a corresponding transient response function. The time-variant output $\varphi_a(t)$ is then the sum of these individual transient functions, and it can be calculated as a Duhamel integral:

$$\varphi_a(t) = \frac{d}{dt} \int_{t_x=0}^{t} dt_x \, \varphi_{\ddot{u}}(t_x) \, \varphi_e(t - t_x) \quad .. \quad (34)$$

This Duhamel integral also enables the transient function $\varphi_{\ddot{u}}(t)$ of the open-loop system to be determined, when the transient functions $\varphi_R(t)$ of the controller, and $\varphi_S(t)$ of the controlled unit are known. We then have

$$\left.\begin{aligned} \varphi_{\ddot{u}}(t) &= \frac{d}{dt} \int_0^t dt_x \, \varphi_S(t_x) \, \varphi_R(t - t_x) \\ &= \frac{d}{dt} \int_0^t dt_x \, \varphi_R(t_x) \, \varphi_S(t - t_x) \end{aligned}\right\} \quad (35)$$

9. CLOSED-LOOP SYSTEMS

When the terminals of the open-loop system are connected together, the input and output quantities become equal: $\varphi_e = \varphi_a = \varphi$. Therefore eq. (31) becomes

$$\Sigma\Sigma T_i s_k \varphi^{(i+k)} + \Sigma r_n \varphi^{(n)} = 0 \quad .. \quad (36)$$

and since in this case $\boldsymbol{F}(i\omega) = \varphi_a/\varphi_e = 1$, we have

$$\boldsymbol{F}_R(i\omega)\,\boldsymbol{F}_S(i\omega) = 1 \quad .. \quad .. \quad .. \quad .. \quad (37)$$

$$-\Sigma r_n (i\omega)^n / [\Sigma T_i (i\omega)^i \, \Sigma s_k (i\omega)^k] = 1$$

or $$\Sigma T_i (i\omega)^i \, \Sigma s_k (i\omega)^k + \Sigma r_n (i\omega)^n = 0 \quad .. \quad (38)$$

Furthermore, the transient function of the system becomes

$$\varphi(t) - \frac{d}{dt} \int_0^t dt_x \, \varphi_{\ddot{u}}(t_x) \, \varphi(t - t_x) = 0 \; .. \quad (39)$$

or if φ_R and φ_S are used

$$\varphi(t) - \frac{d}{dt} \int_0^t \left\{ \frac{d}{dt} \int_0^t dt_{x_1} \, \varphi_S(t_{x_1}) \, \varphi_R(t - t_{x_1}) \right\} \times \varphi(t - t_{x_2}) \, dt_{x_2} = 0 \quad .. \quad .. \quad .. \quad (40)$$

An example illustrating the use of Duhamel integrals is given at the end of this article. The most appropriate way of solving integral equations such as eq. (40) is by employing Laplace transformations of the types

$$z_u(p) = \int_0^\infty dp \, z(t) \, e^{-pt},$$

and $$z_{1u}(p) \, z_{2u}(p) = \int_0^t dt_x \, z_1(t_x) \, z_2(t - t_x).$$

10. REFERENCE-DATUM CONTROL ELEMENTS

The relation in this case is

$$\varphi_e = \varphi_a - \psi \; .. \quad .. \quad .. \quad (41)$$

where ψ is the reference datum. The differential equation is then of the same type as eqs. (31) and (36), but with additional terms in ψ (terms with r_{-1}, r_0, and r_1), so that

$$\Sigma\Sigma T_i s_k \varphi^{(i+k)} + \Sigma r_n \varphi^{(n)} = \Sigma r_n \psi^{(n)} \; .. \quad (42)$$

This equation enables some of the typical features of the deviations under equilibrium conditions to be determined. As then all the derivatives vanish, we have

$$\varphi_{Gl}/\psi_{Gl} = r_0/(s_0 + r_0) \text{ when } r_{-1} = 0$$

$$\varphi_{Gl}/\psi_{Gl} = 0 \text{ when } r_{-1} \neq 0;$$

where the subscript *Gl* denotes equilibrium conditions. The transfer function is then (see Fig. 1 and eqs. (26) and (41)):

$$-\boldsymbol{F}_\psi(i\omega) = \frac{\varphi}{-\psi} = \frac{1}{\dfrac{1}{\boldsymbol{F}(i\omega)} - 1} \quad .. \quad (43)$$

where $\boldsymbol{F}(i\omega)$ is the transfer function of the open-loop system. Substituting in eq. (43) the value of $\boldsymbol{F}(i\omega)$ determined by eq. (32) gives

$$\boldsymbol{F}_\psi(i\omega) = \Sigma r_n (i\omega)^n / [\Sigma r_n (i\omega)^n + \Sigma s_k (i\omega)^k \, \Sigma T_i (i\omega)^i] \quad (44)$$

Conversely, if $\boldsymbol{F}_\psi(i\omega)$ is known, the transfer function of the open-loop system can be obtained from

$$\boldsymbol{F}(i\omega) = 1 \Big/ \left[1 - \left\{1/\boldsymbol{F}_\psi(iw)\right\}\right] \quad .. \quad (45)$$

Eq. (45) is useful in practice if the open-loop circuit is unstable so that its behaviour cannot be determined by direct measurements. Loci of the reference-datum transfer function can also be plotted. However, $\boldsymbol{F}_\psi(i\omega)$ can be obtained directly from the $\boldsymbol{F}(i\omega)$ locus of the open circuit by virtue of eq. (41), as shown in Fig. 19, the reference-datum being then determined as the vector connecting the input φ_e to the output quantity φ_a. The transient function is

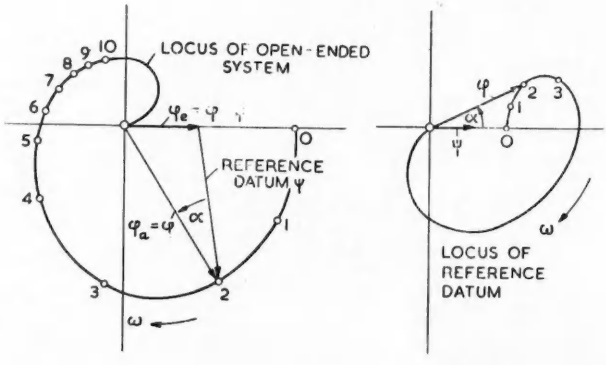

Fig. 19. **Determination of locus of reference-datum from locus of open-ended system.**

$$\varphi(t) - \frac{d}{dt}\int_0^t dt_x\, \varphi_{\ddot{u}}(t_x)\, \varphi(t-t_x)$$

$$= -\frac{d}{dt}\int_0^t dt_x\, \varphi_{\ddot{u}}(t_x)\, \psi(t-t_x) \quad .. \quad (46)$$

the left-hand side of this equation is the integral equation of the closed-loop circuit.

11. LOAD DISTURBANCE

To consider the effect of the load disturbance σ on the controller output μ_R, it is necessary to subdivide the system into a controller R and a controlled network S. The effective output μ_S is then

$$\mu_S = \mu_R - \sigma \quad .. \quad .. \quad .. \quad (47)$$

the negative sign of σ indicating that the disturbance is assumed to reduce the effect of the controller output μ_R on the controlled quantity φ. The differential equation of the disturbed control system is therefore

$$\Sigma\Sigma T_i\, s_k\, \varphi^{(i+k)} + \Sigma r_n\, \varphi^{(n)} = \sigma + T_1\sigma' + T_2\sigma'' + T_3\,\sigma''' \quad (48)$$

Control Factor: Eq. (48) can be applied to obtain some information regarding the deviations of the controlled quantity from the equilibrium condition. As the derivatives then vanish, we have

$$\left.\begin{array}{ll} \varphi_{GI}/\sigma_{GI} = 1/[r_0 + s_0] & \text{when } r_{-1} = 0, \text{ and} \\ \varphi_{GI}/\sigma_{GI} = 0 & \text{when } r_{-1} \neq 0 \end{array}\right\} \quad (49)$$

Eqs. (49) show that the inclusion of an integral term r_{-1} in the input-control elements has the advantage of eliminating deviations after the control process is in operation. These equations also show that there are some controlled units which even without a controller tend to seek a new state of equilibrium after a disturbance. Controlled networks of this type are known as "*static*" networks, and are characterised by the condition: $s_0 \neq 0$; whereas $s_0 = 0$ denotes "*astatic*" controlled networks. For static networks we can define the "control factor" R:—

$$R = \varphi_{GI}/[\varphi_{GI} - \varphi^*] \quad .. \quad .. \quad (50)$$

where $\varphi^* = \varphi$ without the controller. The control factor is thus the ratio of the deviations of the system with and without the controller network. After substitution in eqs. (49) the control factor can be expressed by means of the magnification V of the open-loop circuit; and since according to eqs. (4) and (32): $V = V_R V_S$ (magnifications of the controller and the controlled unit), we have

$$R = 1/[1 + V] = 1/[1 + (V_R V_S)].$$

The transfer function $\boldsymbol{F}_\sigma(i\omega)$ of the system with load disturbance is given by

$$-\boldsymbol{F}_\sigma(i\omega) = \frac{\varphi}{-\sigma} = \frac{\varphi}{\mu_S}\frac{\mu_S}{-\sigma} = \frac{\varphi}{\mu_S}\frac{\mu_S}{\mu_S - \mu_R}$$

$$= \frac{\varphi}{\mu_S}\,\frac{1}{1-(\mu_R/\mu_S)} \quad .. \quad .. \quad .. \quad (51)$$

since $\mu_R/\mu_S = \boldsymbol{F}(i\omega) =$ transfer function of the open-loop system

$$-\boldsymbol{F}_\sigma(i\omega) = \boldsymbol{F}_S(i\omega)/[1 - \boldsymbol{F}(i\omega)] \quad .. \quad .. \quad (52)$$

and as $\boldsymbol{F}(i\omega) = \boldsymbol{F}_S(iw)\,\boldsymbol{F}_R(i\omega)$ we can write

$$-\boldsymbol{F}_\sigma(i\omega) = \boldsymbol{F}_S(i\omega)/[1 - \boldsymbol{F}_R\boldsymbol{F}_S] = 1/[(1/\boldsymbol{F}_S) - \boldsymbol{F}_R]$$

$$= 1/[\boldsymbol{F}_R\{1/\boldsymbol{F}(i\omega)\} - 1] \quad .. \quad .. \quad (53)$$

On substitution we obtain

$$\boldsymbol{F}_\sigma(i\omega) = \Sigma T_i\,(i\omega)^i/[\Sigma r_n\,(i\omega)^n + \Sigma T_i\,(i\omega)^i\,\Sigma s_k\,(i\omega)^k]$$

The various transfer functions are therefore all related to one another, so that they can be determined by either direct or indirect measurements. Thus,

$$\left.\begin{array}{ll} \boldsymbol{F}_S(i\omega) = -\boldsymbol{F}_\sigma(i\omega)/[1 - \boldsymbol{F}_\psi(i\omega)] & \\ \text{and} \quad \boldsymbol{F}_R(i\omega) = \boldsymbol{F}_\psi(i\omega)/\boldsymbol{F}_\sigma(i\omega) & \end{array}\right\} \quad (54)$$

The load disturbance σ can also be determined as a vector $\sigma = \mu_R + \mu_S$ from the loci of the controller and the controlled unit. The transient function is

$$\varphi(t) = \frac{1}{2\pi i}\int_{-\infty}^{+\infty} \frac{dw}{\omega}\,\frac{\boldsymbol{F}_S(i\omega)}{\boldsymbol{F}(i\omega) - 1}\, e^{i\omega t} \quad .. \quad (55)$$

If instead of $\boldsymbol{F}_S(i\omega)$, the transient functions of the open loop system $\varphi_{\ddot{u}}$ and of the controlled unit φ_S are given, then

$$\varphi(t) - \frac{d}{dt}\int_0^t dt_x\, \varphi_{\ddot{u}}(t_x)\, \varphi(t-t_x)$$

$$= \frac{d}{dt}\int_0^t dt_x\, \varphi_S(t_x)\, \sigma(t-t_x) \quad .. \quad (56)$$

(To be concluded)

Sonic and Ultrasonic Dust and Smoke Precipitators

(From *The Iron Age*, Vol. 163, Nos. 14 and 15, April 7, 1949, p. 104, and April 14, 1949, p. 88.)

At a recent meeting of the American Chemical Society in San Francisco, Dr. H. W. St. Clair, of the U.S. Bureau of Mines Eastern Experiment Station, College Park, Maryland, stated that powerful sound generators, with frequencies of 5,000 to 50,000 cps, have been developed, which are capable of removing dust, smoke and other particles from the air. Utilisation of the effect is practical on an industrial scale.

Excitation at frequencies above 18,000 cps results in an increased rate of collisions between particles, and the kinetic effects due to particle rotation and other factors cause the particles to agglomerate in thin cohesive wafers at intervals equal to one-half of the wavelength of the sound produced. The agglomeration time, depending on particle size and concentration, varies from 2-3 to 10-15 seconds, and the wafers formed then settle out of the atmosphere. The intensity of the sound generated is sufficient to maintain lead shot in suspension in the air, and the method has been successfully used to clear tubes filled with smoke, fogs of oil and water, quartz dust, and other pollutants.

Further details regarding equipment used for similar work were given by H. W. Danser and E. P. Neumann, of the Ultrasonic Corporation, Cambridge, Massachusetts. The high-intensity ultrasonic generator produced by this Corporation is a siren-type unit. One generator has been completed for the recovery of fine sulphuric acid fog particles carried in the exhaust stacks of an acid manufacturing plant. It is now possible to produce units large enough to treat 10,000-100,000 cubic feet of gas per minute, and particles are agglomerated without fire hazard, regardless of temperature and electric charges. Visible fine particles smaller than one twenty-five thousandth of an inch in diameter can be recovered or captured, and even particles of less than 0·01 microns in diameter have been readily agglomerated. Ultrasonic agglomeration is said to be more economical than other methods, and ultrasonic dust control systems are expected to have a wide range of industrial applications.

DESIGN TRENDS AND E
OF MACHINE TO

By TIBOR HAAS, A.M.I.MECH.E., A.F.

LATHES—PART

General

MACHINE tools represent the most important equipment for industrial production, and, therefore, their quality is of the utmost significance for the national economy of any country. Their function being to produce machined parts, they are factory equipment, not show-pieces. Yet their good appearance in addition to functional perfection is indirectly of great economic value, inasmuch as a good "clean-lined" appearance in machine tools is suggestive of quality and, consequently, tends to give the operatives a feeling of pride in their work. They will also show partiality for a good-looking machine tool and will look after it more carefully.

Meticulous care in the grouping of functional units results in a number of advantages, such as reduced fatigue, with consequent reduction of accident risk while unbroken lines and smooth surfaces facilitate cleaning and are thus conducive to both higher machining accuracy and increased life of the machine tool itself.

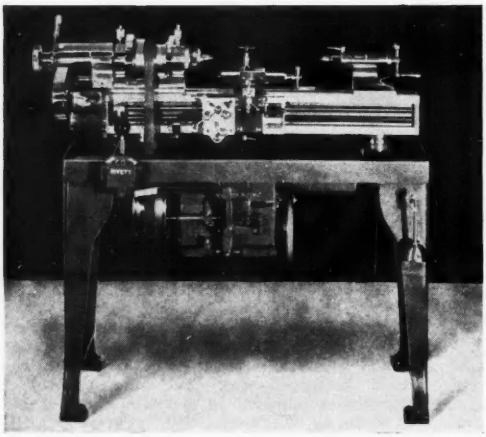

Fig. 1. **Rivett lathe, old design.**

The lathe was the earliest type of machine tool. It still remains the one in most general use and to-day represents the most versatile tool in the machine shop. From its primary uses for turning and screw-cutting, it has been adapted for drilling[1], boring, milling, grinding and other operations.

Design for Appearance

The appearance of early lathes was characterised by the crude features present in all machines in their initial stages of evolution, such as exposed step-pulleys and mechanisms, out-of-reach and often inaccessible controls, and unwieldy legs. Later, with the introduction of the single-pulley drive, some attempts were made to improve appearance, but these were only tentative and did not result in the integration of the functional units. The outward contours still followed the loosely grouped functional units, particularly the gears, and presented a rather irregular appearance.

Around the thirties, a start was made in cleaning up the appearance of machine tools, resulting in an improvement of form achieved by attention to detail and an integration of the functional groups. However, this left much to be done at a later stage, as a logical development of the first stage.

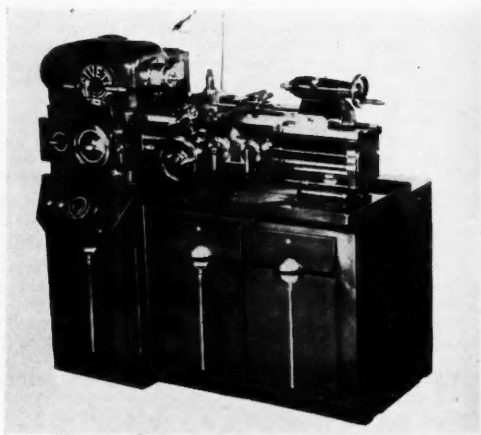

Fig. 2. **Rivett lathe, re-designed.**

The present-day objectives of aesthetic design as applied to machine tools can best be demonstrated by reference to an example of re-design of an obsolete lathe following the principles of modern industrial design. Fig. 1 shows a Rivett lathe which, although the forerunner of the contemporary type, still had too many exposed mechanisms, giving the impression of complexity and awkwardness in operation. The lathe of Fig. 2 is a re-design carried out by Designers for Industry, Inc., Cleveland, Ohio, and although this machine is now a few years old, it already has an improved disposition of controls which facilitates operation and not only gives the impression of compactness but also reveals careful thought in the lay-out of data plates and gauges which we have come to regard as basic requirements of good design.

Taking the lathe as a "theme", an infinite number of variations on the basic form is possible. However,

notwithstanding the existence of different schools of thought and national characteristics, the contemporary industrial designer will aim at improving the utility, safety and ease of maintenance of the lathe. He will succeed in his task only if he is able to combine with each such improvement a harmony of form and a balance of often contradictory specifications. As in every product design, the appearance of machine tools is greatly enhanced by proper surface treatment, comprising colour, texture and quality. The question of colour being extremely important in machine tools from the human aspect, this subject justifies separate treatment in an independent article.* Apart from the fact that colour can be used as an aid in the unification of a complex form, it has special significance as regards the fatigue of the machine operator and must be considered in conjunction with the colours of the surroundings; colour codes have lately been developed in several countries. As to surface texture and quality in machine tools, it will be appreciated that smooth surfaces can easily be kept clean and are conducive to accuracy and ease of maintenance. An example of good surface treatment is that used in the Monarch lathe, Fig. 3; this machine is coated with an oil-resistant enamel which retains its appearance and protective qualities under machine shop conditions, but to avoid glare, an "egg-shell" finish is preferable to a glossy coating. This lathe is also in other respects a representative example of modern industrial design as practised in the United States. It will be noted that the headstock, traverse gear, Norton gear and leg are combined into a single body. This is not only suggestive of sturdiness

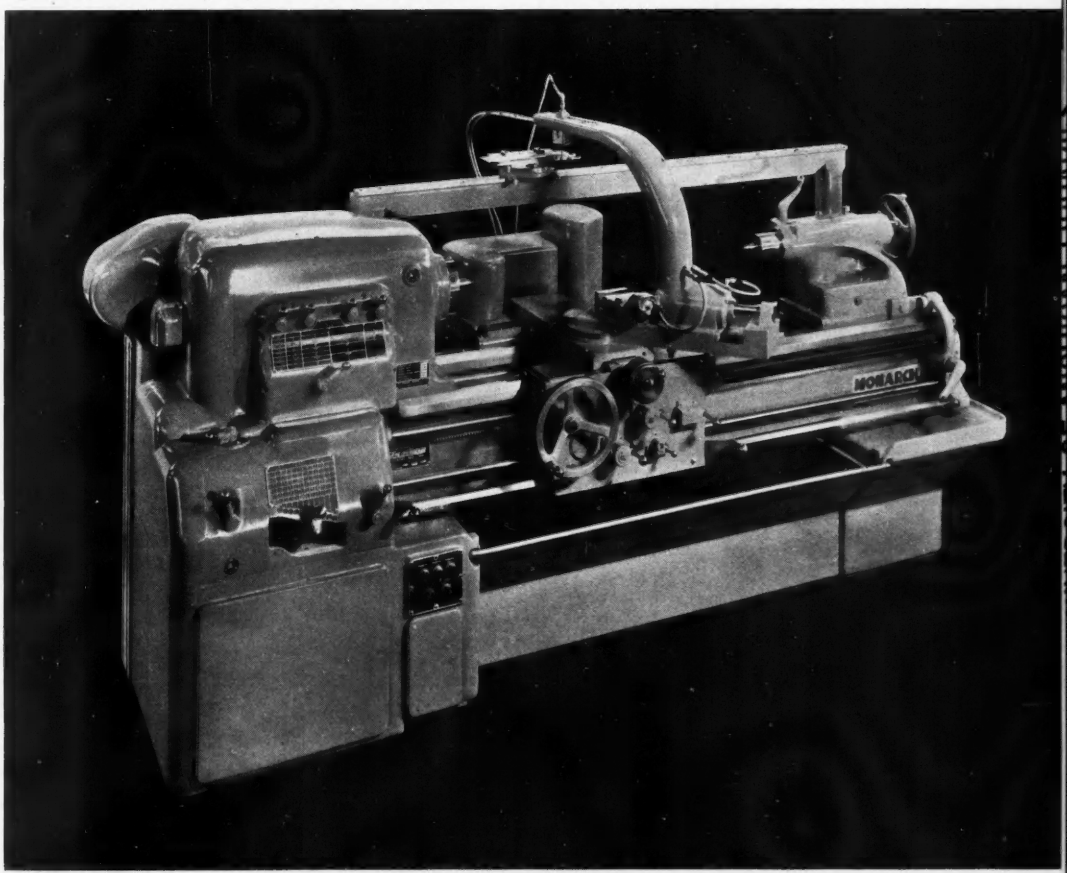

Fig. 3. **The Monarch lathe, one of the latest American designs.**

*Such an article is under consideration.—EDITOR, E.D.

Fig. 6. **The Loewe lathe (Ludwig Loewe & Co., A.G., Berlin), a representative example of modern trends in Germany.**

with rounded-off corners. A full size mock-up is built before deciding the final radii of the corners, because the correct amount of curvature in relation to other dimensions must be carefully tried out to achieve distinctive appearance. Such mock-ups are necessary in any case to test the control arrangements with a view to reducing operator fatigue to a minimum. The German idea is that aesthetics in engineering is dictated solely by functional objectives[2]. They insist that non-functional streamlining is a perversion of taste. In other words, a machine so designed that it is functionally perfect will not necessarily have a pleasing appear-

and of what the Americans term " operator assurance," but, due to the box-shaped legs, also results in greater rigidity and stability. Contrary to former designs, in which the

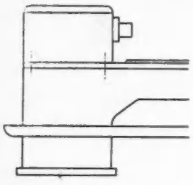

Fig. 4. **Horizontal division.**

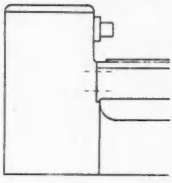

Fig. 5. **Vertical division.**

Figs. 4 and 5. **Schematic representation of headstock end of lathes.**

lathe had a horizontal division (Fig. 4), the integration of all gear castings with the leg results in a vertical division (Fig. 5). For a German parallel to the Monarch, the Loewe

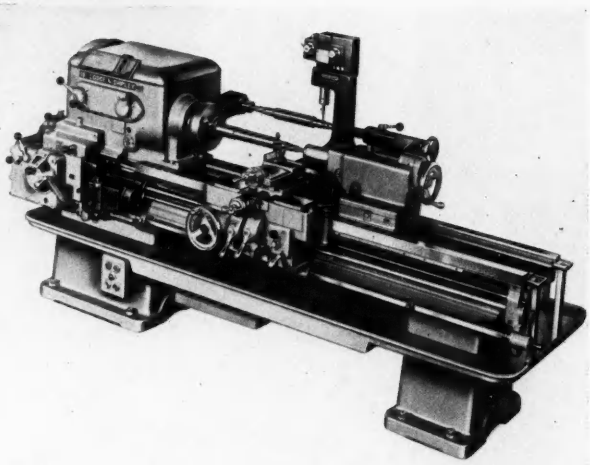

Fig. 7 (left). **LeBlond tool room lathe.**

Fig. 8 (above). **Lodge and Shipley lathe, standard model X, fitted with " Copymatic " copying attachment.**

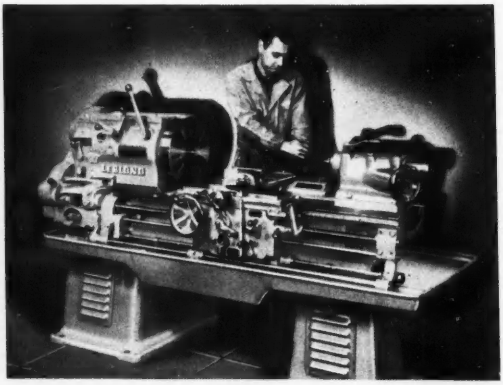

lathe could be quoted as a representative example of modern trends in Germany (Fig. 6). This lathe also conforms to the vertical division shown schematically in Fig. 5. The most striking difference between these two conceptions lies in the American preference for curvilinear shapes, while the Germans tend to keep to rectilinear shapes for the principal lines and are satisfied

ance, but it is the prevalent German view that " streamlining " in the American sense will not improve appearance. It follows that the Germans have no use for the stylist as a designer for appearance, and they consider aesthetics as applied to machines to be the province of the functional designer, that is to say, the engineer.

They argue that there is no yardstick for beauty; if the engineer cannot appreciate it, why should he recognise the outsider as a critic of taste, whose criteria may be alien to the engineer's outlook ? If we understand it rightly, this opinion could best be summarised by the following statement : A machine provided with non-functional embellishments, even if these do not detract from its functional perfection, cannot be considered an improvement from the aesthetic point of view.

It appears that the industrial designer as known in England and America exists neither in Germany nor in most of the other Continental countries. However, aesthetic design in machines is not neglected. In fact, the Continental technical Press indicates great interest in this aspect of engineering. The value of the Consultant Designer is clearly recognised there to represent a more detached viewpoint and broader interest than

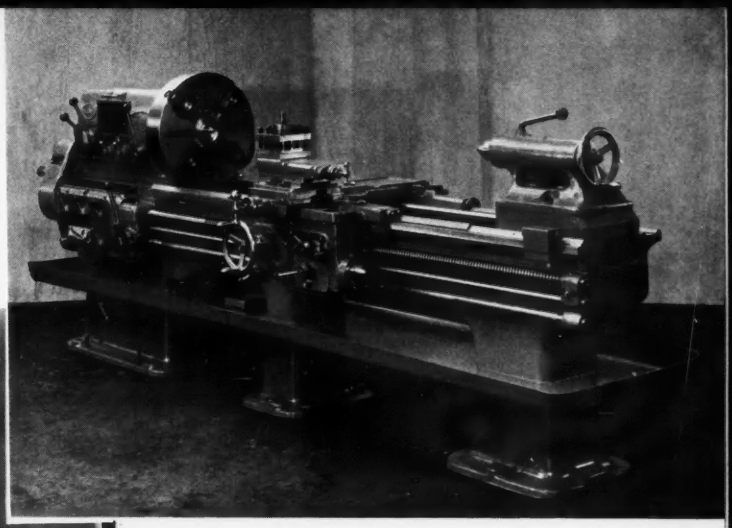

Fig. 9 (right). **VDF-Standard lathe, type V3 (Vereinigte Drehbank-Fabriken, Hamburg).**

Fig. 10 (below). **Reiden lathe, type T185 (Maschinen & Werkzeug Fabrik A.G., Reiden, Switzerland).**

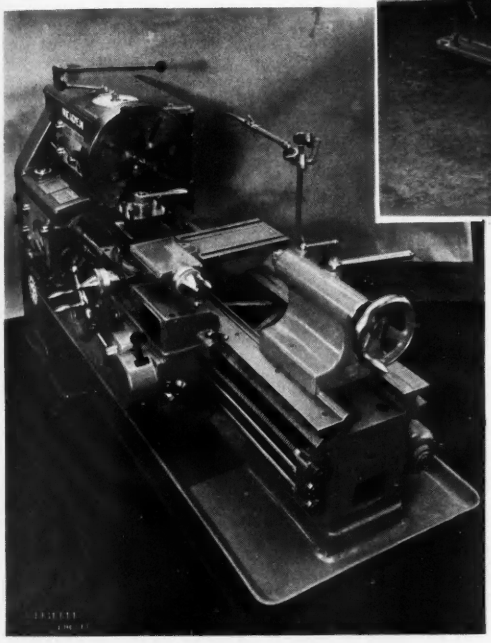

engineering personnel not having the same wide circle of interests. This professional man, who is generally a graduate engineer, may well have great influence on aesthetic problems of engineering design, but it may well be assumed that he will be inclined to dictate his own views rather than accept what the public may think a better-looking machine.

This outlook, let us call it "the Continental outlook," puts the criteria of aesthetic design in engineering at the same level as those of the visual arts. One does not expect the artist to create what the public likes. It might, of course, happen that the public likes what the artist creates.

The Americans regard the Industrial Designer as an artist in and for industry, yet, in his book, Van Doren says "The acid test of design is: WILL IT SELL ? Abstract beauty is well enough, but educating the public is an expensive pastime—one that business can ill afford in these days of bitter competition. As a designer you must strike a middle course. You must give the public the very best it will absorb, and not one bit more" (p. 54). On another page (p. 72) he says that the primary object of industrial design is "to build sales, to increase profits." The same thought is expressed in his introduction to a representative group of successful product designs which are displayed at the end of his book (plate 1): "The latter were chosen chiefly for sales success. Attractive appearance as an end in itself was subordinated, for beauty as such is meaningless unless it brings the client increased revenue." These views are cited here, not with a view to entering polemics, but as a background for the appraisal of the designs of different nations. Obviously, the crucial question is whether the public taste and understanding has reached maturity, and if not, just how much education of the public is necessary should industrial designers have a serious and lasting contribution to make without degenerating into mere agents of fashion.

In the light of these facts it will perhaps be interesting to look for the guiding principles in foreign designs. Let us consider, for instance, the Loewe lathe; there is nothing "stylish" about it, yet it cannot be denied that it is of a very appealing design. Its adherence to flat surfaces enables the provision of handy tool and gauge trays, one of which can be seen on top of the headstock, the other above the traverse gear at lathe bed level. These tool trays are integral with the casting and have flanged rims. The top of the tailstock of the Loewe lathe also carries a tool tray, and perhaps a com-

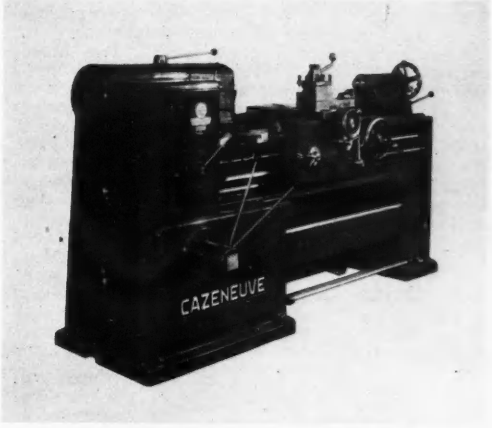

Fig. 11. **Cazeneuve lathe, Model HB (Etablissements A. Cazeneuve, La Plaine-St. Denis, France).**

*Harold Van Doren: *Industrial Design*, McGraw Hill, New York, London, 1940.

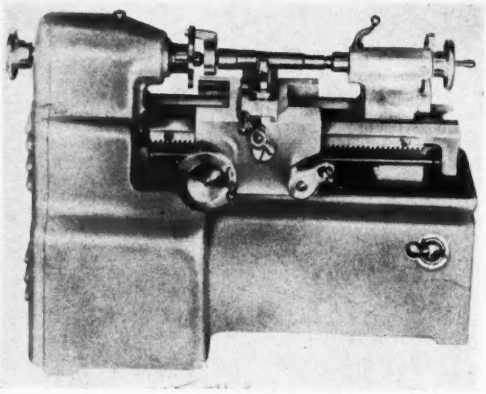

Fig. 12. **The ManSon lathe is a tiny lathe for precision work in the home workshop and laboratory.**

parison of this part of the lathe with that in Figs. 2 and 3 could serve best to illustrate the different trends of thought in various countries on machine aesthetics. However, there are no clearly defined national characteristics. Generally speaking, American lathes are practically devoid of forms not derived from functional requirements. For instance, the Le Blond lathe, Fig. 7, on its two cabinet legs, or the Lodge and Shipley lathe shown in Fig. 8, is strictly functional. It is often the case that a measure introduced for purely functional reasons brings in its train an improved appearance. For instance, the increase in the number of lathes with vertical division according to Fig. 5 is functionally justified by the claim that can be made to smoothness of running and noiseless operation of the headstock, as well as ease of machining in the manufacture of the lathe. It so happens that this division is also more satisfactory from an aesthetic standpoint. In the slow process of evolution the gears were totally enclosed and provided with automatic lubrication, thus facilitating maintenance. To prevent oil loss and access of grit, the tendency is to abandon the Norton gear and adjust thread pitches by sliding gears. (See Fig. 6).

Another example of a representative German lathe, but of a type suitable for heavier duty, is shown in the VDF lathe (Fig. 9). No attempt is made here at "streamlining," it is rather the case of systematic approach and meticulous attention to detail which gives this machine a good-looking appearance. The curved rear wall of the tailstock is functional in this case, inasmuch as it enables the provision of a long base and at the same time permits of placing the handwheel further inwards to save space. Reminiscent of the Loewe lathe is the Swiss Reiden Type T185 shown in Fig. 10. The photograph is taken from an unusual angle to reveal the design of the bed with its diagonal reinforcing ribs, mounted on a full-length box-type base. The latter, apart from imparting rigidity and stability to the lathe, overcomes the inconvenience experienced by the operator by stubbing his toes against the machine legs. The swarf and coolant tray is cast integral with the base. Flat surfaces are predominant, and the lay-out of the headstock conforms to Fig. 5. All thread pitches and feeds are changed by means of sliding gear wheels.

A very original design is the French Cazeneuve lathe, Fig. 11. It is noteworthy for its clean-cut lines and careful grouping of controls. Further examples of modern designs could be given here, but it is thought that before doing so, some comments on trends in mechanical design would be desirable.

Mechanical Design

Among the most important parts of machine tools are the slides. They must ensure high machining accuracy as well as even and steady motion, combined with the least possible wear. Three basic types of machine tool slides are in use: flat slides, prismatic slides and cylindrical slides. The first two types are in general use either separately or in combination; cylindrical slides represent a more recent principle, at least as regards their application to lathes[3]. As an example of combined slides, the Reiden lathe shown in Fig. 10 employs two prismatic front slides for saddle and tailstock, respectively, while the rear slides are flat. The VDF lathe, Fig. 9, has double prismatic slides for the saddle. Bolted to the saddle, guard strips can be seen which are destined to protect the slides from swarf and accidental damage. Least machining inaccuracy occurs if wear of the slides takes place in a plane perpendicular to the plane of machining. This happens —as can be proved by calculation—when, in conventional types, the front prismatic side is obliquely inclined, and if its surface facing the workpiece is about double the width of the outer face[2]. It is believed that what the LeBlond Machine Tool Co. calls the "compensating vee-way" principle conforms to this idea.

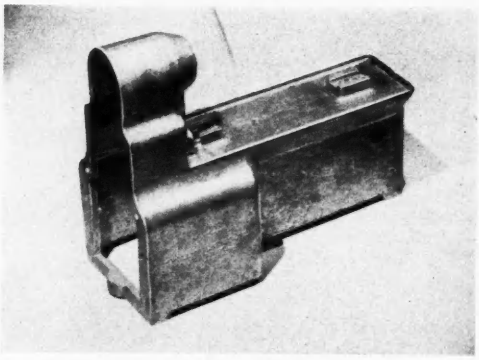

Fig. 13. **Frame of the ManSon lathe shown in Fig. 12.**

To reduce slide wear, alloy cast iron slides have been tried out. Chill cast[3] slide faces also improve wear qualities; a minimum of 200 Brinell hardness is normally required. However, an increase in Brinell hardness does not necessarily mean improved wear resistance. The most promising development was originated in 1936 by the Monarch Machine Tool Company who introduced surface-hardening of the cast iron lathe bed. Flame-hardened beds are now a standard with Monarch; LeBlond supply slides flame-hardened to 600 Brinell as standard equipment. The steel slide strips are replaceable. The surface-hardened cast iron as well as the hardened steel strips have a drawback in that free graphite, which is so necessary for good lubrication, is absent. The Timken Company in America claims to have developed a special steel of high wear qualities which eliminates this drawback.

Next in importance for the development of mechanical design are the possibilities presented by the introduction of welded steel sheet and tubular construction for lathes. Great saving in material should be possible, which would be reflected in the price, as material cost amounts to about half the total manufacturing cost. The behaviour of such lathes with respect to vibration and damping requires a great deal of research work

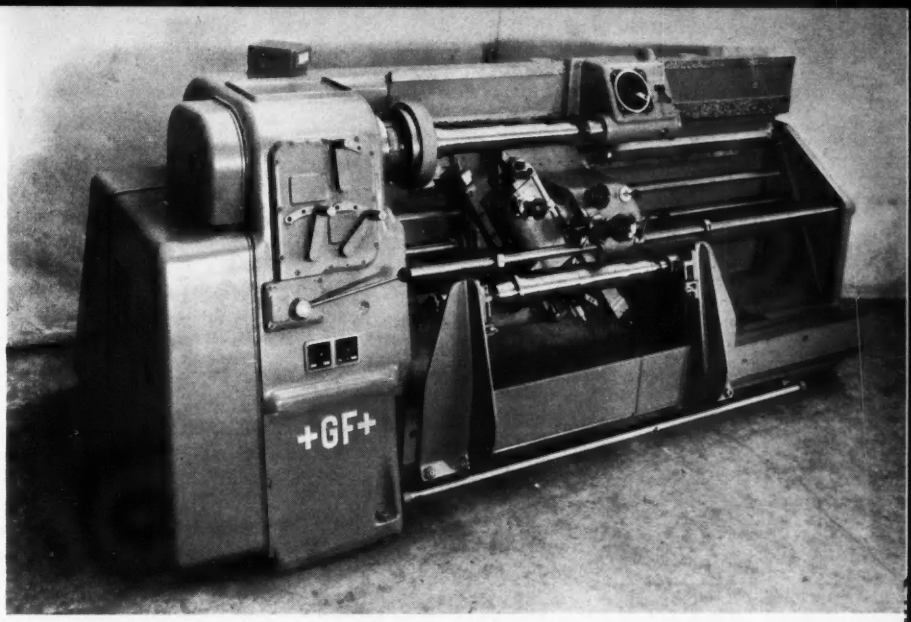

Fig. 14.
Copying lathe, type KDM (George Fischer A.G., Schaffhausen, Switzerland).

before they can generally be adopted. It is obvious that the employment of these new methods would radically alter the appearance of the lathe, leading to simplification of line and shape by the use of the minimum of raw materials. In this respect, the objectives of functional and aesthetic design coincide: the optimum result from the minimum of expenditure.

There are also promising developments inherent in the replacement of cast iron by aluminium alloy castings, even for large beds and bases[4].

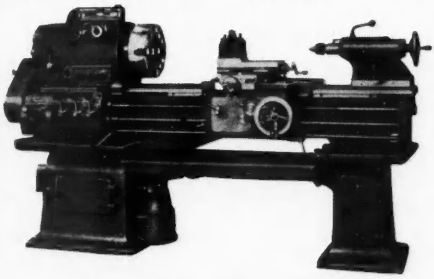

Fig. 15. **Urbinate lathe, type TP200.**

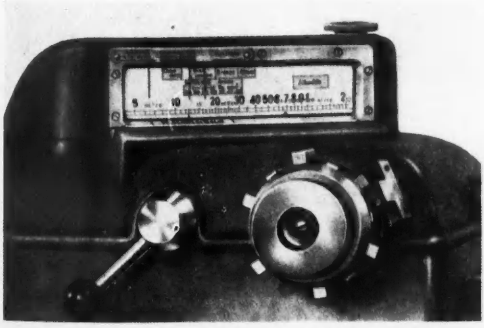

Fig. 16. **Speed Preselector of Urbinati lathe shown in Fig. 15**

For small laboratory lathes, the objectives, i.e., to minimize production costs and to provide a superior surface smoothness, has been achieved by the use of aluminium diecastings. Fig. 12 shows the ManSon lathe manufactured by Small Machines Inc., of West Los Angeles, California, many parts of which are made as aluminium die-castings[5]. Its frame, shown in Fig. 13, has a uniform wall thickness of $\frac{1}{16}$ in. Two thick sections for added strength are located at the headstock and apron, where greater stresses occur. The carriage, cross-slide and many small parts are produced by the diecasting process.

Further design trends are characterized by changes necessitated by tool developments. Early in this century, the power of the driving motors had to be increased to enable the use of high-speed steels which were introduced at that time. This led to stronger and heavier designs, and notably to an increase in the size of the gear boxes, the reduction or partial elimination of which could possibly be achieved by improvements in the design of electric motors, especially of d.c. motors for continuous speed control. Fresh impetus was given to lathe design during the thirties by the introduction of carbide-tipped tools, which still further increased the demand for power and for a wide range of spindle speeds. In addition, difficulties arose in connection with the removal of the large flow of chips resulting from heavier cuts. This led the Swiss firm, George Fischer, to depart from present-day practice by machining the workpiece in a vertical plane, thus enabling the easy unobstructed removal of chips. The machine built on this principle is the KDM type copying lathe, and its appearance (Fig. 14) clearly reveals the novelty of its conception. Upward tool approach at an angle of 60 degrees to the centre line made it possible, perhaps for the first time, to carry out copy turning at right angles without resorting to the use of in-feed tools. This design, with its tailstock on vertical slides, also made possible a great increase in the distance between centres. The continuous box-type rear console is well ribbed and provides increased rigidity and stability, resulting in silent running and high machining accuracy. Copy turning is tantamount to automatic turning, and as work produced by the machine becomes economical for a minimum batch number of four as compared with

an ordinary lathe, it is likely to supersede the latter entirely for certain types of work. Generally speaking, there is a tendency in lathe design towards increased automaticity. The aim is to cut down idle machine time to a minimum. The fitting of switchboxes to the longitudinal and transverse feeds makes it possible to turn stepped shafts to fine tolerances without intermediate gauging[6]. A well-known equipment is the "Man-Au-Trol" of Bullard and the "Electro-Cycle" of Warner and Swasey. These enable pre-selection of speed, sense of rotation, rate of feed and direction of feed for the next operation while the lathe is working.

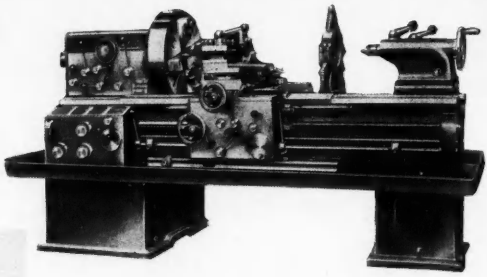

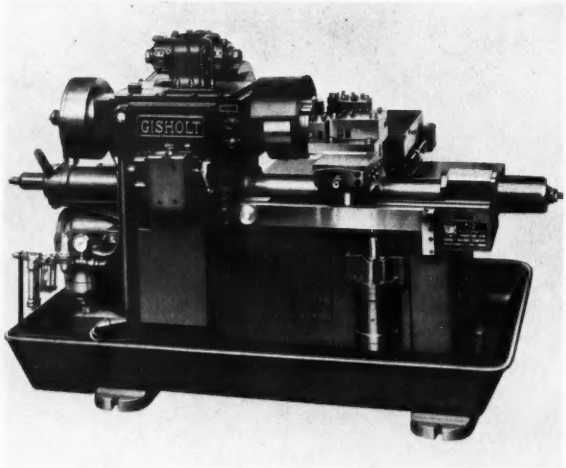

Fig. 17 (above). **Demoor lathe equipped with "Magic Eye" (Ateliers Demoor, S.A., Bruxelles-Forest, Belgium).**

Fig. 18 (left). **Gisholt Hydraulic Automatic Single-spindle lathe, type 12.**

Fig. 19 (below). **Gisholt Hydraulic Automatic Single-spindle lathe, type 24.**

Such a preselector for speed is incorporated in the Italian Urbinati lathe (Fig. 15 and 16). An important aid to ease of control is provided by the "magic eye" of the Belgian Demoor lathe shown in Fig. 17. This visual aid enables quick two-lever control.

Another tendency in the same direction is the provision of copying attachments to normal lathes so that the lathe can be used for regular lathe work or copying, without limiting the range in either case.

The Monarch 20 lathe is equipped with an "Air Gauge Tracer" (Fig. 3) and the Lodge and Shipley lathe (Fig. 8) with the "Copymatic" fully hydraulic tracer control.

Pneumatic, hydraulic, electric and electronic means are being more and more employed for increasing automaticity of operation and will be dealt with more fully in a continuation of this article.

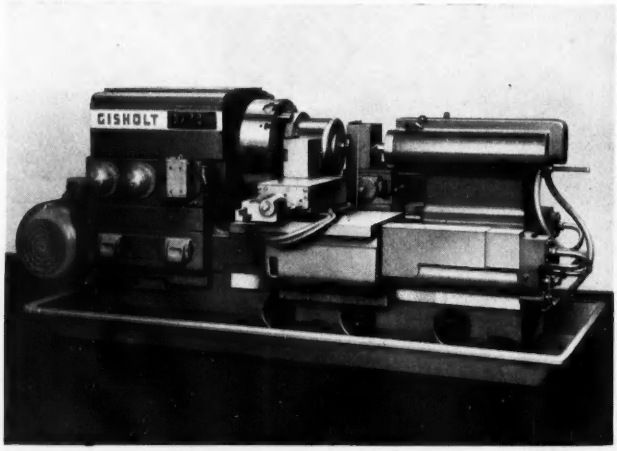

As a culmination of these efforts (applicable to certain types of work) the Gisholt No. 24 hydraulic automatic lathe is shown in Fig. 19. It is an excellent example of modern industrial design, combining sturdiness with simplicity. This is a machine for the production of large parts, having the versatility of the smaller Gisholt No. 12 Automatic (Fig. 18) from which it has been evolved. There is a great similarity in function and detail between these two machines, but the No. 24 is doubtless the one in which industrial design has been allowed to play a most prominent part.

(To be continued)

Bibliography

(1) Using the Lathe as a Horizontal Drilling Machine.—THE ENGINEERS' DIGEST, Vol. 9, No. 7, July, 1948, p. 233.

(2) R. LAMBERTZ.—Entwicklungslinien im Werkzeugmaschinenbau. *VDI-Zeitschrift*, Vol. 91, No. 4, 1949, pp. 73-81 (38 references to literature given).

(3) O. LICH.—New Principles for the Design of Machine Tool Slides. THE ENGINEERS' DIGEST, Vol. 9, No. 7, July, 1948, pp. 234-236.

(4) E. G. WEST.—Aluminium Alloy Casting Developments.—*Engineering*, Vol. 166, August 27, 1948, pp. 213-216.

(5) Diecastings, May, 1948, pp. 33-34, and p. 43.

(6) T. PIČ.—Skoda Universal Lathes.—THE ENGINEERS' DIGEST, Vol. 8, No. 5, May, 1947, pp. 166-168.

WORKSHOP TECHNOLOGY

Miniature Thermionic Valve Handling Equipment

WITH the increasing use of miniature glass-based thermionic valves in many fields of equipment, including radio, television, and electronic devices, mechanical difficulties have arisen due to the small dimensions of the valves in question.

These problems resolve themselves into two main fields. The most important is that of obtaining maximum electrical contact between the small contact pins of the valves and the likewise small contacts of the valveholder. Owing to the fact that the contact pins of the valves are moulded directly into the glass envelope, it is essential that perfect alignment with the valveholder contacts is maintained, in order to avoid risk of damage to the valve, and, of course, to obtain satisfactory functioning. As will be recognised, should only a single valve pin be mis-aligned with its mating contact in the holder, it is possible to render the valve inoperative, and damage may be caused to the valve itself. Intermittent contact, on the other hand, will result in noisy operation, while a high-resistance contact will reduce the efficiency of the entire piece of equipment.

Adequate contact pressure and area were comparatively easy to maintain with the older types of valve, the contact pins of which were of the solid or 'Banana' pattern, and the massive types of valveholders used. However, the miniature glass-based valve has contact pins of small diameter very closely spaced, and to avoid the presence of large masses of solid dielectric, the holders must essentially be of miniature and light construction.

Two types of valve pins are at present in use, one being made from chrome iron, and the other from nickel, the latter being particularly soft. It is with this type that a number of these problems arise.

The spacing and positions of the valve pins, as received from the valve manufacturers, conform to specification, but much may have happened to render these dimensions inaccurate by the time the valve is inserted into its final position. It may have been pushed into a valveholder and withdrawn several times during the process of testing. Side pressure on the valve is sufficient to bend all the pins, and careless handling of the valve in store and workshop all contribute to troubles on installation.

In order to satisfy the requirements of B.S.I. Specifications, it was found that the only safe method of correcting mis-aligned or bent valve pins was to insert the valve into a miniature drawing die, Fig. 1, with an adequate lead on each of its bores, in order to guard against undue stress being placed on the tiny pins. These dies are dimensionally correct to the closest tolerances, and are of hardened steel. The die is housed in a body with four vertical guides, to ensure the valve being held upright while using the tool.

It is recommended that, in order to be certain that the valves having soft pins are satisfactory before use, they are inserted in a pin-straightening tool immediately before being placed in their respective valve holders.

Fig. 1. **Valve pin straightening tool.**

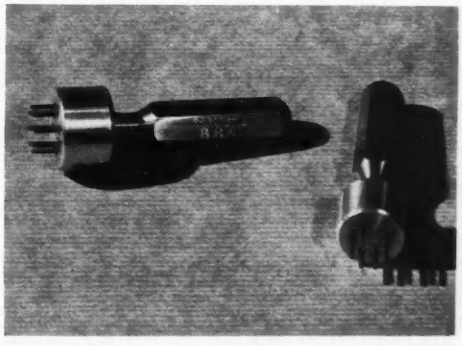

Fig. 2. **Wiring jigs of two types.**

In order to maintain the necessary accuracy of the valveholder contacts during wiring operations, it is recommended that a jig be inserted to ensure holding the contacts in their respective positions. The jig must be as light in weight as is reasonably practical, and embody a head with accurately spaced and dimensioned hardened steel pins. (See Fig. 2.) In use, the appropriate jigs are inserted in the valveholders and hold the contacts in the nominal position during wiring operations.

Yet another problem presents itself with the use of miniature glass-based valves, this problem having entailed considerable experiment and research before it was solved.

Owing to the very small dimensions of the valves, chassis have become more compact, and thus the valves may now be so hemmed in by other components that their withdrawal for servicing becomes a very difficult operation indeed. In many cases, the valves cannot be reached by the fingers, and, in addition, are often in the most inaccessible positions in the equipment.

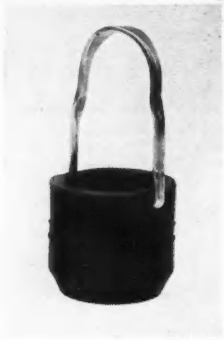

Fig. 3.
Valve extracting tool.

The solution of the problem was the design and manufacture of a valve-extracting tool. This tool, in form, is of tubular construction, fitted with a swivelling handle, thus enabling the body to align itself automatically on the glass envelope of the valve to be extracted. The tool is then pushed by the handle on to the valve. A steady pull on the handle than extracts the valve from its holder. This operation is carried out with the use of one hand only. Several types of these valve-extracting tools are now made, and include one capable of withdrawing valves requiring a 28-lb pull without damage to the valve. (See Fig. 3.)

The whole range of these patented miniature valve-handling tools are described and marketed as " Spearette " Industrial and Service Aids, and are obtainable from the Spear Engineering Company Ltd., Titan Works, Limpsfield Road, Warlingham, Surrey.

A New Trimming Fixture for Deep-Drawn Parts

By H. SCHLICK. (From *Werkstatt und Betrieb, Germany* Vol. 82, No. 2, February, 1949, p. 58, 1 illustration.)

DEEP-DRAWN parts of small size and round shape can easily be trimmed on a lathe. Special fixtures are needed, however, for parts of medium size and irregular shape. Fig. 1 shows a fixture which can be attached to a 60 to 80 ton crank or eccentric press with pneumatic ejector, and which can be used for trimming parts 7 by 5 by 1½ inches deep with a sheet thickness of up to 0·1 inch. The time taken for trimming is approximately the same as for the deep-drawing operation itself.

The part to be trimmed is inserted into the opening of cutting plate *a* which fits round the work piece with a clearance of 0·02 inch. The cutting plate is closely fitted into the bearing plate *c* which carries two hardened and ground driving bushes *h* with internal threads, secured by thrust washers. During the down-stroke of the press, the distance plate *d* first presses the work-piece against the ejector plate until the two stop pins *k* touch the cutting plate *a*. Then the driving screws *g* impart a slight horizontal eccentric movement to the bearing plate *c* and the cutting plate *a*. Pitch and V-angle of the threads must be suitably chosen so that friction is reduced as much as possible. Moreover, the surfaces of screw and nut must be of a high quality and the materials highly wear-resisting, and ample lubrication must be provided. The horizontal eccentric movement of the cutting plate *a* effects the trimming operation by scissor-like action against the cutting edge of the cutting punch *b*. The stop pins *k* are adjusted to suit the sheet thickness of the work piece, whilst the distance plate *d* accurately determines the trimmed depth and fits into the work piece, leaving clearance for the cutting action only. The eccentric motion produces a slowly starting, uniformly proceeding cutting action, so that fairly thick sheet can be cut.

Cylinder *e* and piston *f* guide the punch action and take the shearing forces exerted during cutting. Air pressure in cylinder *e* produces a uniform pressure on cutting punch and work-piece. Four distance bolts *l* and thrust washers *m* prevent the bearing plate *c* from lifting and secure a clean sliding action. The up-stroke of the press takes the fixture back into the starting position. The cutting edges are made from hard alloy, deposited by welding, so that expensive material is saved and the plates can be straightened after quenching and before grinding. The fixture can easily be fitted to a press since the stroke of the press need not be accurately limited. The pneumatic ejector must be adjustable. Consumption of compressed air is very small indeed.

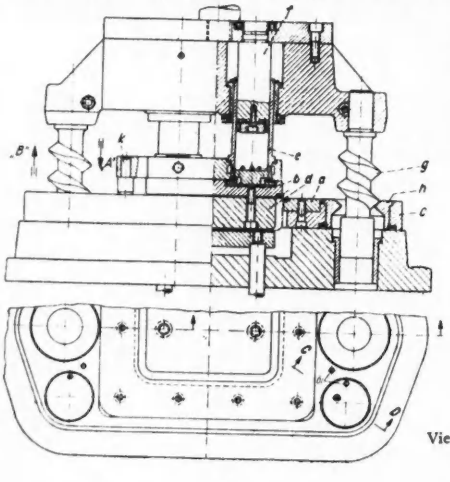

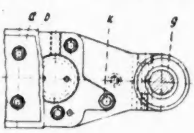

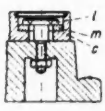

Fig. 1. **Trimming fixture for deep-drawn work pieces.**

a = Cutting plate,
b = cutting punch,
c = bearing plate for *a*,
d = distance plate,
e = 2 compressed-air cylinders,
f = pistons,
g = 2 driving screws,
h = driving bushes with internal thread,
k = 2 stop pins,
l = 4 distance bolts,
m = 4 thrust washers.

CLASSIFIED ABSTRACTS

Numerous important abstracts which, for lack of space, cannot be published in our main editorial columns, are regularly included in condensed form in this section. Subscribers may obtain photostat copies of all original articles at cost.

CERAMIC ENGINEERING

Ceramic Materials with a High Dielectric Constant

By E. J. W. VERWEY and R. D. BÜGEL. (From *Philips Technical Review, Holland*, Vol. 10, No. 8, February, 1949, pp. 231-238, 5 illustrations.)

IN electrical engineering, ceramic materials are very widely used for insulation purposes and as dielectrics for capacitors. In the latter instance, preference is given to a material having a high dielectric constant and low dielectric losses, and here the choice is limited almost exclusively to pure titanium dioxide (rutile), or a mixture in which the latter figures as chief ingredient. Admixtures, sometimes necessary for the purpose of reducing the dielectric losses to a value below the permissible maximum, tend also to reduce considerably the dielectric constant of the TiO_2, and the purpose of this article is to investigate to what extent the value of this constant is related to other properties of the material. A disadvantage of pure titanium dioxide is that the temperature coefficient of its dielectric constant is highly negative. The Philips Laboratories at Eindhoven have worked out various methods for reducing this temperature coefficient to zero by using suitable admixtures. By way of example, a description is given of a series of capacitors of small dimensions with a ceramic dielectric as used in radio receivers and other equipment incorporating high-frequency circuits.

ELECTRIC FURNACES

High-Speed Electro-Hydraulic Arc-Furnace Control

By A. GARDE. (From *Asea Journal, Sweden, Vol.* 22, No. 1-2, January-February, 1949, pp. 3-9, 9 illustrations.)

A NEW system of high-speed electro-hydraulic arc furnace control is described in this paper. Practical experience with this new regulator has shown that the problems confronting earlier regulator designers have been successfully solved, and the combination of stability and speed of response, in a manner hitherto considered feasible only in theory, has opened up great possibilities for future applications. This great advance in design presents attractive features, both economic and technical, to the steel manufacturer. Important economic considerations are the increased capacity of existing furnaces resulting from the reduction in melting time, together with the appreciable saving in energy and electrode costs. Also of great importance is the substantial reduction in maintenance requirements. From the technical point of view, the reduction in current fluctuation with attendant improvement in load factor is an important consideration.

ELECTRICAL INSTRUMENTS AND METERS

A Direct-Reading Dynamic Electrometer

By J. VAN HENGEL and W. J. OOSTERKAMP. (From *Philips Technical Review, Holland*, Vol. 10, No. 11, May, 1949, pp. 338-346, 11 illustrations.)

A DESCRIPTION is given of a direct reading d.c. electrometer. It is based on the dynamic principle, the direct voltage being converted into an alternating voltage with the aid of a parallel-plate capacitor, the capacitance of which changes periodically as one plate is kept stationary while the other is kept in vibration. The alternating voltage is applied to an amplifier with conventional valves; the output voltage is rectified and the conducted direct voltage measured with a moving-coil meter. In order to keep the amplification constant, a high degree of negative feedback is applied by connecting the output d.c. voltage wholly or partly in opposition to the voltage to be measured. This makes it necessary to use a special rectifying circuit which is sensitive to the polarity of the a.c. input voltage. Due in part to the direct-voltage feedback, the (apparent) input resistance reaches extremely high values (more than 10^{15} Ohms). Two instruments are discussed: a millivoltmeter (full deflection at 100 mV) for laboratory measurements, and a dosimeter for X-rays (in combination with an ionization chamber and a measuring resistor). The dosimeter has a scale calibrated in r/min and covers a very wide measuring range, from 4×10^{-7} r/sec (fraction of the tolerance dose) to 200 r/sec (contact therapy). For the calibration a standard-current generator has been designed which supplies a calibrated current of 10^{-9} A.

ELECTRIC TRANSFORMERS

New Trend in the Design of Large Power Transformers

By H. B. CHEVALIER. (From Bulletin Scientifique de l'Association des Ingenieurs Electriciens sortis de *l'Institut Electrotechnique Montefiore, Belgium*, No. 12, December, 1948, pp. 463-517, 34 illustrations.)

AMONG the main criteria which characterise the modern transformer are, first of all, its impulse strength, and, secondly, the thermal characteristics of the "hot spot" at normal and over-load. These two criteria determine the useful life of the transformer. The exceptional magnetic properties of transformer sheet with an oriented crystal structure have led to the construction where output is above a certain limit of wound-core shell-type transformers. In addition to the possibility of designing this type of transformer for very favourable impulse strength and thermal conditions, there is a number of other advantages: reduced losses, short-circuit strength, reduced size, simple dismantling, etc. From the manufacturing point of view, mass production methods can easily be applied.

A highly detailed account of theory and practice of this type of transformer is given, which has only recently been adapted for large power units. A description is given of the composition, manufacture, characteristics and application of cold-rolled strip, with a high degree of grain orientation, magnetic phenomena in wound cores, design of wound-core transformers as compared with the ordinary concentric coil transformers, workshop problems, thermal behaviour of the transformer, cooling and ageing. Oscillograms taken on a 8000-kVA, 115-kV experimental transformer show the behaviour of the winding under varying shock conditions up to the point where a breakdown occurs in the insulation.

to resist steam

And to make it strong, hard and free from galling and "wire-drawing". There are nickel-containing non-ferrous alloys which will give these properties at steam temperatures. For any given set of conditions, the wide range of alloys available provides the right material but necessitates a wise choice. Whatever your problem may be, we will gladly give you every assistance in making this choice.

The Mond Nickel Company Ltd.

SUNDERLAND HOUSE · CURZON STREET · LONDON · W.1

12/La/1

METALLURGICAL ENGINEERING

Effect of Niobium on the Fatigue Strength of Chrome-Molybdenum Steel at a Temperature of 550° C.

By Y. S. GINSBURG, K. A. LANSKAYA and A. V. STANYUKOVICH. From *Kotloturbostroyenie, Russia*, No. 1, 1948, pp. 17-19, 4 illustrations.)

THE object of the investigation reported in the present article was to clarify the effect of niobium on heat resistance of chrome molybdenum steel when subjected to creep tests to destruction. The samples contained 1 to 8·24 per cent chromium and 0·44 to 0·52 per cent molybdenum with an addition of niobium varying from 0·56 to 2·0 per cent.

Steel with a chromium content of 1 to 4 per cent in tests ranging up to 1000 hours in duration did not show any appearance of fracture as a result of brittleness. Steel with a chromium content of 2 per cent usually gave an elongation of 20-35 per cent, and it was found that with steel of this composition the introduction of niobium generally produces unfavourable fatigue test results, inasmuch as the ultimate strength is lowered in comparison with steel not containing niobium.

On the other hand, steel with a chromium content of 6 to 8 per cent shows increased strength when niobium is added within the limits of 1 to 1·3 per cent, but with a higher niobium content the strength decreases sharply.

Generally, the investigation shows that niobium produces a strong spheroidization of the pearlite, which always leads to a reduction of the ultimate fatigue strength and to an increase of plasticity, with the one exception stated above.

It is interesting to note that for tests conducted over a period of 100,000 hours, the composition of the steel did not seem to affect the ultimate strength.

An Investigation of Creep, Fracture, and Bending of Lead and Lead Alloys for Cable Sheathing

By CURTIS W. DOLLINS. (From *University of Illinois Bulletin, U.S.A.*, Vol. 45, No. 65, July 1, 1948, 86 pages, 29 illustrations.)

RESULTS of creep tests on strips and full sections of lead cable sheathing are reported. Mathematical analysis of the creep properties is difficult, if not impossible, because of the nature of creep in lead, both flow at the grain boundaries and slip within the grains (the amount of each varying with different stress conditions), and because of the further fact that many of these alloys are unstable supersaturated solutions. Extrusion conditions and the biaxial state of stress in sheath samples make a comparison of tests on strip and full-size sheath difficult.

Lead alloys show considerable recovery during cyclic loading. Data are given which may account for the wide difference in the amount of creep obtained in laboratory tests and field tests.

Stress rupture tests are reported, in which the loss of ductility as time for fracture is increased is very marked for some alloys. If the tensile stress is too low to cause slip within the grains, failure occurs at the grain boundaries, resulting in reduced elongation. The arsenical lead alloys maintain fair ductility under low as well as high stress conditions.

Bending machines are described for testing the bending resistance of sheathing in strip form or extruded on cables. In the repeated bending of lead, the rate of strain is very important. Since the lead may creep during the test and some corrosion takes place during slow-speed testing, the importance of testing lead in bending with a rate of strain as near as possible to service conditions is pointed out. The marked superiority in bending resistance of the arsenical leads is shown in the test results of both strip and cable bend tests.

NON-FERROUS METALS

Some Precipitation-Hardening Silver Alloys

By M. BALLAY and P. VOGT. (From *Revue de Métallurgie, France*, Vol. 45, No. 8, August, 1948, pp. 254-260, 9 tables.)

SILVER alloys with a high silver content (Class A, above 95 per cent, Class B, above 80 per cent) tarnish easily and are too weak and soft for many industrial applications. The authors have systematically investigated the influence of alloying elements, such as Sn, Zn, Ni, Be, Al, which could improve the hardness and strength of the alloy. Various percentages of these elements were added to the main Ag-Cu body and the alloyed materials were tested as rolled, or annealed, quenched, quenched and tempered, and quenched and cold-worked with or without subsequent tempering. The hardness of the finished material was determined by Brinell tests, and the capacity for deformation by a folding test.

It is shown that Class B alloys (over 80 per cent Ag, remainder Cu) can already be hardened by artificial ageing, but a greater hardness of up to 200 Brinell (20 kg, 1 mm ball) can be obtained if 2·5 to 3 per cent of the copper is replaced by aluminium. The deformability still remains satisfactory. Class A alloys (over 95 per cent Ag, remainder Cu) can be improved if half the copper content is replaced by aluminium. A hardness of up to 125 Brinell can then be attained. If the material (Class A or B) has to undergo appreciable deformation in the finished state, the best treatment is water quenching from 700 to 800° C, finish-forming in the quenched state, and then artificial ageing at 250 to 325° C. A greater hardness, with a reduction in deformability, can be obtained if the material is heavily cold-worked after quenching and then hardened by heat treatment. Silver springs can be manufactured by this method.

STRESS ANALYSIS

Stress Studies on Piping Expansion Bellows

By F. J. FEELY, Jr., and W. M. GORYL. (From a Paper presented at the National Meeting of the Applied Mechanics Division of *The American Society of Mechanical Engineers*, June 13-15, 1949, Paper No. 49–APM-22, 7 pages, 13 illustrations.)

As a result of numerous and costly failures of the stainless-steel bellows used to take up thermal expansion in the piping of petroleum and chemical processing equipment, a basis has been developed for designing these bellows to operate within reasonable stresses. A formula has been derived to show the total stress induced in the material as a result of the combined effects of pressure and movement. The validity of the approximations used in this formula has been verified by laboratory strain-gauge measurements on an experimental bellows. A relationship between several variables in the design of the discs has also been determined and serves as a basis for dimensioning them to achieve the most economical proportions. When this relationship is satisfied, the maximum permissible movement per disc can be obtained. This is shown graphically. Several supplementary formulae are given for determining bellows characteristics which may affect the design of adjacent piping. The problem of designing an expansion joint for high-pressure service is discussed briefly, and some preliminary laboratory data are presented on a commercial joint of this type.

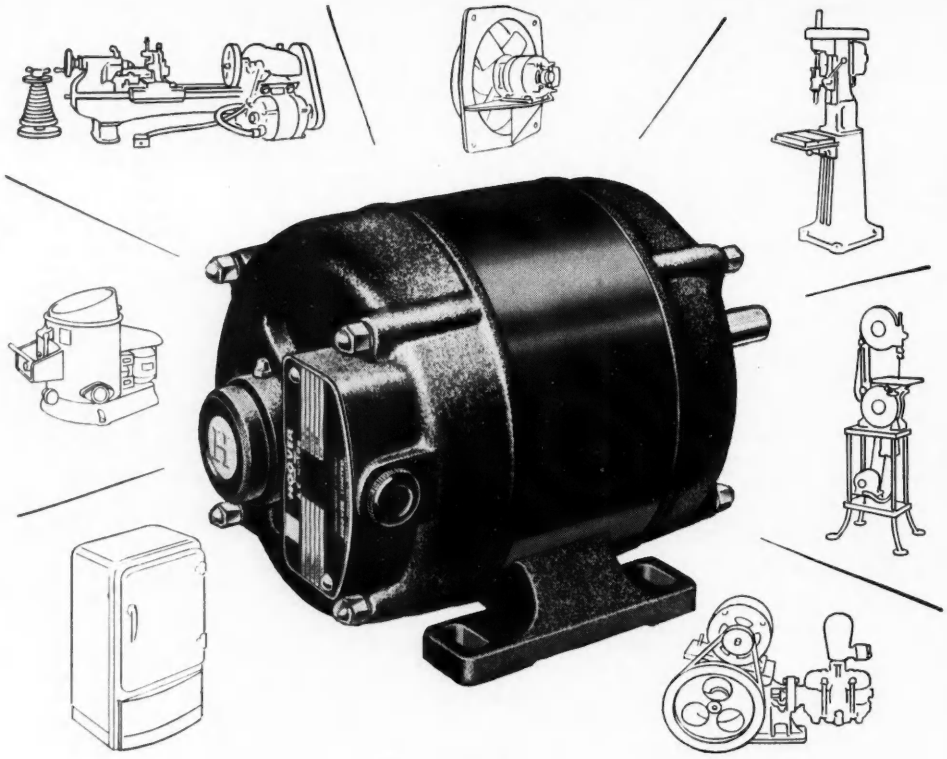

FIT
HOOVER F.H.P. MOTORS
TRADE MARK

for smooth, trouble-free power

When you need Fractional H.P. Motors that will stand up to the hard test of constant daily usage—that will give years of smooth, efficient, trouble-free service—fit "HOOVER". These strong, sturdy motors have inherited the same dependability and stamina that characterizes every product that carries the name of Hoover.

Wherever Hoover Motors are used to provide power in electrical appliances INCREASED CUSTOMER SATISFACTION is the inevitable result.

HOOVER LIMITED

INDUSTRIAL PRODUCTS DEPARTMENT · PERIVALE · GREENFORD · MIDDLESEX

NEWS OF THE MONTH

PERSONAL

Mr. K. S. Arnold, B.Sc., M.I.Mech.E., has been appointed director and assistant general manager of Duncan Stewart & Co., Ltd., Glasgow.

Mr. R. W. Ayers has been elected chairman of the Resistance Welding Machine Manufacturers' Section of the British Electrical and Allied Manufacturers' Association, 36-38, Kingsway, London, W.C.2. **Mr. F. Simmons** has been elected deputy chairman, and **Mr. E. S. Waddington,** vice-chairman.

Mr. L. W. Baldwin has been appointed export manager of Simplex Electric Co., Ltd., Broadwell, Oldbury, Birmingham.

Mr. W. J. Borrowman has been appointed manager of the diesel engine department of Sulzer Bros. (London) Ltd.

Professor E. C. Bullard, M.A., D.Sc., F.R.S., has been appointed Director of the National Physical Laboratory.

Mr. O. V. S. Bulleid, C.B.E., M.I.Mech.E., has been elected President of the Institute of Welding. **Mr. C. S. Milne** has been elected vice-president.

Dr. Maurice Cook has been re-elected President of the Institution of Metallurgists, 4, Grosvenor Gardens, London, S.W.1.

Mr. E. M. Deloraine, vice-chairman of Standard Telecommunication Laboratories Ltd., has received the degree of Ingenieur-Docteur from the University of Paris.

The Rt. Hon. The Viscount Falmouth, M.I.Mech.E., Comp.I.E.E., has been re-elected President of the British Internal Combustion Engine Research Association. **Vice-Admiral (E.) Sir Denys C. Ford, K.C.B., C.B.E., Lieut.-General Sir Frederick G. Wrisberg, K.B.E., C.B., Dr. S. F. Dorey, C.B.E., M.I.C.E., M.I.Mech.E., F.R.S., Air Commodore F. R. Banks, C.B., O.B.E.,** and **Sir Lynden Macassey, K.B.E., K.C.,** have been re-elected vice-presidents. **Major-General E. H. Clayton, C.B.E.,** has also been elected vice-president, and **Mr. Joseph Jones, M.I.Mech.E.,** has been elected chairman of the Council.

Mr. H. M. Goody has been appointed managing director of Cantie Switches Ltd., which moved from Chester to a new and larger factory at New Ferry, Bromborough, Cheshire. **Mr. P. J. Shipton, A.M.I.E.E.,** director and general manager, who has been intimately concerned with the growth of the company in recent years, continues in this position.

Mr. R. J. Gregg has been appointed publicity manager of the Gas Council.

Mr. S. B. Hainsworth, managing director of J. H. Fenner & Co., Ltd., and associated companies, has been elected chairman of the Association of Solid Woven Belting Manufacturers.

Mr. F. W. Halliwell, M.I.Mech.E., M.I.P.E., has been re-elected President of the Gauge and Tool Makers' Association. **Mr. H. S. Holden** has been re-elected chairman, **Mr. A. L. Dennison, M.I.P.E.,** vice-chairman, and **Mr. R. Kirchner, M.I.P.E., A.M.I.Mech.E.,** honorary treasurer.

Mr. Donald McCullough has been appointed public relations adviser to the Fe eration of British Industries, 21, Tothill Street, London, S.W.1.

The Rt. Hon. Sir Roland Nugent, D.L., Minister in the Senate of Northern Ireland, has been appointed to be Chairman of the Council of Scientific Research and Development in place of **Sir David Lindsay Keir, M.A.,** who has resigned in view of his impending departure for Oxford.

Mr. G. E. Savory, B.Eng., A.M.I.Mech.E., has been appointed sales director to Ruston-Bucyrus Ltd., Excavator Works, Lincoln.

Mr. D. A. Shepard, chairman of the Anglo-American Oil Co., Ltd., 36, Queen Anne's Gate, London, S.W.1, has resigned to take up the position of executive assistant, in New York, to the President of the Standard Oil Co. (New Jersey). **Mr. R. A. Carder,** managing director of the Anglo-American Oil Co. since 1939, has been appointed chairman and **Mr. Leonard Sinclair** has been appointed an additional managing director. **Mr. H. W. Page** has been appointed director of the Anglo-American Oil Co.

Mr. B. W. Silverwood has been appointed technical commercial welding engineer to the Industrial Department of Philips Electrical Ltd. He has also been elected secretary of the North London branch of the Institute of Welding.

Mr. H. R. Walton, technical sales manager, and **Mr. L. E. Meeks,** works manager, have been appointed directors of Electroflo Meters Co., Ltd. **Mr. G. H. Barker,** sales director, has been appointed joint managing director with **Mr. B. Dunglinson,** chairman of the company.

Mr. R. A. West, B.Sc. (Eng.), A.M.I.E.E., has been elected a director of the Igranic Electric Co., Ltd., Bedford.

BUSINESS NOTES

B.S.A. Tools Ltd., Mackadown Lane, Marston Green, Birmingham, announce that their Glasgow branch and that of the distributing organisation, Burton, Griffiths & Co., Ltd., has been moved to new premises at 46, Carlton Place, Glasgow, C.5. Tel. South 1121-2.

V. L. Farthing & Co. have moved into larger premises at 329, Tower Building, Liverpool 3. Tel. CENTral 5002 and 1768.

Sheepbridge Engineering Ltd. has opened a new sales office for its light engineering division at 351, Sauchiehall Street, Glasgow, C.3. **Mr. L. Harrop** is the local representative.

Brooks & Walker Ltd., 41, Dockhead, London, S.E.1, has become sole world concessionnaire for C. A. Gray, Bishops Stortford, Herts, manufacturers of vernier gauges. **Mr. M. Pryce** has been appointed sales manager of the precision tool department.

Change of Name. The title of the Transmitting and Industrial Valve Division of Mullard Electronic Products Ltd. has been changed to "Communications and Industrial Valve Department."

The telegraphic address of the Mullard Radio Valve Co., Mitcham, Surrey, has been changed from EMVALCO PHONE LONDON to EMVALCO SOUPHONE LONDON.

"Hot" Laboratory at Harwell. One wing of the new Radiochemical Laboratory at the Atomic Energy Research Establishment, Harwell, is now ready. Scientists are to start work in it almost immediately.

The laboratory will be used primarily for research on the chemical problems of separating the fissile element plutonium from uranium rods that have been irradiated in a pile. The rods also contain very radioactive "fission products," and the chemical separation problem involved means that the scientists will be tackling one of the most difficult jobs in the Atomic Energy programme.

The laboratory will also be used for other chemical work with radioactive materials, including the separation of radio-isotopes produced in BEPO (British Experimental Pile), and processing materials that have been irradiated in the pile.

This 32pp. brochure contains just the information the engineer requires about the Brailey Process for reclaiming worn or undersized parts or for resisting wear and corrosion—preparation before deposition, machining of deposits, type of deposition required for specific applications—write for it today.

BRAILEY ELECTROPLATERS LTD.
CHAPEL ST · SALFORD 3 · LANCS.

Ⓜ B.38

DEPOSITION FACILITIES AT

FESCOL

The plant is equipped to treat components between the extremes illustrated.

Executives are invited to write for fully descriptive booklet E.D.4.

Illustrated in the background is a 3,000-ton Schloemann Forging Press, the property of Messrs. High Duty Alloys Ltd., Forging Division, Redditch, for whom we deposited the 8 ft. 6 in. main rams and to whom we are indebted for permission to publish.

FESCOL LIMITED

FESCOL REGISTERED TRADE MARK

ORIGINATORS OF HEAVY DEPOSITION

SOLE LICENSEES FOR FRANCE: SOCIETE FESCOL, 140, RUE DU CHATEAU, BOULOGNE-SUR-SEINE.
SOLE LICENSEES FOR AUSTRALASIA: DE HAVILLAND AIRCRAFT PTY. LTD., MILPERRA ROAD, BANKSTOWN, N.S.W.

Scottish Address: PORT GLASGOW

Northern Address: KARRIER WORKS, CABLE ST. HUDDERSFIELD

NORTH ROAD LONDON N.7

TELEPHONE · NORTH 3025.6.7
TELEGRAMS FESCOLDOM · PHONE · LONDON

BOOKS

Metal Cutting Tools. By P. S. Houghton, A.M.I.Mech.E. Publishers: Chapman & Hall Ltd., 37 Essex Street, London, W.C.2. 283 pp. 273 figures. PRICE: 25/-.

This book is intended for students of production engineering, tool room, machine shop and drawing office personnel. It deals with a wide range of metal cutting tools and is well illustrated with diagrams and tables.

Design for Welding. Publishers: The James F. Lincoln Arc Welding Foundation, Cleveland 1, O. Over 1000 pages, profusely illustrated. PRICE $2.00 in the United States, $2.50 elsewhere.

The book is composed of abstracts of 82 award papers, selected and edited by Professor R. S. Green, Acting Chairman of the Department of Welding Engineering of the Ohio State University, Columbus, O., in the recent Foundation "Design-for-Progress" Award Program.

In the preface of the book Professor Green states that he has prepared the book with the purpose of making available a record of representative welded designs. He has placed emphasis on projects produced and in operation with the objective of providing engineers and industry generally with a variety of ideas which may be adaptable to their own products or structures. The book contains a liberal presentation of cost data on the various designs which afford a sound means of making a comparative study of methods.

Papers included in the book are classed into the following categories: Aircraft, Automotive, Railroad, Watercraft, Containers, Furniture, Structures, Machinery and Welderies. Each section contains papers describing outstanding accomplishments in that particular field. The machinery and Structures sections are especially strong and the quality of the papers evidences the advance in design in these fields.

Assisting Professor Green were associate editors Professor Douglas C. Williams and Professor Charles B. Smith, both of the Ohio State University, in addition to numerous consulting editors chosen from industry.

Ports of the World. Edited by Sir Archibald Hurd. Publishers: The Shipping World, Ltd., Effingham House, Arundel Street, London, W.C.2. PRICE 40/-.

This publication, which extends to some 1,200 pages, gives detailed information of practically every port in the world of any importance. It has been possible for the first time since the war to include up-to-date particulars of the majority of the Japanese ports. New features which have been added include tables of steaming distances. Further information about the incidence of public and local holidays has been incorporated in the text. Other features include a table of foreign currencies and a 16-page map section.

Mechanical Vibrations. Their Calculation, Design Effects and Suppression. By R. A. Collacott, Ph.D., B.Sc.(Eng.), A.M.I.Mar.E. Publishers: Sir Isaac Pitman & Sons, Ltd., Parker Street, Kingsway, London, W.C.2. 130 pp. 82 illustrations. PRICE 15/-.

General and Industrial Management. By Henry Fayol. With a Foreword by L. Urwick, O.B.E., M.C., M.A., F.I.I.A. Publishers: Sir Isaac Pitman & Sons, Ltd., Parker Street, Kingsway, London, W.C.2. 110 pp. PRICE 15/-.

Engineering Contracts and Specifications. 2nd Edition. By Robert W. Abbett. Publishers: John Wiley & Sons, Inc., 440-4th Avenue, New York 16, N.Y. and Chapman & Hall Ltd., 37, Essex Street, London, W.C.2. 237 pp. PRICE $3.75 or 22/6.

Engineering Materials and Processes. By L. H. Hancock, A.M.I.Mech.E. Publishers: Sir Isaac Pitman & Sons, Ltd., Parker Street, Kingsway, London, W.C.2. 214 pp. 107 figures. PRICE 15/-.

The Nickel Bulletin. The article "Nickel Alloy Steel Castings" in the May issue of The Nickel Bulletin, discusses the selection of steels to meet the new British Standards Specifications for steel castings.

The article deals at some length with methods of testing and includes a table which will assist in the choice of steels for a wide range of applications. The illustration shows a group of aircraft quality, high tensile steel castings, indicating something of the design flexibility, accuracy of form and excellence of finish possible by modern steel foundry practice.

The May edition, which includes a number of interesting abstracts, can be obtained on application to The Mond Nickel Co. Ltd., Sunderland House, Curzon Street, London, W.1.

The Institute of Industrial Supervisors has announced the election of the following members of the Educational Advisory Panel:—Sir Anthony Bowlby, Bt., director and joint general manager, Guest, Keen & Nettlefolds (Midlands) Ltd., Screw Division; Mr. Michael Clapham, M.A., Imperial Chemical Industries Ltd., Metals Division Personnel Director; Mr. E. W. Hancock, M.B.E., M.I.Mech.E., F.R.S., M.I.P.E., F.I.I.A., director and general works manager Humber Ltd., Coventry; Mr. David H. Bramley, A.M.I.Mech.E., A.M.I.P.E., A.M.I.I.A., Head of Department of Industrial Administration, Central Technical College, Birmingham; Mr. H. Garratt, B.Sc., Principal of the Chance Technical College, Smethwick and Mr. J. V. A. Long, F.B.S.I., F.I.A.C., A.M.I.I.A., Leicester College of Technology & Commerce.

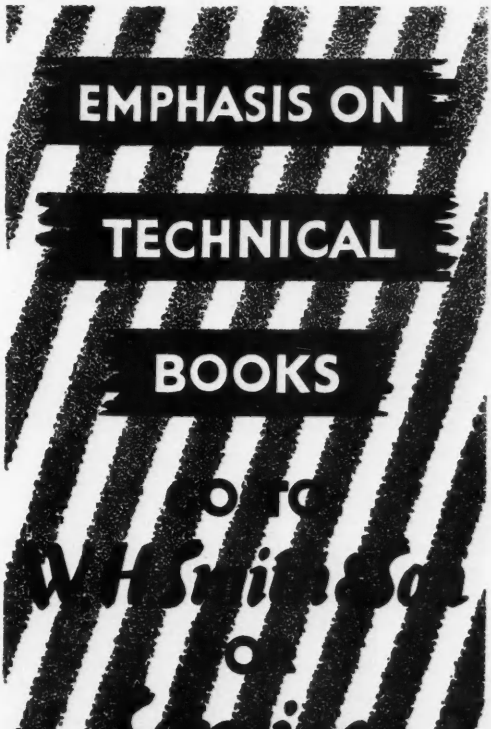

EXECUTIVES, technical training officers, and works librarians who are constantly seeking the newest technical publications will find a quick and competent service at any branch of W. H. Smith & Son.

Each is in daily contact with Head Office in London and your orders, either for single copies or complete works libraries will be fulfilled within the shortest possible time.

W.H.SMITH & SON

1500 BOOKSHOPS AND BOOKSTALLS THROUGHOUT THE COUNTRY

RUINED

by the tests which should have saved them

but this would have saved them

High Voltage Testing of insulated components has hitherto meant, in many instances, complete destruction of units below standard. Furthermore, such tests have involved appreciably long periods of time.

This Airmec non-destructive high voltage insulation tester will give immediate indication of weakness in insulation before breakdown voltage is reached. It will indicate the maximum safe voltage at which insulation can be worked and will show whether or not ionisation is present within the insulation. The instrument is self-contained, portable, low in cost, and safe to operate. It may be used by unskilled personnel and is many times faster in use than other test equipment. Voltages up to 5kV are available.

For testing radio and electrical components, motor and transformer windings, insulated wire and cables, and determining deterioration of insulation after storage.

AIRMEC

AIRMEC LABORATORIES LIMITED

HIGH WYCOMBE, BUCKINGHAMSHIRE, ENGLAND

Tel: High Wycombe 2060 · Cables: Commlabs

Manufacturers of all types of industrial electronic equipment and test gear

PUBLICATIONS OF THE NATIONAL BUREAU OF STANDARDS

(Copies may be obtained at listed prices from the Superintendent of Documents, U.S. Government Printing Office, Washington 25, D.C.)

PHYSICS

RP1965. Accurate Determination of the Deadtime and Recovery Characteristics of Geiger-Müller Counters, Louis Costrell, 9 pp., 10 cents :—Description of an electronic gating instrument for the determination of deadtime and recovery characteristics of Geiger-Müller counters to an accuracy of 2 microseconds.

The theory of operation of Geiger-Müller counters is briefly presented, emphasizing deadtime and recovery characteristics. Experimental data are given showing variation of deadtime and recovery time with counter pressure and overvoltage.

RP1962. The International Temperature Scale of 1948, H F. Stimson, 9 pp, 10 cents :—The first revision of the International Temperature Scale since its adoption 21 years ago is described.

The new scale is designed to conform as nearly as practicable to the thermodynamic centigrade scale as now known, while incorporating certain refinements, based on experience, which make the scale more uniform and reproducible. A new value for the temperature of the silver point and the use of Planck's law with a new value for the radiation constant, c_2, are the only changes having significant effects on numerical values assigned to temperatures.

RP1960. Expansion Effects of Annealing Borosilicate Thermometer Glasses, Arthur Q. Tool and James B. Saunders, 12 pp., 10 cents :—By changing the equilibrium temperatures of a number of the better known borosilicate thermometer glasses, the increase in expansivity per degree in equilibrium temperature was found to be about 2.4×10^{-9} at 100° C.

As these effects are important in the performance of thermometers, the results obtained are used to demonstrate their relation to certain ice point fluctuations where, under particularly adverse conditions, the ice point reading may be changed as much as 30° C.

RP1969. Optical Glass of Interferometer and Schlieren Quality for Wind-Tunnel Optics, Leroy W. Tilton, 8 pp., 10 cents :—An analysis of some of the factors involved in producing large glass disks of uniform optical thickness for wind-tunnel optics.

These disks should be uniform in optical thickness within $\pm$ 1/16 λ to ensure highest accuracy in interference measurements. Evidence is cited to show that differences in chemical composition in good glass may not prevent realization of the desired uniformity, and that stress birefringence cannot be an important preventing factor. The remaining source of non-uniformity in glass is the existence of temperature gradients during annealing, and it has been found that these can be reduced within required limits simply by encasing the glass annealing in a sufficient number of concentric boxes composed of alternate heat-conducting and insulating layers.

RP1970. A Standard of Small Capacitance, Chester Snow, 22 pp., 15 cents :—Derivation of a formula for computing the electrical capacitance of an absolute standard consisting of a modification of the ordinary parallel-plate condenser with coplanar guard.

In this modification, the circular face of the electrode is placed at the bottom of a cylindrical hold in the guard. The analogous two-dimensional arrangement is considered, and the two cases are formulated as special cases of a more general one, so as to show that certain approximate formulae have errors of the same order of magnitude in each case. The magnitude of the error is then determined by comparison with an exact formula obtained for the two-dimensional case by conformal transformation.

RP1961. Zeeman Effect and g-Values for Neutral Nitrogen and Oxygen, Carl C. Kiess and George Shortley, 25 pp., 15 cents :—Zeeman patterns of red and infra-red lines of nitrogen and oxygen, as observed in magnetic fields of 35,000 and 86,000 gauss, show various degrees of distortion due to Paschen-Back interaction.

The interpretation of these patterns has afforded an interesting application of quantum theory to the elucidation of the Paschen-Back effect. The g-values derived for the energy levels of N I and O I are the first to be announced for neutral atoms of atomic number less than neon, 10, and are found to conform with those required for LS-coupling despite the fact that the term intervals do not conform with the Lande ratios.

ENGINEERING

RP1949. Weather Resistance of Porcelain Enamels Exposed for Seven Years, William N. Harrison and Dwight G. Moore, 14 pp., 10 cents :—Report on a seven-year study of the weather resistance of porcelain-enamelled architectural panels.

Eight hundred and sixty-four 1-foot square panels and a like number of 4- by 6-inch laboratory specimens were weathered at four widely separated test sites. Results show a good correlation between acid resistance of enamels and their resistance to weathering. Where initial coverage was complete and no mechanical damage had occurred, protection of the metal by the enamel for all specimens was unimpaired.

RP1955. Laboratory Wear Tests with Automotive Gear Lubricants, Samuel A. McKee, James H. Swindells, Hobart S. White, and Wayne Mountjoy, 6 pp., 10 cents :—Use of the SAE extreme-pressure lubricants testing machine for determination of the wear with gear lubricants under conditions simulating high torque and low speed is described.

Data were obtained with a straight mineral oil and 11 representative samples of commercial lubricants commonly used in automotive gears, operating at 225° F and at various constant loads. Marked differences are shown in the performance of the lubricants in the higher-load range.

GLACIER
BEARING PRODUCTS

PLAIN BEARINGS
Thin and thick wall bearings to customers' specifications—steel or bronze shells lined with white metal, copper lead or lead bronze.

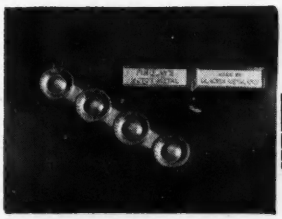

WHITE METALS
Tin and lead-base white metal alloys in a wide range of specifications to meet all engineering needs.

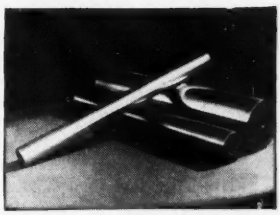

BRONZE BARS
Machined Chill Cast Phosphor Bronze and Lead Bronze Bars in a wide range of cored and solid stock sizes.

STANDARD WRAPPED BUSHES
Nearly 400 sizes, English and Metric, in stock; steel backed, lead bronze lined, ready for assembly with a burnishing allowance in the bore.

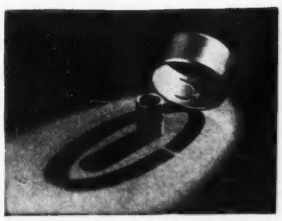

GLACIER METAL CO. LTD.
Europe's Largest Makers of Plain Bearings
ALPERTON, MIDDX., ENGLAND
Telephone : PERIVALE 4271
Telegrams : BEAUCOUP, PHONE, LONDON

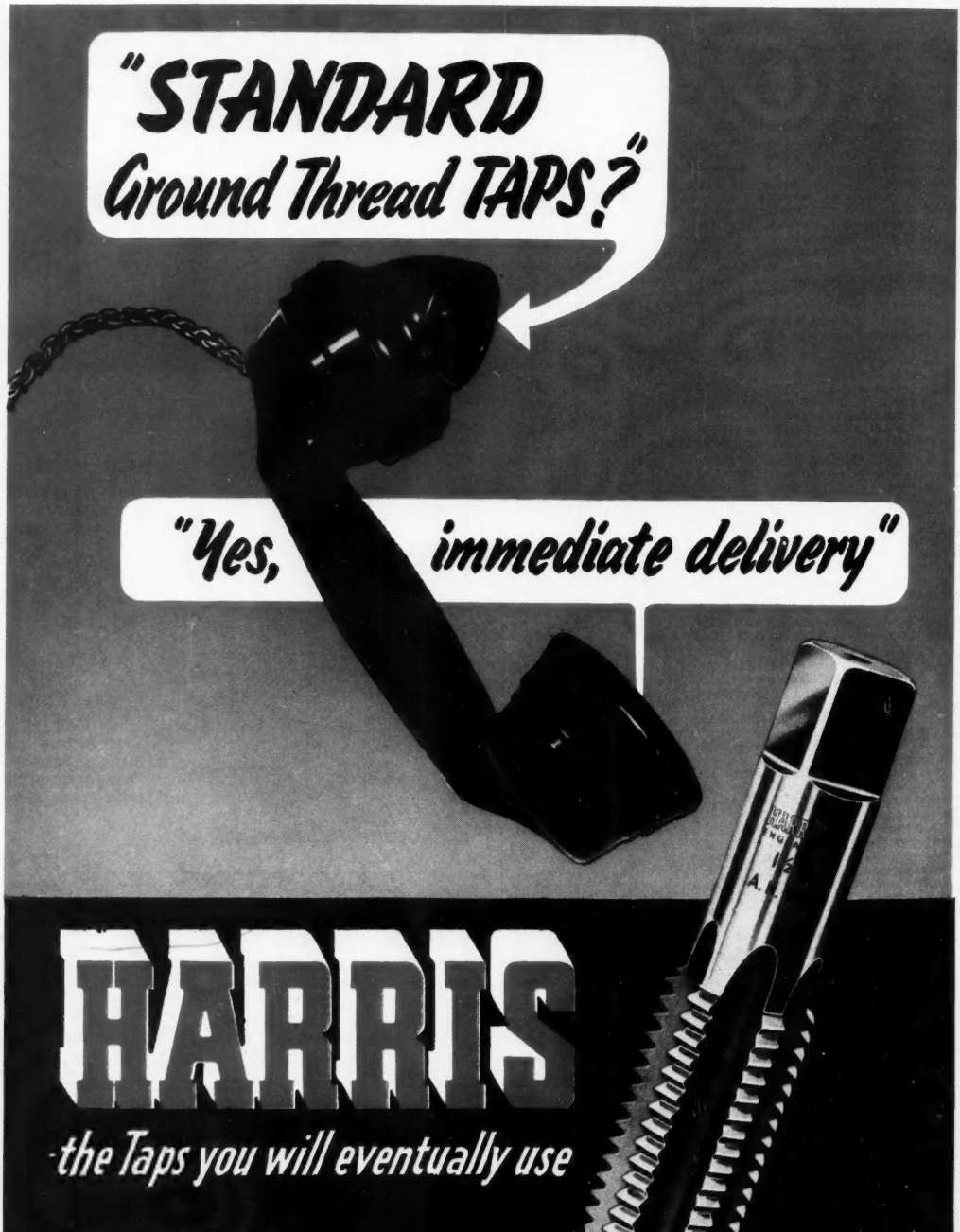
"STANDARD
Ground Thread TAPS?"
"Yes, immediate delivery"
HARRIS
the Taps you will eventually use
JOHN HARRIS TOOLS LTD., WARWICK
Phone 741 (4 lines)

BRITISH STANDARDS

(Copies of British Standards may be obtained from the British Standards Institution, 24, Victoria Street, London, S.W.1)

Rust and Acid Resisting Steel Wire. (B.S. 1554 : 1949). This British Standard is to provide more fully for rust, acid and heat resisting steels commonly supplied in the form of wire for general engineering purposes. The first section covering general clauses includes details of manufacture, methods of test and tolerances; section 2 gives for each steel the chemical composition and mechanical properties. PRICE 2/-.

Silver Anodes and Silver Salts for Electroplating. (B.S. 1561 : 1949). As in the former standards of this series, details of the composition and maximum limits for insoluble matter are provided. Methods for determining the percentage of silver present and the quantity of insoluble matter are included. PRICE 2/-

Nickel and Nickel Alloy Products. (B.S. Nos. 1525-1530 and 1534-1537 : 1949). These Standards form part of the series of standards for nickel and nickel alloys covering the various forms of wrought material.

1537 : 1949 Nickel alloy castings for general purposes.
1525 : 1949 Hot rolled malleable nickel sheet and cold rolled malleable nickel sheet and strip.
1526 : 1949 Hot rolled nickel-copper alloy sheet and cold rolled nickel-copper alloy sheet and strip.
1527 : 1949 Hot rolled nickel-chromium-iron alloy sheet and cold rolled nickel-chromium-iron alloy sheet and strip.
1528 : 1949 Malleable nickel bars, rods and sections.
1529 : 1949 Nickel-copper alloy bars, rods and sections.
1530 : 1949 Nickel-chromium-iron alloy bars, rods and sections.
1534 : 1949 Malleable nickel wire.
1535 : 1949 Nickel-copper alloy wire.
1536 : 1949 Nickel-chromium-iron alloy wire.

The standards do not cover products of special compositions.

Standards for nickel and nickel alloy tubes are being prepared and will be published shortly.

The standards for sheet and strip, bars rods and sections and wire lay down the chemical composition, condition, mechanical properties and tolerances and specify the procedure to be adopted in selecting test pieces and carrying out tests. Details are also given in regard to test certificates, independent tests and facilities for testing and appendices give a summary of the information to be given by the purchaser in enquiries and/or orders.

The subject of the casting standard is continually under revision and its scope will be extended when this is considered to be justified. Castings conforming to this standard are intended primarily for pressure vessels excluding wear-resisting surfaces. They are intended specially for the use with chemical plant suitable for services up to 480 deg. C. and the silicon content is therefore limited to a maximum of 1·2 per cent in order to prevent age hardening occurring in service.

Moulded Electrical Insulating Materials for Use at High Temperatures and at Radio Frequencies. (B.S. Nos. 1539 : 1949 and 1540 : 1949). Intended mainly to assist designers of electrical equipment each Standard takes into account all the types of material that meet the requirements of the branch of electrical work with which it deals. This series of Standards provides, as far as possible, similar methods of test to permit comparison of technical data.

B.S. 1539 deals with moulded electrical insulating-material for use where temperatures may exceed 180 deg. C. It defines three broad classes of material: (1) arc-resisting; (2) non-ignitable; (3) self-extinguishing. The Standard specifies requirements for the electrical and mechanical properties of each of these classes, together with standard methods of test for these properties.

B.S. 1540 covers moulded electrical insulating-materials for use under working conditions where they may be subjected to alternating electric fields having a frequency greater than 10,000 cycles per second. While the Standard nominally covers only moulded materials, it may be applied by agreement to all the extruded materials as well. Necessarily of some length, it deals with six classes of materials—fused silica, vitreous materials, ceramic materials for insulators, ceramic materials for dielectrics, rubber-base materials, and synthetic resins. It specifies requirements for the electrical and mechanical strength of each of these classes of material and gives a standard method of test for each property. PRICE B.S. 1539—3/- and B.S. 1540—5/-.

Wrought Aluminium Rainwater Goods. (B.S. 1543 : 1949). Two grades of gutters, pipes and fittings made from aluminium sheet strip or extrusions are dealt with in this British Standard. Gutters may be of the half-round or ogee types, pipes being limited to the round type. Valley gutters are dealt with by the specification of the minimum thicknesses appropriate to a range of girths.

The general requirements relate to quality of materials, manufacture and workmanship, inspection, finish and certification. The range of fittings for gutters comprises outlets, 90 deg. internal and external angles, obtuse (120 deg. and 135 deg.) internal and external angles and stop ends. The range of fittings for pipes includes offsets, shoes, 90 deg. and 135 deg. elbows and typical rainwater heads.

The specification is fully illustrated by line drawings and tables of dimensions with tolerances are provided. PRICE 5/-.

Office Equipment (Metal). (B.S. 1558 : 1949). The main purpose of this Standard is to specify standard dimensions of equipment which will ensure lining-up and will facilitate the planning of office and factory layouts while, at the same time, assisting economic production.

This first Standard deals with desks, tables, filing cabinets and plan cabinets; it specifies dimensions of desks and tables and of drawers, the arrangement of drawers in standard pedestals, and general requirements such as for sliding shelves and the tops of desks and tables. The Standard covers vertical filing cabinets of the type intended for current filing, and deals with dimensions to provide for lining-up, drawer sizes, drawer checks, drawer suspension, compressor plates and locks. Similar requirements are given for plan cabinets.

The Standard also specifies sizes of strongroom doors, of thickness up to Branch Bank quality: these sizes have been reduced, by agreement, from forty which were formerly quoted, to two sizes, which meet all normal requirements. PRICE 2/-.

Classified Advertisements.

The Rate for all classified advertisements is 6d. per word; in bold print 9d. per word; minimum order 6s. Box number advertisements 1s. extra. Instructions together with remittance must be received not later than the 3rd of each month for advertisements to appear in the same month's issue.

SITUATIONS VACANT

ADMIRALTY (C.E. in C. Department). Vacancies exist for Architectural and Civil Engineering Assistants in the Drawing Office at H.M. Dockyards and Establishments at Home and Abroad.

Applicants must be competent draughtsmen and designers with experience in some of the following types of Building and Civil Engineering Structures and Works:—Structural Steelwork, Reinforced Concrete, Dock and Harbour Works, Accommodation, Residential, Office, Store and Factory Buildings, Oil Fuel Tanks and Pipe Lines, Airfield Construction and Maintenance, Rail, Road, Water, Sewerage and Heating services, etc.

The salary for Architectural and Civil Engineering Assistants is £300-£525 (consolidated London rate) subject to Provincial differentiation of £20 at the minimum and £30 at the maximum, with a weight for age allowance above or below the age of 21 up to a total addition of seven increases of £20 each on the London rate. Appropriate rates of Colonial Allowance are payable in addition at Foreign Stations.

Vacancies exist at present at: Pinner, Broughton Moor, Caerwent, Chatham, Devonport, Liverpool, Arbroath, Portland, Rosyth, Fareham, Birmingham, Sheerness, Portsmouth, Leeds, Milford Haven, Ceylon, Gibraltar, Malta, Singapore, and West Africa.

The appointments are temporary.

Applications should be made, giving full particulars of experience, to the Civil Engineer-in-Chief, Admiralty, Chamberlain Way, Pinner, Middlesex.

£50 FOR ONE JOB. Scale Model-making Pays! We supply Plans, Instructions, and buy your work.—Write: B12, BILTEX, Chiswick, London.

WANTED

WANTED TO BUY Second-hand Machinery, Milling Machines, Lathes, Shaping Machines, Planing Machines, and all types of Modern Machine Tools.—Morgan Fairest, Ltd., Fairway Works, Sorby Street, Sheffield 4. Tel.: 23068 (4 lines).

WORK WANTED

BOTTLENECK IN CASTINGS? We can probably help you. Small part of our capacity available at the moment for precision ALUMINIUM gravity die castings, ZINC pressure die castings. High standard of workmanship; established 1828.—Write or 'phone **Thos. Ashworth & Co., Ltd.** (Dept. A/15/7), Vulcan Works, Burnley, Lancs. (Burnley 3505).

MACHINERY, ETC., FOR SALE

CRAIG & DONALD PRESS BRAKE, all steel; capacity 1000 tons; suitable for handling 8 ft. wide by 1 in. thick; motor driven 400/3/50; length of bed 8 ft. 6 in.; weight approx. 55 tons.—Full details: **F. J. Edwards Ltd.,** 359, Euston Road, London, N.W.1. EUSton 4681.

ADDRESSOGRAPH MACHINE, Hand Operated, in good order, with wooden cabinet; capacity, 10,000 address plates. Price, which also includes approximately 5,000 frames and used plates, £40 or near offer.—Phone: "The Engineers' Digest," WELBECK 9357—Mrs. AYLES.

NISSEN TYPE HUTS, ex-Government stock, reconditioned and supplied ready for erection. All sizes in 6 ft. multiples. 36 ft. by 16 ft., £65 & £54; 24 ft. by 16 ft., £46 & £38; 72 ft. by 16 ft., £122 & £97; delivered U.K. Plasterboard huts and other buildings. Some 24 ft. span Nissens.—Write, call or telephone, **Universal Supplies (Belvedere) Ltd.,** Dept. 50, Crabtree Manorway, Belvedere, Kent. Telephone No. ERITH 2948.

Our technical representatives will gladly advise you on the varying types of the Weston Seals. These include our Gitseals and Weston Oil Retainers fitted with best quality chrome leather inserts, also the Weston Synthetic Rubber Oilseals all precision made to give the lightest possible contact consistent with efficient sealing.

WESTON
OIL SEALS

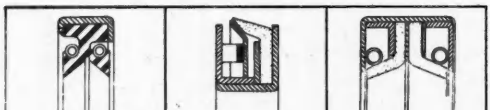

CHARLES WESTON & CO. LTD., IRWELL BANK WORKS, DOUGLAS GREEN, PENDLETON, SALFORD, 6.
PHONE: PENDLETON 2857-8-9. BIRMINGHAM, MIDLAND 6952. LONDON, HOLBORN 0414

Smee's W 58

Specify

CASTLE V F FIBRE

for

Machined Components

Unaffected by age or climate

Vulcanised Fibre Ltd
BROADFORD MILLS, GUILDFORD, ENGLAND
Phone: Guildford 5214-6. Grams: Vulcanised, Guildford

LONDON OFFICE:
8, KING WILLIAM ST., LONDON, E.C.4
Phone: Mansion House 0452
Grams: Fibremil, Stock, London